Introduction to aero-acoustics of internal flows

A. Hirschberg
Laboratory for Fluid Dynamics
Faculty of Applied Physics
Technische Universiteit Eindhoven
Postbus 513
5600 MB Eindhoven, Nederland
A.Hirschberg@tue.nl

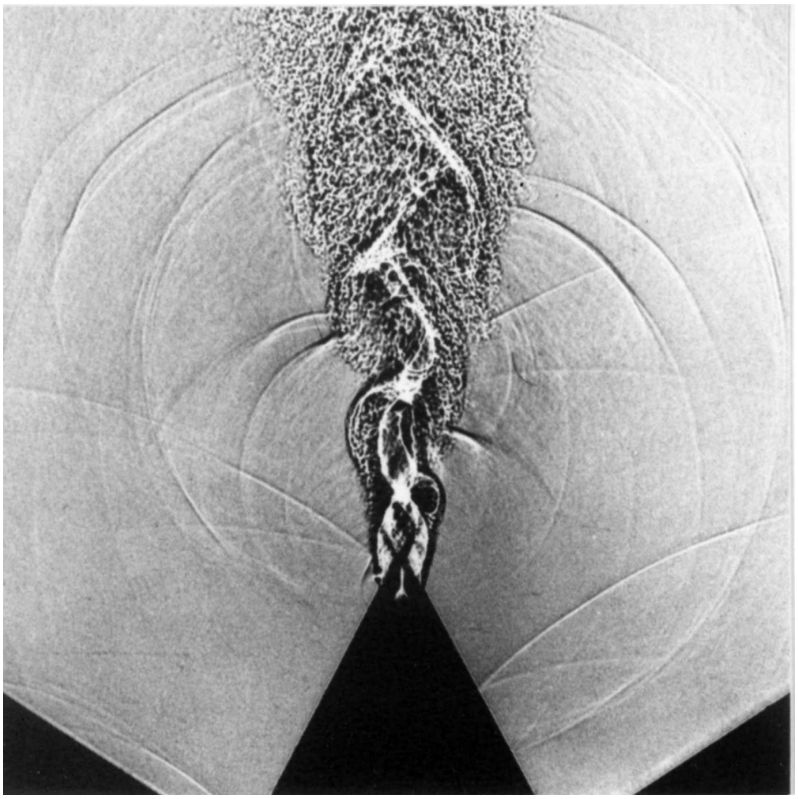

Revised version of chapter from the course *Advances in Aeroacoustics* (VKI, 12-16 March 2001) [1].

[1]Acknowledgement: The author wishes to express his gratitude for the support of Mrs. B. van de Wijdeven and Mr. D. Tonon in the revision of this manuscript. The flow visualization of jet screech has been provided by L. Poldervaard and A.P.J. Wijnands.

Contents

1 Introduction **4**

2 Fluid dynamics **5**
2.1 Conservation laws 5
2.2 Constitutive equations 8
2.3 Entropy equation 11
2.4 Boundary conditions 13
2.5 Vorticity and potential flows 13

3 Lighthill's analogy **14**

4 Acoustics of a quiescent fluid **17**
4.1 Wave equation 17
4.2 Elementary solutions 18
4.3 Acoustical energy and acoustical impedance 19
4.4 Range of validity of acoustical approximation 21
4.5 Acoustical field of a harmonically pulsating or translating sphere 23
4.6 Green's function and integral formulation 29
4.7 Multipole expansion 32
4.8 Doppler effect 34
4.9 Influence of walls 36
4.10 Influence of a compact body on radiation 38

5 Waves in pipes **41**
5.1 Pipe modes 41
5.2 One dimensional Green's function for infinite pipe 45
5.3 Reflections at pipe discontinuities at low frequencies. 46
5.4 The open pipe termination in quiescent fluid 51
5.5 Simple resonators in pipe systems 53
5.6 Helmholtz resonator 58
5.7 Bubble resonance 61
5.8 Self-sustained oscillations 62
5.9 The clarinet 67

6 Vortex-sound theory **70**
6.1 Paradox of D'Alembert and flow separation 70
6.2 Vortex-sound analogy 74
6.3 Vortex dynamics 76
6.4 Dipole character of vortex sound 77
6.5 Grazing flow along a Helmholtz resonator 80
6.6 Low frequency behaviour of an open pipe termination 86
6.7 High amplitude response of resonators 92

7 Turbulent noise **94**
7.1 Turbulence 94
7.2 Isothermal free jets 96
7.3 Low frequency behaviour of a jet in an infinite pipe 99
7.4 Low frequency turbulent sound production by a diaphragm. 100
7.5 Free jet in a bubbly liquid 103

1 Introduction

Due to the essential non-linearity of the governing equations it is difficult to predict accurately fluid flows under conditions at which they do produce sound. This is typically high speeds for which non-linear inertial terms in the equation of motion are much larger than viscous terms (high Reynolds numbers). Direct simulation of such flows is very difficult. When the flow velocity remains low compared to the speed of sound waves (low Mach numbers) the sound production is a minute fraction of the energy in the flow. This makes numerical simulation even more difficult. It is even not obvious how we should define the acoustical field in the presence of flows. Aero-acoustics provides such definitions. The acoustic field is defined as an extrapolation of an ideal reference flow. The difference between the actual flow and this reference flow is identified as sources of sound. Using Lighthill's terminology, we call this an "analogy" [68].

In free field conditions the sound intensity produced by flows is usually so small that we can neglect the effect of acoustics on the flow. Furthermore the listener is usually immerged into a uniform stagnant fluid. In such cases the convenient reference flow is the linear inviscid perturbation of this stagnant uniform fluid. It is convenient to use an integral formulation of the aero-acoustical analogy. This integral equation is a convolution of the sound source by the Green's function: the response of the reference state to a localized impulsive source. The advantage of the integral formulation is that random errors in the source term average out. One therefore also often uses such an integral formulation to extract acoustical information from direct numerical simulations of the flow which are too rough to predict directly the acoustical field. Such an approach is used to obtain scaling laws for sound production by turbulent flows when only global information is available on the flow. When the flow dimensions are small compared to the acoustical wave length (compact flow) we can locally neglect the effect of wave propagation. Lighthill provides here again a procedure which guarantees that we keep the leading order term where brute force would predict no sound production at all or would dramatically overestimate the sound production. In compact flows at low Mach numbers the flow is most efficiently described in terms of vortex dynamics. This allows a more detailed study of the sound production by non-linear convective effects.

Walls have a dramatic effect on the production of sound because it becomes much easier to compress the fluid than in free space. In internal flows acoustical energy can accumulate into standing waves which correspond to resonances. Even at low Mach numbers acoustical particle velocities of the order of magnitude of the main flow velocity can be reached when hydrodynamic flow instabilities couple with the acoustical standing waves. Those self-sustained oscillations are most efficiently described in terms of vortex dynamics. Furthermore in a pipe the main flow does not necessarily vanishes when we travel away from the source region. For those reasons another analogy should be used which we call the vortex-sound theory. This theory was initially developed by Powell [92] for free space and generalized by Howe [52] for internal flows. In Howe's approach the acoustical field is

defined as the unsteady irrotational component of the flow, which again stresses the fact that vortices are the main sources of sound in isentropic flows. An integral formulation can also be used in this case. When considering self-sustained oscillations: one is interested in conditions at which they appear and the amplitude they reach. While a linear theory does provide information on the conditions under which self-sustained oscillation appears, the amplitude is determined by essentially non-linear saturation mechanism. We will show that when the relevant non-linear mechanism is identified, the order of magnitude of steady self-sustained pulsation amplitude can easily be obtained. A balance between the acoustical power produced by the source and the dissipated power will be used.

We provide a summary of the equations of fluid dynamics (section 2). We introduce the acoustic field by means of Lighthill's analogy (section 3). We then describe some elementary concept of the acoustics of a stagnant uniform fluid such as elementary solutions of the wave equation, acoustical energy, acoustical impedance, the Green's function, multipole expansions, Doppler effect and influence of plane walls on radiation (section 4). We then discuss the acoustics of pipes for stagnant fluids. We introduce the concepts of modes, resonators and self-sustained oscillations (section 5). The next section is dedicated to an introduction to Vortex-sound theory (section 6). We use this theory to analyse in detail the aero-acoustic of the Helmholtz resonator which is an acoustical mass-spring system (section 6). In the last section (7) we provide some information on the sound production by turbulent flow in pipes.

Our discussion is inspired by the book of Dowling and Ffowcs Williams [28] which is an excellent introductory course. Basic acoustics is discussed in the books of Morse and Ingard [74], Pierce [90], Kinsler et al [60], Temkin [109] and Blackstock [7]. Aero-acoustics is treated in the books of Goldstein [37], Blake [8], Crighton [20], Hubbard [53], Howe [52] and Howe [51]. We ignore in this introduction the effect of wall vibration which are discussed by Cremer [17], Junger and Feit [57], Blevins [9] and Norton [82]. The acoustics of musical instruments which we use as examples is treated by Fletcher and Rossing [33]. In an earlier course [13] we discussed the aero-acoustics of woodwinds. In the lecture notes of Rienstra and Hirschberg [98] more details on mathematical aspects are provided. An overview of acoustics is provided by Crockler [22].

2 Fluid dynamics

2.1 Conservation laws

We consider the motion of fluids in the continuum approximation ([65], [110], [102], [64]). This means that quantities such as the velocity $\vec{v}$, the density ρ, the pressure p,... can be described by means of smooth functions of space and time coordinates $(\vec{x}, t)$. We consider the fundamental equations of mass, momentum and energy conservation applied to an infinitesimal fluid particle of volume V (material element). For such a small particle we can

neglect the variation of density within the particle. The mass of the particle is then the product ρV of its volume and the density. The mass conservation law states that the mass remains constant. As we move with the particle we can write this statement in the form:

$$\frac{D\rho V}{Dt} = 0 \tag{1}$$

where the convective time derivative:

$$\frac{D}{Dt} = \frac{\partial}{\partial t} + \vec{v} \cdot \nabla \tag{2}$$

is the time derivative as experienced by an observer which moves with the fluid particle, at the velocity $\vec{v}$. We can for cartesian coordinates write equation (2) in the index notation:

$$\frac{D}{Dt} = \frac{\partial}{\partial t} + v_i \frac{\partial}{\partial x_i} \tag{3}$$

where we use the convention of Einstein: the repetition of index i implies that we have a summation over this (dead) index:

$$v_i \frac{\partial}{\partial x_i} = v_1 \frac{\partial}{\partial x_1} + v_2 \frac{\partial}{\partial x_2} + v_3 \frac{\partial}{\partial x_3} \ . \tag{4}$$

The dilatation rate of an infinitesimal cubic volume $V = L_1 L_2 L_3$ is simply the sum of the strain rates:

$$\frac{1}{V}\frac{DV}{Dt} = \frac{1}{L_i}\frac{DL_i}{Dt} \ . \tag{5}$$

Considering the one dimensional flow sketched in figure 1 we can easily understand that the rate of change of the length is given by $DL_1/Dt = [v_1(x_1+L_1) - v_1(x_1)] = (\partial v_1/\partial x_1)L_1$. We then can understand that:

$$\frac{1}{V}\frac{DV}{Dt} = \frac{1}{L_i}\frac{DL_i}{Dt} = \frac{\partial v_i}{\partial x_i} \ . \tag{6}$$

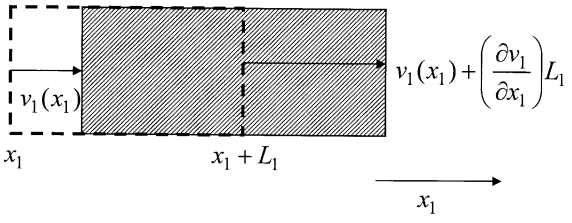

Figure 1: *Mass conservation law in one dimensional flow. The dilatation rate* $\frac{DL_1}{Dt}$ *of a fluid particle of length* L_1 *is equal to* $\frac{\partial v_1}{\partial x_1} L_1$.

Hence the mass conservation law (1) can be written in the familiar form:

$$\frac{1}{\rho}\frac{D\rho}{Dt} = -\nabla \cdot \vec{v} \tag{7}$$

or in the conservative form:

$$\frac{\partial \rho}{\partial t} + \nabla \cdot (\rho \vec{v}) = 0 \ , \tag{8}$$

which in index notation becomes:

$$\frac{\partial \rho}{\partial t} + \frac{\partial \rho v_i}{\partial x_i} = 0 \ . \tag{9}$$

The same equation applied to a finite controle volume V delimited by a surface S with outer normal $\vec{n}$ (see figure 2) becomes:

$$\frac{d}{dt}\int_V \rho dV + \int_S \rho(v_i n_i) dS = 0 \ . \tag{10}$$

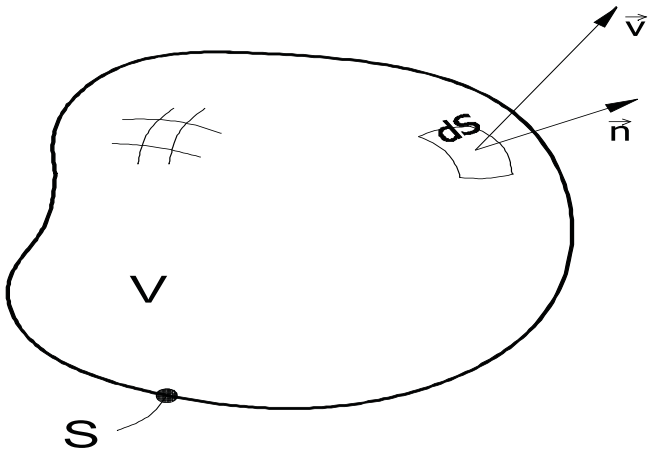

Figure 2: *Macroscopic controle volume V enclosed by surface S with outer normal $\vec{n}$ used for integral conservation law. The volume flux through an element dS of the surface is $\vec{v} \cdot \vec{n} dS = v_i n_i dS$. An element of volume dV has a mass ρdV.*

This conservative equation stresses the interpretation of the equation as a balance between the change of mass content $\partial\rho/\partial t$ of a control volume fixed in the reference frame of the laboratory as a result of the net flow of fluid into the control volume $\partial \rho v_i/\partial x_i$ through the surface delimiting the control volume. The integral form of the conservation law is more general than the differential form because it allows for discontinuities in the flow field such as shock-waves.

The second law of Newton applied to a fluid particle (material element) can be written as:

$$\rho \frac{D\vec{v}}{Dt} = -\nabla \cdot \vec{\vec{P}} + \vec{f} \tag{11}$$

where the ρ is the mass per unit volume, $\vec{f}$ is the density of the force field acting on the bulk of the fluid and $-\nabla \cdot \vec{\vec{P}}$ is the net force acting on the surface of the particle divided by the volume of the particle, which we express in terms of the stress tensor $\vec{\vec{P}}$. The force per unit surface acting on the surface enclosing the particle is $-\vec{n} \cdot \vec{\vec{P}}$ where $\vec{n}$ is the outer normal on the surface. In index notation Newton's law becomes:

$$\rho \left(\frac{\partial v_i}{\partial t} + v_j \frac{\partial v_i}{\partial x_j} \right) = -\frac{\partial P_{ij}}{\partial x_j} + f_i \ . \tag{12}$$

and using the mass conservation law we obtain the conservation form:

$$\left(\frac{\partial \rho v_i}{\partial t} + \frac{\partial \rho v_i v_j}{\partial x_j} \right) = -\frac{\partial P_{ij}}{\partial x_j} + f_i \ . \tag{13}$$

which states that the change in momentum content ρv_i of a fixed controle volume is due to external forces and flux $-\rho v_i v_j n_j$ of momentum through the surface of the particle. The tensor $\rho v_i v_j$ is called the Reynolds stress tensor. An integral formulation of the momentum equation (13) in the same form as equation (10) can easily be derived:

$$\frac{d}{dt} \int_V \rho v_i dV + \int_S \rho v_i (v_j n_j) dS = -\int_S P_{ij} n_j dS + \int_V f_i dV \tag{14}$$

The energy conservation law applied to a fluid particle is:

$$\rho \frac{D}{Dt} \left(e + \frac{1}{2} v^2 \right) = -\nabla \cdot \vec{q} - \nabla \cdot \left(\vec{\vec{P}} \cdot \vec{v} \right) + \vec{f} \cdot \vec{v} + Q_w \tag{15}$$

where e is the internal energy per unit of mass, $v = |\vec{v}|$, $\vec{q}$ is the heat flux vector and Q_w is the heat production per unit of volume. The source term Q_w depends on effects which we do not take into account in either $\vec{f}$ or $\vec{q}$. This can be chemical reactions or electrical heating.

In conservation form, the energy equation becomes:

$$\frac{\partial}{\partial t} \rho \left(e + \frac{1}{2} v^2 \right) + \frac{\partial}{\partial x_i} \rho v_i \left(e + \frac{1}{2} v^2 \right) = -\frac{\partial q_i}{\partial x_i} - \frac{\partial P_{ij} v_j}{\partial x_i} + f_i v_i + Q_w \tag{16}$$

2.2 Constitutive equations

The conservation laws of mass, momentum and energy presented in the previous section do not form a complete set of equations [110]. They involve more unknowns (14: $e, \rho, v_i, P_{ij}, q_i$)

than equations (5). The additional information needed is provided by the so-called constitutive equations. First of all we assume the fluid to be in a state of local thermodynamic equilibrium. This implies for a homogeneous fluid that two intrinsic state variables are sufficient to specify the thermodynamic state of the fluid. We chose as basic variables the density ρ and the specific entropy s (entropy per unit of mass). We assume that a thermal equation of state:

$$e = e(\rho, s) \tag{17}$$

or in differential form:

$$de = \left(\frac{\partial e}{\partial \rho}\right)_s d\rho + \left(\frac{\partial e}{\partial s}\right)_\rho ds \tag{18}$$

has been determined from quasi-static experiments. Relationships between this equation of state and other variables are provided by the thermodynamics. The temperature T and the pressure p are introduced by the fundamental equation:

$$de = Tds - pd\left(\frac{1}{\rho}\right) \tag{19}$$

which implies that:

$$T = \left(\frac{\partial e}{\partial s}\right)_\rho \tag{20}$$

and:

$$p = \rho^2 \left(\frac{\partial e}{\partial \rho}\right)_s \tag{21}$$

Furthermore as $p = p(\rho, s)$ we have:

$$dp = \left(\frac{\partial p}{\partial \rho}\right)_s d\rho + \left(\frac{\partial p}{\partial s}\right)_\rho ds. \tag{22}$$

The speed of sound $c = c(\rho, s)$ is defined as the thermodynamic variable:

$$c = \sqrt{\left(\frac{\partial p}{\partial \rho}\right)_s}. \tag{23}$$

We will see later that indeed acoustic waves do propagate with this velocity.

In most applications which we consider, the fluid will be assumed to be an ideal gas, so that:

$$p = \rho RT \tag{24}$$

where R is the specific gas constant, the ratio $R = k_B/m_w$ of the Boltzmann constant k_B and the mass m_w of a gas molecule. It can be shown that for an ideal gas:

$$c^2 = \gamma RT \tag{25}$$

where $\gamma = c_p/c_v$ is the Poisson ratio of specific heat c_p at constant pressure and specific heat c_v at constant volume:

$$c_v = \left(\frac{\partial e}{\partial T}\right)_v \tag{26}$$

and:

$$c_p = \left(\frac{\partial i}{\partial T}\right)_p \tag{27}$$

where i is the specific enthalpy defined by:

$$i = e + \frac{p}{\rho} \ . \tag{28}$$

For an ideal gas it follows from those definitions that $R = c_p - c_v$.

In many cases we assume that the gas has a constant specific heat c_v so that $e = c_v T$. Combining this assumption with the ideal gas law and the fundamental law of thermodynamics (19), we find the equation of state:

$$\frac{p}{p_0} = \left(\frac{\rho}{\rho_0}\right)^\gamma \exp\left(\frac{s - s_0}{c_v}\right) \tag{29}$$

where the (ρ_0, s_0) is a reference state at which the pressure is p_0. For an isentropic flow $(s - s_0) = 0$ we recover the more familiar equation $(p/p_0) = (\rho/\rho_0)^\gamma$.

As we assume local thermodynamic equilibrium, it is logical to assume that the transport processes are determined by linear functions of the gradients of the flow variables ([104], [102], [4], [110]). This corresponds to a so-called Newtonian behaviour for the stress tensor P_{ij}. We introduce the viscous stress tensor τ_{ij} defined by:

$$\tau_{ij} = -(P_{ij} - p\delta_{ij}) \tag{30}$$

where $\delta_{ij} = 1$ for $i = j$ and zero otherwise. For a Newtonian fluid, the viscous stress τ_{ij} is given by:

$$\tau_{ij} = 2\eta(D_{ij} - \frac{1}{3}D_{kk}\delta_{ij}) + \mu_v D_{kk}\delta_{ij} \tag{31}$$

where D_{ij} is the rate of strain tensor defined by:

$$D_{ij} = \frac{1}{2}\left(\frac{\partial v_i}{\partial x_j} + \frac{\partial v_j}{\partial x_i}\right) \tag{32}$$

which is the symmetric part of the tensor $\nabla\vec{v}$. The bulk viscosity μ_v is taken to be zero according to Stokes hypothesis for a fluid in thermodynamic equilibrium. The dynamic viscosity η is a function of the thermodynamic state of the fluid. For an ideal gas η is a function of the temperature. A typical empirical relationship is for air at ambient conditions:

$$\frac{\eta}{\eta_0} = \left(\frac{T}{T_0}\right)^{0.75} . \tag{33}$$

While the assumption of local thermodynamic equilibrium is a reasonable first approximation, many examples of significant deviations are observed in acoustics. Due to the finite relaxation time of rotational degrees of freedom of molecules the absorption of sound is in air much larger than expected when $\mu_v = 0$.

The equivalent approximation for the heat flux is Fourier's law:

$$q_i = -K\left(\frac{\partial T}{\partial x_i}\right) \tag{34}$$

where K is the heat conductivity which for an ideal gas is also a function of the temperature only. It is convenient to introduce the kinematic viscosity ν and the heat diffusivity a, which are the diffusion coefficients for respectively momentum transport:

$$\nu = \eta/\rho \tag{35}$$

and for heat transport:

$$a = K/(\rho c_p) . \tag{36}$$

Following elementary kinetic theory of gasses those diffusion coefficients are proportional to the product of a thermal velocity and of the mean-free path for the particular transport process (memory distance). A typical thermal velocity is the speed of sound. The ratio of the two diffusion coefficients is called the Prandtl number $Pr = \nu/a$. For ambient air $Pr = 0.72$ is almost constant, indicating that both heat and momentum transport are controlled by the same molecular collisional processes.

2.3 Entropy equation

As the entropy is a convenient state variable we now combine the energy conservation law with the second law of thermodynamics and we subtract from the energy equation the mechanical energy conservation law (the scalar product of $\vec{v}$ and the momentum conservation law) to obtain an equation for the entropy [110]:

$$\rho T\frac{Ds}{Dt} = -\nabla\cdot\vec{q} + \vec{\vec{\tau}} : (\nabla\vec{v}) + Q_w \tag{37}$$

Using the fact that $\vec{\vec{\tau}} : (\nabla \vec{v}) = \frac{1}{2}\vec{\vec{\tau}} : \vec{\vec{D}}$ we can re-write this equation as:

$$\rho T \frac{Ds}{Dt} - Q_w + T\nabla \cdot \left(\frac{\vec{q}}{T}\right) = -\left(\frac{\vec{q}}{T}\right) \cdot \nabla T + \frac{1}{2}\vec{\vec{\tau}} : \vec{\vec{D}} \tag{38}$$

in which the right hand term corresponds to irreversible heat conduction and viscous dissipation. As the right hand side of the equation is always positive we can verify that deviation from an reversible process leads to an increase of entropy as we expect from the laws of thermodynamics.

When $Q_w = 0$, heat transfer and dissipation are negligible the entropy equation reduces to:

$$\frac{Ds}{Dt} = 0 \tag{39}$$

we call a flow satisfying this equation: isentropic. When the fluid is uniform (we have initial conditions with uniform entropy) and the flow is isentropic, the entropy is uniform and constant ($ds = 0$). We call such a flow homentropic.

In subsonic flows, at low Mach numbers ($M = U_0/c_0 \ll 1$) and high Reynolds numbers ($Re = U_0 D/\nu \gg 1$), entropy production is due to combustion, condensation, ... processes. When the flow is laminar, heat conduction and dissipation are limited to thin boundary layers. In turbulent flows, kinetic energy is very efficiently dissipated by a transfer of energy from large scales towards small (viscous dominated) scales. However the kinetic energy density $\frac{1}{2}\rho v^2$, of the flow is only a fraction M^2 of the specific internal energy $e(\rho, s)$, and the entropy production by viscous dissipation is usually neglected. The significance of this dissipation for the production of sound in subsonic turbulent flows is subject to some controversy[84], but it is certainly quite small compared to other sources of sound.

In supersonic flows ($M = U_0/c_0 > 1$), the kinetic energy density of the flow will by definition be large. Viscous dissipation involves large entropy production and temperature gradients in boundary layers on walls. The appearance of shock waves, which are in nature essentially non-isentropic even in the frictionless limit ($Re \gg 1$), involves specific sound production mechanisms. Of course such effects become even more significant in hypersonic flows($M \gg 1$).

In summary:

- a high Reynolds number non-reacting gas flow is in first approximation isentropic ($Ds/Dt = 0$). Deviations occurring in boundary layers and turbulent flow regions remain small unless a temperature gradient is imposed by the boundary conditions. An homentropic flow is often a reasonable model.

- in supersonic flows, even if the bulk of the flow is isentropic, viscous dissipation is an essential source of entropy in boundary layers and shock waves. Deviations from an homentropic flow are essential.

2.4 Boundary conditions

The boundary conditions for a fluid at a solid impermeable wall with velocity $\vec{v}_w$ and temperature T_w are, in the continuum approximation:

$$\vec{v} = \vec{v}_w \tag{40}$$

and:

$$T = T_w \tag{41}$$

The first condition expresses the fact that due to viscosity the fluid sticks to the wall. The second condition is the continuity of temperature.

2.5 Vorticity and potential flows

In the absence of sources ($Q_w = 0$) when friction and heat transfer are negligible the flow is isentropic:

$$\frac{Ds}{Dt} = 0 \tag{42}$$

If we further assume an homogeneous fluid then ($\nabla s = 0$) the flow is homentropic. In a frictionless approximation, the momentum conservation law reduces to the equation of Euler:

$$\rho \frac{D\vec{v}}{Dt} = -\nabla p + \vec{f} \, . \tag{43}$$

It is important to realize that if we neglect friction we have to admit the existence of a finite slip velocity tangential to the wall. The boundary condition $\vec{v} = \vec{v}_w$ for a rigid impermeable wall is replaced by $\vec{n} \cdot \vec{v} = 0$, where $\vec{n}$ is the outer unit normal to the wall.

We now derive from these equation the Bernoulli equation for an unsteady compressible flow. We introduce for convenience the specific enthalpy i defined by:

$$i = e + \frac{p}{\rho} \, . \tag{44}$$

Using the fundamental laws of thermodynamics we find:

$$di = de + \frac{1}{\rho} dp + p \, d\left(\frac{1}{\rho}\right) = T ds + \frac{1}{\rho} dp \tag{45}$$

Which implies that for an homentropic flow ($\nabla s = 0$) we have $\frac{\nabla p}{\rho} = \nabla i$ and the equation of Euler can be write as:

$$\frac{D\vec{v}}{Dt} = \frac{\partial \vec{v}}{\partial t} + (\vec{v} \cdot \nabla)\vec{v} = -\nabla i + \frac{\vec{f}}{\rho} \, . \tag{46}$$

The convective acceleration term can be split into a gradient term (acceleration along the stream- line) and a Coriolis acceleration due to the rotation of the fluid particle [101]:

$$(\vec{v} \cdot \nabla)\vec{v} = \frac{1}{2} \nabla \left|\vec{v}\right|^2 + (\vec{\omega} \times \vec{v}) \tag{47}$$

where $\vec{\omega}$ is the vorticity of the velocity field:

$$\vec{\omega} = \nabla \times \vec{v} \ . \tag{48}$$

Substitution into the equation of Euler yields the Crocco's form of the equation of motion:

$$\frac{\partial \vec{v}}{\partial t} = -\nabla B - (\vec{\omega} \times \vec{v}) + \frac{\vec{f}}{\rho} \tag{49}$$

where we have defined the *total enthalpy* B as:

$$B = i + \frac{v^2}{2} \ . \tag{50}$$

For an irrotational flow ($\vec{\omega} = \nabla \times \vec{v} = 0$) we can introduce a potential:

$$\vec{v} = \nabla \varphi \tag{51}$$

or in integral form:

$$\varphi_2 - \varphi_1 = \int_{\vec{x}_1}^{\vec{x}_2} \vec{v} \cdot d\vec{x}$$

we call such a flow a *potential flow* ([94], [4], [86], [101], [64], [2]). If we further assume that $\frac{\vec{f}}{\rho} = -\nabla \Phi_f$ we can then integrate the equation of movement and we obtain the equation of Bernoulli:

$$\frac{\partial \varphi}{\partial t} + B + \Phi_f = g(t) \tag{52}$$

The function $g(t)$ is determined by the boundary conditions.

3 Lighthill's analogy

Aeroacoustics is the art of predicting sound generation by flows. In principle acoustical waves are an intrinsic part of the flow. One could therefore consider simply the solution of the equations describing the flow. As the flow equations described in the previous section are non linear and are therefore extremely difficult to solve, one therefore has to seek for suitable approximations.

In figure 3, we see schlieren flow visualization of self-sustained oscillations of an under-expanded supersonic jet. Due to the under-expansion, expansion waves are formed at both sides of the flow-exit to adapt the pressure in the jet to the environment. The intersection of those expansion waves in the middle of the jet flow results into an overexpansion. At the edges of this overexpansion zone the expansion waves reflect, as compression waves, at the shear-layer separating the jet from the environment (one on each side of the jet). The interaction of these two compression waves results into a compression of the jet above the environment pressure. The process is then repeated. This results into the oscillatory

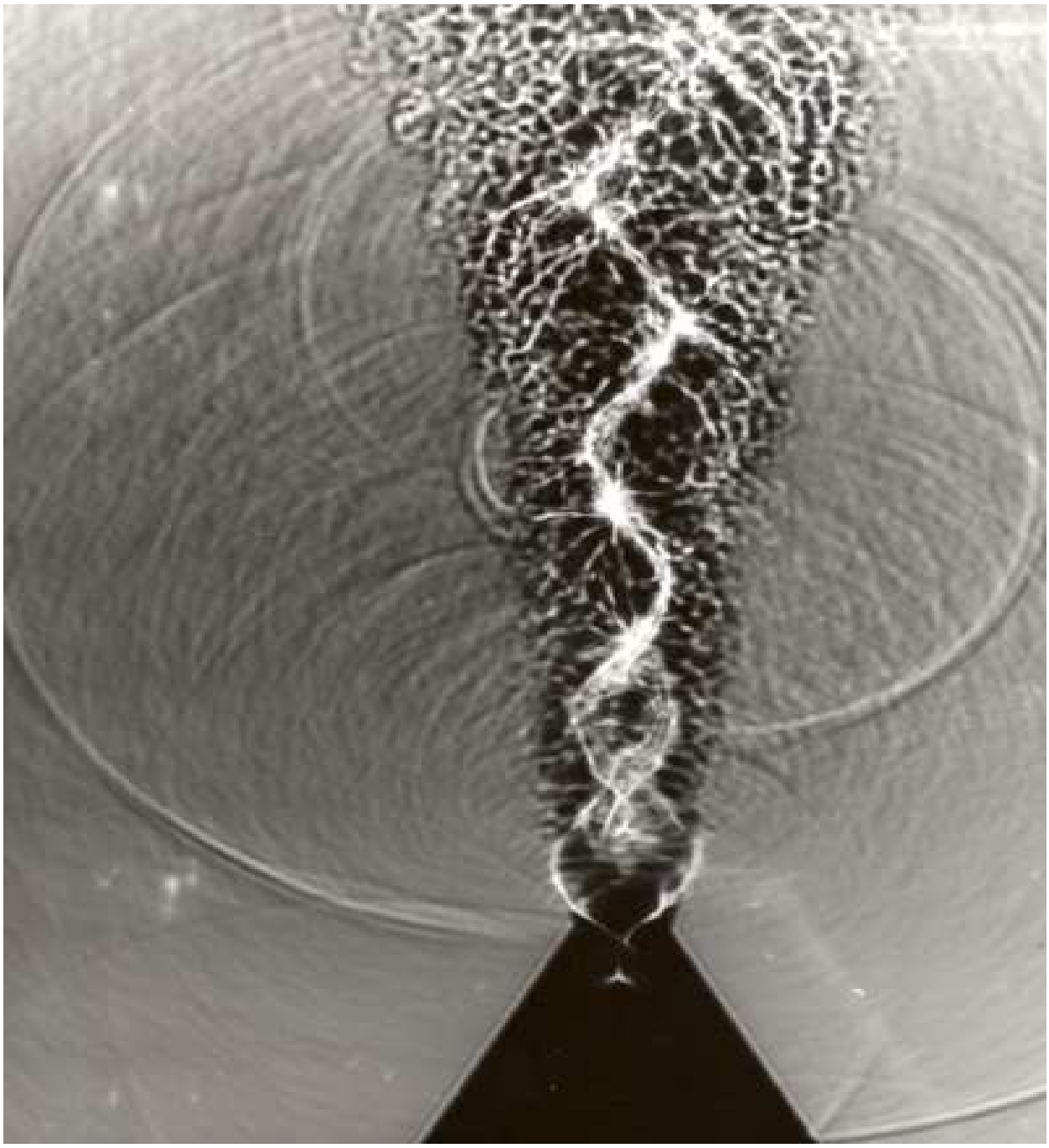

Figure 3: *Schlieren flow visualization of self-sustained oscillation of an under-expanded free jet.*

pattern of the steady flow. As compression waves tend to steepen up, shock waves are formed. The jet oscillation is due to a feedbackloop. Interaction of vortices in the shear layer of the jet with the standing shock-waves results into a radiation of sound waves. These waves cannot travel upstream within the jet because the jet is supersonic. However the surrounding air is stagnant. The acoustic waves expand radially into this stagnant air and reach the flow exit. This perturbation of the flow triggers the formation of a vortex as a result of the instability of the shear layer separating the jet flow from the environment. This vortex is convected downstream by the jet and interacts with the shock.

The picture shows a striking difference between the very complex jet flow with its waves, vortices and turbulence and the relatively simple acoustic wave propagation in the surrounding air. We therefore will consider two different approximations, one for the "wave" region outside the jet and one for the "source" region in the jet. We would like to establish a relationship between those two approximations. In the example of the free jet discussed above it will appear that the outer flow is reasonably described as a linear inviscid and isentropic perturbation of a uniform stagnant fluid. We will call further the uniform stagnant fluid a quiescent fluid. We will introduce this approximation by using the so-called aeroacoustical "analogy" of Lighthill.

We take the time derivative of the mass conservation law (9):

$$\frac{\partial^2 \rho}{\partial t^2} + \frac{\partial^2 \rho v_i}{\partial t \partial x_i} = 0. \tag{53}$$

and subtract from it the divergence of the momentum equation (13):

$$\left(\frac{\partial^2 \rho v_i}{\partial x_i \partial t} + \frac{\partial^2 \rho v_i v_j}{\partial x_i \partial x_j} \right) = -\frac{\partial^2 P_{ij}}{\partial x_i \partial x_j} + \frac{\partial f_i}{\partial x_i}. \tag{54}$$

to obtain the exact equation:

$$-\frac{\partial^2 p}{\partial x_i^2} = \frac{\partial^2 (\rho v_i v_j - \tau_{ij})}{\partial x_i \partial x_j} - \frac{\partial f_i}{\partial x_i} - \frac{\partial^2 \rho}{\partial t^2} \ . \tag{55}$$

This equation has no simple physical meaning. When however we add on both sides the term $\frac{1}{c_0^2}\frac{\partial^2 p}{\partial t^2}$ we obtain a non-homogeneous wave equation which is called the analogy of Lighthill:

$$\frac{1}{c_0^2}\frac{\partial^2 p}{\partial t^2} - \frac{\partial^2 p}{\partial x_i^2} = \frac{\partial^2 (\rho v_i v_j - \tau_{ij})}{\partial x_i \partial x_j} - \frac{\partial f_i}{\partial x_i} + \frac{1}{c_0^2}\frac{\partial^2 p}{\partial t^2} - \frac{\partial^2 \rho}{\partial t^2}. \tag{56}$$

This equation is valid for any value of the velocity c_0. One could introduce here the velocity of propagation of light in vacuum! With such a choice for c_0 the equation is rather meaningless. The equation becomes interesting when we use here the speed of sound c_0 in the reference quiescent state (ρ_0, s_0) of the fluid surrounding a listener. We furthermore introduce deviations from this reference state:

$$\rho' = \rho - \rho_0 \ , \tag{57}$$

$$p' = p - p_0, ... \tag{58}$$

to obtain:

$$\frac{1}{c_0^2}\frac{\partial^2 p'}{\partial t^2} - \frac{\partial^2 p'}{\partial x_i^2} = \frac{\partial^2(\rho v_i v_j - \tau_{ij})}{\partial x_i \partial x_j} - \frac{\partial f_i}{\partial x_i} + \frac{\partial^2}{\partial t^2}\left(\frac{p'}{c_0^2} - \rho'\right). \tag{59}$$

which is still exact because ρ_0, p_0 and c_0 are constants. While the analogy of Lighthill is exact, its power is that it forms a suitable starting point to obtain approximate solutions. Furthermore the analogy provides a definition of the acoustical field in the presence of a flow. When the right-hand terms in the analogy are negligible we have an homogeneous wave equation. The solution of this equation is determined by initial or boundary conditions (vibrating walls). In such cases we call the flow acoustical. Aero-acoustics is the study of flow conditions in which the right hand side of the analogy is the most important source of sound. We will later consider alternative to this analogy such as the vortex-sound theory.

4 Acoustics of a quiescent fluid

4.1 Wave equation

We now consider the behaviour of small perturbations of a uniform stagnant fluid ($\vec{v}_0 = 0$). We assume that friction and heat transfer are negligible. In that case the linearized mass conservation equation is:

$$\frac{\partial \rho'}{\partial t} = -\rho_0 \frac{\partial v_i'}{\partial x_i} \tag{60}$$

and the corresponding momentum equation is:

$$\rho_0 \frac{\partial v_i'}{\partial t} = -\frac{\partial p'}{\partial x_i} + f_i \ . \tag{61}$$

The energy equation becomes:

$$\frac{\partial s'}{\partial t} = \frac{Q_w}{\rho_0 T_0} \tag{62}$$

and the equation of state (22) can therefore be written as:

$$p' = c_0^2 \rho' + \left(\frac{\partial p}{\partial s}\right)_\rho s' \ . \tag{63}$$

Taking the time derivative of the linearized mass conservation law (60) and subtracting the divergence of the linearized momentum equation (61) we eliminate the velocity v_i'. Using the equation of state (63) we eliminate the density ρ' and obtain:

$$\frac{1}{c_0^2}\frac{\partial^2 p'}{\partial t^2} - \frac{\partial^2 p'}{\partial x_i^2} = \frac{1}{c_0^2}\left(\frac{\partial p}{\partial s}\right)_\rho \frac{\partial^2 s'}{\partial t^2} - \frac{\partial f_i}{\partial x_i} \ . \tag{64}$$

or:

$$\frac{1}{c_0^2}\frac{\partial^2 p'}{\partial t^2} - \frac{\partial^2 p'}{\partial x_i^2} = \frac{1}{\rho_0 c_0^2 T_0}\left(\frac{\partial p}{\partial s}\right)_\rho \frac{\partial Q_w}{\partial t} - \frac{\partial f_i}{\partial x_i} \ . \tag{65}$$

We see that unsteady heat productions and non-uniform force fields are sources of sound. If we neglect those sound sources we have the homogeneous wave equation:

$$\frac{1}{c_0^2}\frac{\partial^2 p'}{\partial t^2} - \frac{\partial^2 p'}{\partial x_i^2} = 0 \ . \tag{66}$$

4.2 Elementary solutions

The homogeneous scalar wave equation (66) satisfies the plane wave solution of d'Alembert:

$$p' = F(\vec{n}\cdot\vec{x} - c_0 t) \tag{67}$$

where $\vec{n}$ is the unit vector in the direction of propagation and F is a function which is determined by initial and boundary conditions. If we consider harmonic waves with a frequency f and a corresponding angular velocity $\omega = 2\pi f$ we can write the solution in the complex notation:

$$p' = A\exp[i(\omega t - \vec{k}\cdot\vec{x})] \tag{68}$$

where A is the amplitude, $\vec{k}$ is the wave vector (in the direction of propagation) and has the magnitude $k_0 = |\vec{k}| = \omega/c_0$. The corresponding velocity field $\vec{v}'$ is obtained by substitution of the solution in the momentum conservation law (61) we find after integration over the time:

$$\vec{v}' = \vec{n}\frac{p'}{\rho_0 c_0} \ . \tag{69}$$

Another elementary solution is a spherical symmetrical wave field with $\vec{y}$ as origin. The mass conservation law can be written as:

$$r^2\frac{\partial \rho'}{\partial t} = -\rho_0\frac{\partial r^2 v_r'}{\partial r} \tag{70}$$

and the radial component of the momentum equation as:

$$\rho_0\frac{\partial v_r'}{\partial t} = -\frac{\partial p'}{\partial r} \tag{71}$$

where $r = |\vec{x} - \vec{y}|$. The corresponding wave equation is:

$$\frac{1}{c_0^2}\frac{\partial^2 r p'}{\partial t^2} - \frac{\partial^2 r p'}{\partial r^2} = 0 \tag{72}$$

for which we have the solution of d'Alembert:

$$p' = \frac{1}{r}[F(r - c_0 t) + G(r + c_0 t)] \ . \tag{73}$$

The function F corresponds to an outgoing wave while G corresponds to a converging wave. In free field conditions there are no converging waves, so that: $G = 0$. For harmonic spherical waves in free space we have the solution:

$$p' = \frac{A}{r} \exp[i(\omega t - k_0 r)] \tag{74}$$

with $k_0 = \omega/c_0$ and where A is an amplitude determined by boundary conditions. The velocity field v'_r is obtained by substitution of the solution (74) into the momentum conservation law (71):

$$v'_r = \frac{p'}{\rho_0 c_0} \left[1 + \frac{1}{ik_0 r}\right] \ . \tag{75}$$

We can distinguish two limit behaviour,

- an incompressible radial flow in the near field $k_0 r << 1$ around the origin:

$$v'_r \sim \frac{1}{r^2} \tag{76}$$

and

- a quasi-plane wave behaviour in the far field $k_0 r >> 1$:

$$v'_r \simeq \frac{p'}{\rho_0 c_0} \ . \tag{77}$$

In the near field the wave propagation effect are negligible and due to the singularity of the solution, in the neighborhood of $r = 0$, the wave equation can locally be approximated by the equation of Laplace $\partial^2 p'/\partial x_i^2 = 0$ which describes an incompressible flow.

In the far field we have:

$$\frac{\partial p'}{\partial r} \simeq -\frac{1}{c_0} \frac{\partial p'}{\partial t} \tag{78}$$

which corresponds to the behaviour of plane waves propagating in the positive r-direction.

4.3 Acoustical energy and acoustical impedance

It is convenient to discuss the acoustical energy generated by a source. If we consider a linear perturbation of a quiescent reference fluid we can use the energy equation derived by Kirchhoff ([65], [76]). We neglect friction and heat transfer. We start from the linearized mass conservation law:

$$\frac{\partial \rho'}{\partial t} + \rho_0 \frac{\partial v'_i}{\partial x_i} = Q_m \ . \tag{79}$$

In this equation we have added a mass source term Q_m which is of course zero if we consider the exact physical situation. The linearized momentum equation for an inviscid flow is:

$$\rho_0 \frac{\partial v'_i}{\partial t} + \frac{\partial p'}{\partial x_i} = f_i \ . \tag{80}$$

We have assumed that the mass injection is carried out in such a way that it is not associated with an injection of momentum. A linear approximation implies of course that both Q_m and f_i should be somehow "small". We eliminate the density fluctuations by using the equation of state $p' = c_0^2 \rho' + \left(\frac{\partial p}{\partial s}\right)_\rho s'$ and equation 62. We obtain:

$$\frac{1}{c_0^2}\frac{\partial p'}{\partial t} + \rho_0 \frac{\partial v_i'}{\partial x_i} = Q_m + \frac{1}{\rho_0 c_0^2 T_0}\left(\frac{\partial p}{\partial s}\right)_\rho Q_w \ . \tag{81}$$

We multiply the mass conservation law by p'/ρ_0 and add the inproduct of the momentum equation with v_i'. We further assume for simplicity that $Q_w = 0$. We find:

$$\frac{\partial E}{\partial t} + \frac{\partial I_i}{\partial x_i} = p' \frac{Q_m}{\rho_0} + v_i' f_i \tag{82}$$

where the acoustical energy E is defined by:

$$E = \frac{1}{2}\frac{(p')^2}{\rho_0 c_0^2} + \frac{1}{2}\rho_0 |\vec{v}'|^2 \tag{83}$$

and the intensity $\vec{I}$ is defined by:

$$I_i = p' v_i' \ . \tag{84}$$

A problem with this equation is that it involves second order quantities in the perturbations p' and v_i', while we used as starting point the linearized conservation laws in which such terms were neglected. It appears after a more careful analysis that this definition of the acoustical energy is correct up to the third order in the perturbations for a quiescent reference state [65]. When the reference fluid is not uniform or there is a mean flow, there is some arbitrariness in the definition of the acoustical field and of the corresponding acoustical energy. Discussions of generalization of the acoustical energy concept are provided by Pierce [90] and Myers [75].

When using the equation for the energy in complex notation one should realize that for harmonic perturbations the average of the acoustical energy $< E >= \frac{1}{T}\int_0^T E dt$, over an oscillation period T, is constant. Hence the acoustical energy equation becomes after averaging over one oscillation period:

$$\frac{\partial < I_i >}{\partial x_i} = < p' \frac{Q_m}{\rho_0} > + < v_i' f_i > \ . \tag{85}$$

When using the complex notation:

$$p' = Re[\hat{p} \exp(i\omega t)] \tag{86}$$

we find for the average of the intensity:

$$< I_i >= \frac{\omega}{2\pi}\int_0^{2\pi/\omega} p' v_i' dt = \frac{\omega}{2\pi}\int_0^{2\pi/\omega} (Re[\hat{p}]\cos\omega t - I_m[\hat{p}]\sin\omega t)(Re[\hat{v}_i]\cos\omega t - I_m[\hat{v}_i]\sin\omega t) dt = \\ = \frac{1}{2}(Re[\hat{p}]Re[\hat{v}_i] + I_m[\hat{p}]I_m[\hat{v}_i]) = \frac{1}{4}[\hat{p}^* \hat{v}_i + \hat{p}\hat{v}_i{}^*] \tag{87}$$

where $\hat{p}^*$ denotes the complex conjugate of the amplitude $\hat{p}$.

We are often interested in the sound radiated out of a control surface S with outer normal n_i. If we assume a locally reacting surface the most general linear boundary condition on the surface is given for harmonic waves by the impedance Z:

$$Z(\omega) = \frac{\hat{p}}{n_i \hat{v}_i} \ . \tag{88}$$

While an impedance condition is easy to implement in the Fourier domain, in the time domain it will in general involve a convolution corresponding to memory effects. In order to stress the fact that the impedance is defined in the Fourier domain we have written $Z(\omega)$.

Using the concept of impedance, we find that:

$$< I_i >= \frac{1}{2} Re[Z] |\hat{v}_i|^2 \ . \tag{89}$$

The real part of the impedance of a surface provides therefore information about acoustical energy transport trough the surface. We call the real part of the impedance the resistance. The imaginary part is an inertance, which induces a phase delay in the reaction of the surface to an imposed acoustical flux. In free space the acoustical impedance of a plane normal to the direction of propagation of a plane wave is $\rho_0 c_0$, we call this the characteristic impedance of the medium.

The integral formulation of equation (85) applied to a control volume V enclosed by a surface S with outer normal $\vec{n}$ is:

$$\int_V \frac{\partial < I_i >}{\partial x_i} dV = \int_S < I_i > n_i dS = \int_V (< p' \frac{Q_m}{\rho_0} > + < v_i' f_i >) dV \ . \tag{90}$$

The right hand side of this equation corresponds to the acoustical power generated by the sources within the control volume V.

4.4 Range of validity of acoustical approximation

Acoustics was originally the study of sound waves propagating in ambient air and having frequencies within the audio-range 20 Hz< f < 20 kHz. We restrict ourselves to this range. The dynamical range of our ear is so large that sound levels are measured on a logarithmic scale. The sound pressure level (SPL), measured in dB, is defined by:

$$SPL = 20 \log_{10} \left(\frac{p'_{rms}}{p_{ref}} \right) \tag{91}$$

with $p_{ref} = 2 \times 10^{-5}$ Pa in gasses ($p_{ref} = 10^{-6}$ Pa in liquids). The reference level corresponds to the threshold of hearing for harmonic sound at $f = 1$ kHz. For ambient pressure

this corresponds to the thermal noise due to fluctuations $\sqrt{N}$ in the average number N of molecules colliding with our hear drum within 0.5 ms ($N = O(10^{20})$). At the threshold of pain $SPL = 120\ dB$ the pressure amplitude is only $p'_{rms} = 20$ Pa. This is a fraction 2×10^{-4} of the atmospheric pressure $p_0 = 10^5$ Pa. It seems therefore quite reasonable to consider a linearized theory. In a liquid the relevant quantity is the ratio of density fluctuation and of mean density $\rho'/\rho_0 = p'/(\rho_0 c_0^2)$, in which $\rho_0 c_0^2$ is the internal pressure of the fluid which determines its compressibility. For plane waves we have following equation (69) $\rho'/\rho_0 = v'/c_0$. So that linearization is allowed when the acoustical Mach number v'/c_0 is small. Typically we have $\rho_0 c_0^2 = 10^9$ Pa in water and $\rho_0 c_0^2 = 10^7$ Pa in liquid alkanes. Hence the linear approximation remains in liquid valid for quite high pressure fluctuations.

If we consider the analogy of Lighthill, in acoustics we neglect the Reynolds stress term $\rho v_i v_j$ this can now be justified by comparing this term in the wave region with the pressure fluctuations p'. Using the plane wave relationship (69) $n_i v'_i = p'/(\rho_0 c_0)$ we find $\rho v_i v_j / p' \sim p'/(\rho_0 c_0^2)$. This seems to justify the fact that we neglect this term in acoustics. One should however be careful, because when considering long distances of propagation even a weak acoustic wave can be significantly disordered by non-linear wave steepening. This is due to the fact that the effective propagation velocity of a simple wave[2] is $n_i v'_i + c$ rather than c_0. At the compression side $p' > 0$ of a wave the velocity $v'_i n_i = p'/(\rho c_o)$ is larger than at the expansion side $p' < 0$ were the convective velocity is opposite to the wave propagation direction. Furthermore as $c = \sqrt{\gamma RT}$ in an ideal gas the speed of sound is larger for $p' > 0$ than for $p' < 0$ [3]. For a plane wave if we neglect visco-thermal dissipation, a shock wave is formed after a distance x_s given by:

$$x_s = \frac{2\gamma p_0 c_0}{(\gamma + 1)\left(\frac{\partial p}{\partial t}\right)_{x=0}} \tag{92}$$

In brass instruments such as trombones the pipe length is typically of the order of x_s at fortissimo playing levels [44]. The shock waves generated at fortissimo level are responsible for the characteristic brassy sound. This effect is enhanced by playing with a longer tube (higher position). Also in mufflers of combustion engines such shock waves are common. The characteristic sounds which they produce are called "rasping sounds". In spherical waves the amplitude decreases proportionally to the distance r of propagation from the origin. Non-linear wave propagation effects are only observed in very strong waves or for very long travel distances. In particular in the propagation of aircraft engine noise in the atmosphere non-linear propagation effects are essential [20].

We assume that the visco-thermal dissipation is negligible. An argument to justify this is the comparison of $(\partial^2 \tau_{ij}/\partial x_i \partial x_j)$ with $(1/c_0^2)(\partial^2 p'/\partial t^2)$. For a plane simple wave we find that the ratio of those terms is of the order of magnitude of $\eta k/(\rho_0 c_0)$. For ambient

[2] Wave propagating without reflection into a uniform region.

[3] $\Delta c/c_0 = (1/2)(\Delta T/T_0) = [(\gamma - 1)/(2\gamma)]\Delta p/p_0$ with $\frac{5}{3} \geq \gamma > 1$ for gases in general and $\gamma = 1.4$ for air in particular.

air we have $\eta/\rho_0 \simeq 1.5 \times 10^{-5} m^2 s^{-1}$, $c_0 \simeq 340 m s^{-1}$. At audio frequencies we have in air $0.3 m^{-1} < k < 3000 m^{-1}$. We therefore have $10^{-8} < \eta k/(\rho_0 c_0) < 10^{-4}$. Viscosity is negligible for propagation over a few acoustical wave length. As $Pr = 0.72$, heat transfer can also be neglected. Hence the flow is in good approximation isentropic $p' = c_0^2 \rho'$. From our simple order of magnitude estimate we see that dissipation will be more important for high frequencies (high values of k) than at low frequencies. This corresponds to our common experience that aircraft noise is dominated by low frequencies when we hear it from large distances (10 km). This is in contrast with the sharp sound which we hear close to the aircraft at the airport.

As mentioned already in section 2.2 this order of magnitude estimate does not take into account deviations from local thermodynamic equilibrium (bulk viscosity effects) which are quite significant [90].

In a pipe, the dissipation is determined by viscothermal dissipation at the walls, which is often much larger than the dissipation in the bulk of the flow. For plane wave propagation in a pipe of cross-sectional area S and of cross-sectional perimeter L_p we have in the range $(S/L_p >> \sqrt{\eta/(\rho_0 \omega)}$ an exponential damping $p' \sim \exp[-\alpha x]$ with ([74], [89], [98]):

$$\alpha = \frac{L_p}{2 S c_0} \sqrt{\frac{\omega \eta}{2 \rho_0}} \left(1 + \frac{\gamma - 1}{\sqrt{Pr}} \right) . \tag{93}$$

For woodwind instruments such as the clarinet, the visco-thermal damping in the pipe is a more important energy loss than sound radiation! For air at atmospheric pressure and room temperature $\frac{\eta}{\rho_0} = 1,5 \times 10^{-5}$ m^2/s. We have for a pipe diameter of 2 cm at 400 Hz a value $\alpha = 0.05$ m^{-1}. So that for a pipe length of 60 cm, the wave losses 7% of its amplitude in one round trip. This means that a frictionless theory is a reasonable first order approximation, but certainly not an accurate theory to describe the acoustical response of such instruments.

4.5 Acoustical field of a harmonically pulsating or translating sphere

As an example of simple acoustical source we consider an harmonically pulsating sphere in free space. The radius a of the sphere is given by:

$$a = a_0 + \hat{a} \exp[i \omega t] \tag{94}$$

We assume that $\omega \hat{a} << c_0$ so that we can applied linear acoustics. The pulsation generates spherical waves (equation (74)):

$$p' = \hat{p} \exp[i \omega t] = \frac{A}{r} \exp[-i k_0 r] \exp[i \omega t] . \tag{95}$$

The corresponding velocity field $\hat{v}_r$ is given by the momentum equation (71):

$$\hat{v}_r = -\frac{1}{i\omega\rho_0}\frac{\partial \hat{p}}{\partial r} \tag{96}$$

which yields equation (75):

$$\hat{v}_r = \frac{\hat{p}}{\rho_0 c_0}\left(1 + \frac{1}{ik_0 r}\right) \ . \tag{97}$$

In linear approximation, we have as boundary condition on the surface of the sphere at $r = a_0$:

$$\hat{v}_r(a_0) = i\omega\hat{a} \ . \tag{98}$$

Substitution in equation (97) in combination with equation (95) yields:

$$\hat{p} = -\frac{\rho_0\omega^2 a_0^2\hat{a}}{r(1 + ik_0 a_0)}\exp[-ik_0(r - a_0)] \ . \tag{99}$$

This corresponds to an impedance seen from the surface of the sphere given by (equation (88)):

$$Z(\omega) = \frac{\hat{p}(a_0)}{\hat{v}_r(a_0)} = \rho_0 c_0 \frac{ik_0 a_0}{1 + ik_0 a_0} = \rho_0 c_0 \frac{(k_0 a_0)^2 + ik_0 a_0}{1 + (k_0 a_0)^2} \ . \tag{100}$$

We see that when the sphere is large compared to the acoustical wave length $k_0 a_0 >> 1$ it acts as a plane wall and sees the characteristic impedance $\rho_0 c_0$ of the surrounding fluid. In the opposite limit $k_0 a_0 << 1$ we have:

$$Z(\omega) = \rho_0 c_0((k_0 a_0)^2 + ik_0 a_0) \ . \tag{101}$$

We see that the real part of the impedance decreases as $(k_0 a_0)^2$ so that a sphere small compared to the acoustical wave length is a very inefficient source of sound. This is due to the fact that the fluid velocity decreases fast $\hat{v}_r \sim r^{-2}$ as we move away from the surface of the sphere. The fluid can easily escape from the compression. Most of the pressure build-up at the surface is simply due to the inertia in an almost incompressible flow $\hat{v}_r \simeq i\omega\hat{a}(a_0/r)^2$. If there is no compression there is no acoustical energy involved because $\hat{p}$ and $\hat{v}_r$ are $\pi/2$ out of phase (equation (87)). Such a body small compared to the acoustical wave length, is called "compact". An example of such a pulsating sphere are the headphones of a portable CD player or iPod. For frequencies corresponding to the most sensitive range of our ears 1 kHz$< f <$ 4 kHz the acoustical wave length is much larger than the loudspeakers. We do not hear those frequencies unless we plug the headphones into our ear. In that case, we literally push directly on the ear-drum through an almost incompressible air cushion. This stresses why this is a very dangerous device.

The inefficiency of compact vibrating objects becomes even more spectacular when we consider oscillatory translation, without change of volume. An elementary example is the translating rigid sphere. We assume that the velocity of the sphere is given by:

$$\vec{v}_s = (U\exp[i\omega t], 0, 0) \tag{102}$$

For comparison with the pulsating sphere we can assume $U = i\omega\hat{a}$, where $\hat{a}$ is the amplitude of the oscillatory movement. The acoustical field around this object is found by considering the spatial derivative of the field around a pulsating sphere taken in the direction x_1 of the translation. This is also a solution of the wave equation because:

$$\frac{\partial}{\partial x_1}\left(\frac{\partial^2 p'}{\partial t^2} - c_0^2\frac{\partial^2 p'}{\partial x_i^2}\right) = \frac{\partial^2}{\partial t^2}\left(\frac{\partial p'}{\partial x_1}\right) - c_0^2\frac{\partial^2}{\partial x_i^2}(\frac{\partial p'}{\partial x_1}) = 0. \tag{103}$$

We have furthermore:

$$\frac{\partial p'}{\partial x_1} = \left(\frac{\partial r}{\partial x_1}\right)\frac{\partial p'}{\partial r} = \frac{x_1}{r}\frac{\partial p'}{\partial r} \tag{104}$$

because $r^2 = x_1^2+x_2^2+x_3^2$ so that $\partial r/\partial x_1 = x_1/r$. For an arbitrary position $\vec{x}$ in space we also have $x_1/r = \cos\theta$, where θ is the angle between the position vector $\vec{x}$ and the x_1 direction. The radial velocity of the sphere surface in direction θ is simply $v_r(a_0) = U\exp[i\omega t]\cos\theta$ (see figure 4). Let us assume that the pressure field $\hat{p}$ is given by:

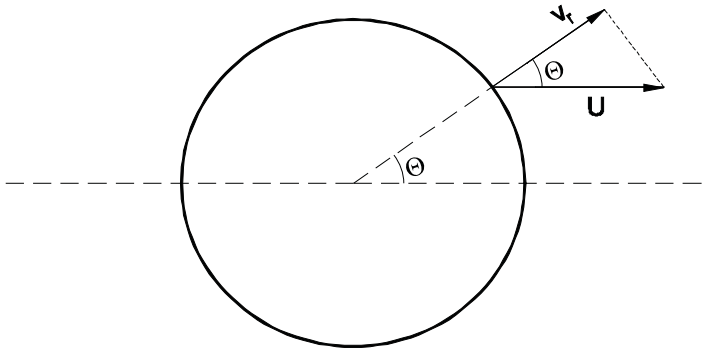

Figure 4: *Velocity normal to the surface of a sphere in the radial direction for a translation* $\vec{v} = (U, 0, 0)$ *in direction* x_1 *is given by* $v_r = U\cos\theta$.

$$\hat{p} = A\cos\theta\frac{\partial}{\partial r}\frac{\exp[-ik_0 r]}{r} \ . \tag{105}$$

We see by substitution of (105) into the radial momentum equation (96), that the velocity dependence of $\hat{v}_r(a_0) = U\cos\theta$ on θ is correct. We find after some algebra the amplitude A:

$$\hat{p} = \frac{-i\omega\rho_0 U a_0^3\cos\theta}{2(1+ik_0a_0) - (k_0a_0)^2}\frac{\partial}{\partial r}\frac{\exp[-ik_0(r-a_0)]}{r} \ . \tag{106}$$

In the limit of a compact sphere $k_0a_0 << 1$ this becomes:

$$\hat{p} = -\frac{1}{2}(k_0a_0)^2\rho_0 c_0 U\frac{a_0\cos\theta}{r}\left(1+\frac{1}{ik_0r}\right)\exp[-ik_0r] \ . \tag{107}$$

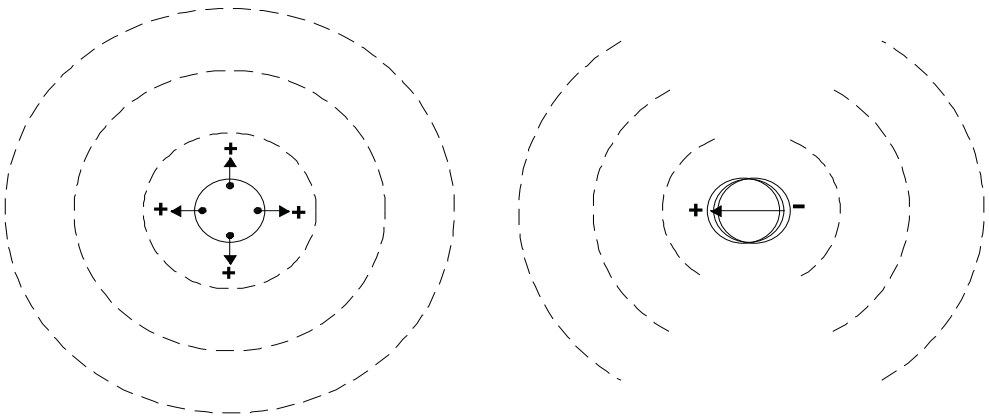

Figure 5: *Sound fields of pulsating and of translating spheres.*

The corresponding acoustical impedance at the surface of the sphere is:

$$Z(\omega) = \frac{\hat{p}}{\hat{v}_r} \simeq \frac{1}{4}\rho_0 c_0 \left[2ik_0a_0 + i(k_0a_0)^3 + (k_0a_0)^4\right] \ . \tag{108}$$

and the radiated power $< P >$ is given by:

$$< P >= \int_S < I_i > n_i dS = \frac{4\pi}{3} a_0^2 \frac{1}{2} Re[z] U^2 = \frac{\pi}{6} a_0^2 (k_0a_0)^4 U^2 \ . \tag{109}$$

We see that the radiated acoustical power is proportional to $(k_0a_0)^4$, which is a very weak sound source!

The fact that the acoustic field of a sphere in oscillatory translation is the spatial derivative of the field found for a pulsating sphere can be understood intuitively. The fluid displaced at the front of the sphere can be though as being produced: a mass source. At the same time the rear part of the sphere acts as a mass sink of equal strength. In principle the acoustical field produced by the two sources would exactly cancel out in the far field if there was no difference in travel time of the waves from the sources to the listener. This difference in travel distance scales as $a_0 \cos\theta$ (see figure 5). When looking in the direction normal to the translation $\theta = \pi/2$ the two waves do indeed exactly cancel. The maximum of sound radiation is in the direction of the translation. The real part of the impedance is an order of magnitude $(k_0a_0)^2$ lower than for a pulsating sphere because the radiated energy scales as the square of the pressure fluctuations in the far field $< I_r > \sim |\hat{p}|^2/\rho_0 c_0$. The limit process of taking the derivative of the pressure field corresponds furthermore to the definition of a dipole: two sources of strength $\pm\dot{m} = \int_{V^\pm} Q_m dV$ placed at a distance δ from each other, which we consider in the limit $(\lim_{\delta\to 0} \dot{m}\delta)$ constant. To leading order the far field of a pulsating compact object is described by a localized point source which we call a "monopole". Following the same nomenclature the far field of a rigid translating compact

body is dominated by the "dipole" component of the field. If however we consider a tuning fork, with two stems oscillating in opposite phase, the dipole term will cancel and we have a "quadrupole". Those concepts are illustrated in figures 6 and 7. In figure 7 we consider

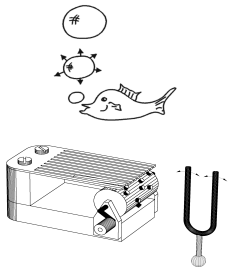

Figure 6: *Examples of object generating respectively monopole, dipole and quadrupole fields, respectively: an oscillating bubble will change volume and create a monopole field, the vibrating stem of a musical box and the vibrating tunning fork.*

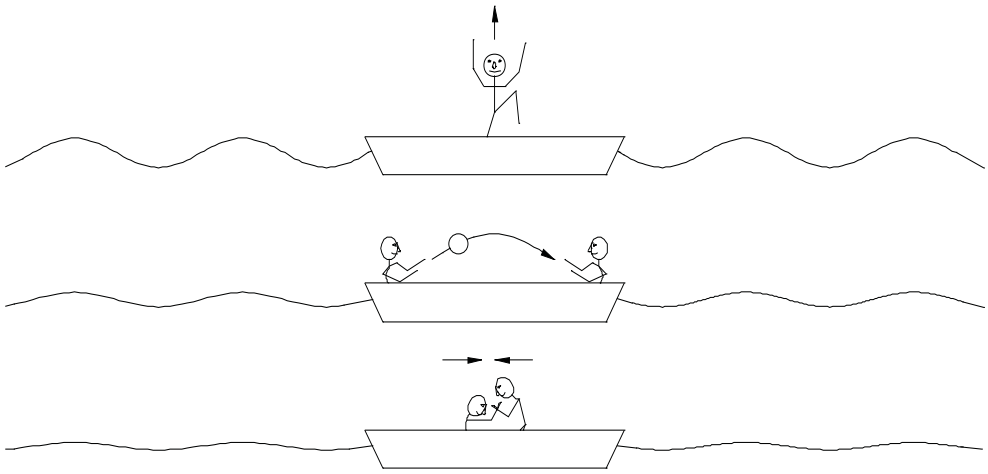

Figure 7: *Monopole, dipole and quadrupole sources for water waves.*

the surface waves generated by a small boat. When a person is jumping up and down in the boat, the immersed volume varies and circular waves are generated around the boat. This corresponds to a monopole field. When two persons play with a ball on the boat, the reaction to the impulse they give to the ball drives a translation of the boat which generates a dipole field. When two persons are fighting in the boat we expect a quadrupole field.

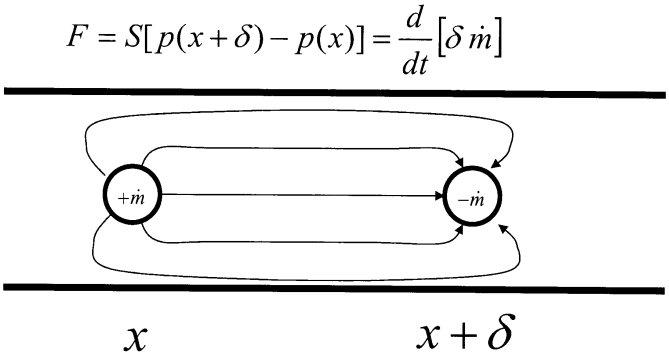

Figure 8: *An acoustical dipole is associated with an oscillatory exchange of mass between a source and a sink which is not possible without an external force acting on the flow.*

The fact that the dipole field is associated with a force field is very fundamental. This can be understood when considering two volume sources placed within a pipe of cross-sectional area S at a distance δ from each other. As illustrated in figure 8, the momentum of the fluid between the two sources is approximatively $\dot{m}\delta = \rho v_1 S\delta$. For an harmonic oscillation of this momentum an external force $F_1 = d\dot{m}\delta/dt$ is needed. Hence such a dipole field is always associated with a force acting on the fluid.

In the analogy of Lighthill (59) we indeed see that the source term corresponding to an external force field f_i has the character of a divergence $\partial f_i/\partial x_i$ and therefore is a dipole field. We also note that a uniform force field does not produce sound because $\frac{\partial f_i}{\partial x_i} = 0$ in such a case.

The second order derivatives $\partial^2 \rho v_i v_j/\partial x_i \partial x_j$ will correspond to a quadrupole. The term $\partial^2[(p'/c_0^2) - \rho']/\partial t^2$ is a monopole field. We will discuss the mathematical aspects of this nomenclature more in detail after we have introduced the Green's function and the integral formulation of the problem.

Before leaving this informal approach to the subject we would like to stress again the importance of the ratio $(k_0 a_0)$ of the dimension of a source compared to the acoustical wave length. We call this the compactness of the source. To illustrate this we consider in figure 9 the experiment of making waves with our hand at the water surface in a bath-tub. We all know that if we move our hand very slowly, the water pushed at the front will simply move around the hand towards the back without any significant production of wave. The water escapes the "compression". However when we move our hand fast, we can make beautiful waves. By increasing the oscillation frequency we make the wave length of the surface waves comparable to the size of our hand and increase $(k_0 a_0)$.

If we do not want to increase the frequency we should use a large plate to make water

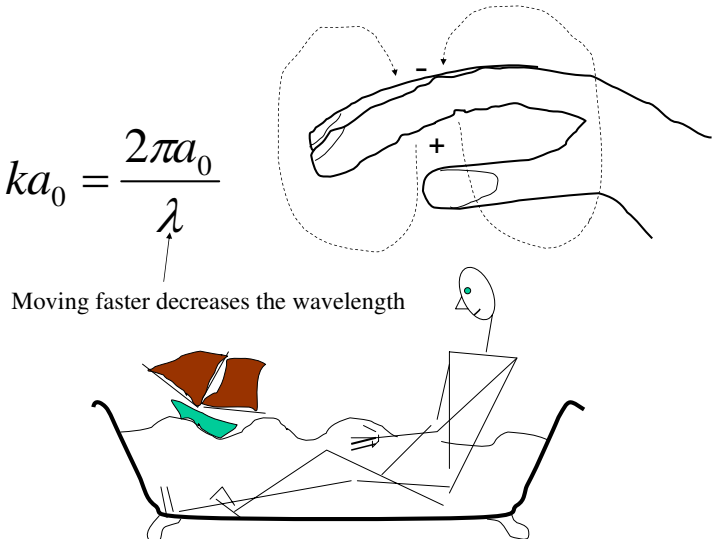

Figure 9: *Making waves.*

waves. This is exactly what we do when we listen to the sound of a tuning fork by pushing it against a table. A minute fraction of the vibration energy is transferred to the table. As this vibrating surface is large compared to the acoustic wave length (85 cm) the table is a very effective acoustical radiator.

Strings of musical instruments do not radiate sound, they transfer vibration energy to a body (violin, guitar,...) or a table of harmony (piano,...) which takes care of the sound production. Typical in such instruments is that the pitch is determined by an oscillator (string) which does not radiate sound. In woodwind instruments, the resonator which determines the pitch (pipe) is also the radiator. However the oscillator and string functions are separated by the fact that the oscillation occurs at low frequencies (10^2Hz). Those low frequency waves are kept in the pipe and form standing waves. Those standing waves drive the oscillation of the instrument and determine the pitch. The sound which we hear is dominated by much higher frequencies (10^3 Hz) which are very efficiently radiated at the pipe exit. We will show later (section 5.4) that this separation in low and high frequency behaviours is due to the fact that the impedance of an open pipe termination is essentially that of a monopole. The real part of the impedance of an open pipe termination is $Re(z) \simeq (k_0 a_0)^2/4$ (where a_0 is the radius of the pipe cross-section).

4.6 Green's function and integral formulation

In the previous section we considered the sound field generated by a pulsating sphere. We called the acoustical field of a compact sphere a monopole field. We now consider the limit of a point source. We call the sound field $G(\vec{x}, t|\vec{y}, \tau)$ observed at $(\vec{x}, t)$ which has been generated by a pulse $\delta(\vec{x} - \vec{y})\delta(t - \tau)$ released at position $\vec{y}$ and time τ, a Green's function.

The delta function $\delta(x)$ is a generalized function defined by the property:

$$\int_{-\infty}^{\infty} F(x)\delta(x)dx = F(0) \tag{110}$$

for any well behaving function $F(x)$. The Green's function is a generalized function which satisfies the non-homogeneous wave equation:

$$\frac{1}{c_0^2}\frac{\partial^2 G}{\partial t^2} - \frac{\partial^2 G}{\partial x_i^2} = \delta(\vec{x}-\vec{y})\delta(t-\tau) \tag{111}$$

where $\delta(\vec{x}-\vec{y}) = \delta(x_1-y_1)\delta(x_2-y_2)\delta(x_3-y_3)$. The Green's function should satisfy the causality conditions $G = 0$ and $\partial G/\partial t = 0$ for any time t smaller than τ, because the source has not yet been fired (initial conditions $t \leq \tau$). The Green's function is further determined by the linear boundary conditions which we impose. Those boundary conditions can correspond to those of the actual acoustical field. In such a case we called it a "tailored" Green's function. This however is not necessary.

Using Green's theorem the solution of the wave equation:

$$\frac{1}{c_0^2}\frac{\partial^2 p'}{\partial t^2} - \frac{\partial^2 p'}{\partial x_i^2} = q(\vec{x},t) \tag{112}$$

can be written in the integral form:

$$p'(\vec{x},t) = \int_{-\infty}^{t^+}\int_V q(\vec{y},\tau)G(\vec{x},t|\vec{y},\tau)dV_y d\tau - \int_{-\infty}^{t^+}\int_S [p'\frac{\partial G}{\partial y_i} - G\frac{\partial p'}{\partial y_i}]n_i dS_y d\tau \tag{113}$$

where n_i is the outer normal on the surface S enclosing the volume V. Please note that in the derivation of this integral equation we made use of the reciprocity relationship has been used [74]. Due to the symmetry of the wave operator and of the delta functions with respect to an exchange of source and listener position we have the general reciprocity principle:

$$G(\vec{x},t|\vec{y},\tau) = G(\vec{y},-\tau|\vec{x},-t)\ . \tag{114}$$

When we exchange the listener and source position the listener time becomes $-\tau$ and the source time $-t$ because we want to keep the time difference $|t-\tau|$ constant but we have to respect the causality condition (observer time greater than source time) [4]. We have $-\tau > -t$ because $t > \tau$. In some cases, the reciprocity principle is very convenient to calculate a Green's function. When we release a sound wave from the far field towards a complex compact object, we are considering the interaction of a plane wave (locally parallel flow) with the object. The acoustical pressure found at a point near the object is the Green's function for a source placed at that point and a listener in the far field(provided

[4] In the presence of a main flow, the direction of this flow has to be inverted in order to keep the travel time of the waves constant when we exchange source and listener position. This leads to the concept of reversed flow Green's function introduced by Howe [51].

we have released a unit pulse). As the acoustical field is an inviscid flow we can use the potential flow theory for incompressible flow in order to obtain the flow around a compact object. This is much easier than calculating first the exact Green's function for a point near the object and then consider the far field approximation of this solution. Howe [51] calls this approximation of the Green's function the low frequency Green's function.

The integral formulation is equivalent to the original differential equation but shows the contribution of initial and boundary conditions explicitly. When the Green's function is tailored the surface integral vanishes, because it satisfies on S the same linear boundary conditions as p'. When we use a different boundary condition for the Green's function and p', the surface integral represents the effect of reflections of the Green's function at the surface.

We often will use the free space Green's function G_0. In order to calculate G_0 we use the Fourier transform:

$$G_0 = \int_{-\infty}^{\infty} \hat{G}_0 \exp[i\omega t] d\omega \tag{115}$$

and its inverse:

$$\hat{G}_0 = \frac{1}{2\pi} \int_{-\infty}^{\infty} G_0 \exp[-i\omega t] dt \ . \tag{116}$$

We known that the source is not directive and we expect therefore spherical symmetric waves:

$$\hat{G}_0 = \frac{A}{r} \exp[-ik_0 r] \tag{117}$$

where:

$$r = |\vec{x} - \vec{y}| \ . \tag{118}$$

Integrating the wave equation (111) over a spherical volume V of radius R around the source position $\vec{y}$ yields:

$$\int_V (k_0^2 \hat{G}_0 + \frac{\partial^2 \hat{G}_0}{\partial x_i^2}) dV_x = -\frac{1}{2\pi} \exp[-i\omega\tau] \tag{119}$$

in which we used $\int_{-\infty}^{\infty} \delta(t-\tau) \exp[-i\omega t] dt = \exp[-i\omega\tau]$ and $k_0 = \omega/c_0$. The first term in the integral is of order $(k_0 R)^2$ and can be made negligible by choosing a compact control volume [5]. Applying the theorem of Gaus $\int_V \nabla \cdot (\nabla G) dV_x = \int_S (\nabla G) \cdot \vec{n} dS$ and using the symmetry of the solution and $(\partial \hat{G}_0 / \partial x_i) n_i \simeq -A/R^2$:

$$\int_V \frac{\partial^2 \hat{G}_0}{\partial x_i^2} dV_x = \int_S \frac{\partial \hat{G}_0}{\partial x_i} n_i dS_x \simeq -4\pi R^2 \left(\frac{A}{R^2} \right) = -4\pi A \tag{120}$$

we find:

$$\hat{G}_0 = \frac{\exp[-i\omega(\tau + \frac{r}{c_0})]}{8\pi^2 r} \ . \tag{121}$$

[5] This of course is the advantage of considering a Fourier component $\hat{G}_0$, because we do know the corresponding wave number k_0 and can define such a compact volume.

The Fourier inversion of equation (121) yields:

$$G_0 = \frac{\delta(\tau - t_e)}{4\pi r} \ . \tag{122}$$

where t_e is the emission time:

$$t_e = t - \frac{r}{c_0} \tag{123}$$

it is the time at which the sound that we hear now (at t in $\vec{x}$) has been emitted at position $\vec{y}$. We note that as the Green's function G_0 is only dependent on $r = |\vec{x} - \vec{y}|$ it satisfies the symmetry property:

$$\frac{\partial G_0}{\partial x_i} = -\frac{\partial G_0}{\partial y_i} \tag{124}$$

because $\partial r/\partial x_i = (x_i - y_i)/r = -\partial r/\partial y_i$. In words we see that in free space moving the gun used to release the pulse towards the listener is equivalent to moving the listener in opposite direction, towards the gun.

In general a Green's function does not satisfy such a simple symmetry relationship.

4.7 Multipole expansion

As a first example of the use of Green's function we propose now a more formal discussion of the concepts of monopole, dipole and quadrupole which we have introduced intuitively in section 4.5. We consider in free space a compact source region $q(\vec{y}, \tau) \neq 0$ around $\vec{y} = 0$ and an observer in the far field $kr >> 1$. The formal solution:

$$p'(\vec{x}, t) = \int_{-\infty}^{t^+} \int_V q(\vec{y}, \tau) G_0(\vec{x}, t|\vec{y}, \tau) dV_y d\tau \tag{125}$$

can be approximated by expanding G_0 in a Taylor series around the origin $\vec{y} = 0$:

$$\begin{aligned} p'(\vec{x}, t) &= \int_{-\infty}^{t^+} \int_V q(\vec{y}, \tau) G_0(\vec{x}, t|0, \tau) dV_y d\tau \\ &+ \int_{-\infty}^{t^+} \int_V q(\vec{y}, \tau) (\frac{\partial G_0}{\partial y_i})_{\vec{y}=0} y_i dV_y d\tau \\ &+ \int_{-\infty}^{t^+} \int_V q(\vec{y}, \tau) \frac{1}{2} [\frac{\partial^2 G_0}{\partial y_i \partial y_j}]_{\vec{y}=0} y_i y_j dV_y d\tau + ... \end{aligned} \tag{126}$$

in which:

$$\begin{aligned} \frac{\partial^2 G_0}{\partial y_i \partial y_j} y_i y_j &= \frac{\partial^2 G_0}{\partial y_1^2} y_1^2 + \frac{\partial^2 G_0}{\partial y_2^2} y_2^2 + \frac{\partial^2 G_0}{\partial y_3^2} y_3^2 \\ &+ 2\frac{\partial^2 G_0}{\partial y_1 \partial y_2} y_1 y_2 + 2\frac{\partial^2 G_0}{\partial y_2 \partial y_3} y_2 y_3 + 2\frac{\partial^2 G_0}{\partial y_3 \partial y_1} y_3 y_1 \ . \end{aligned} \tag{127}$$

Using the symmetry relationship (124) we can replace all the derivative with respects to the source coordinate by derivatives with respect to the listener coordinate $\partial G_0/\partial y_i = -\partial G_0/\partial x_i$. As the integration is carried out over the source coordinate we can take the space derivative with respect to the listener coordinate out of the integral. Furthermore we use the far field approximation $\partial/\partial x_i \simeq -\partial/c_0\partial t$ (equation (78)). Using the filter property of the delta function in the Green's function (122) we can carry out the time integration to obtain:

$$\begin{aligned} p'(\vec{x},t) &\simeq \frac{1}{4\pi|\vec{x}|}\int_V q(\vec{y},t_e)dV_y \\ &+ \frac{x_i}{4\pi|\vec{x}|^2}\frac{\partial}{c_0\partial t}\int_V q(\vec{y},t_e)y_i dV_y \\ &+ \frac{x_i x_j}{4\pi|\vec{x}|^3}\frac{\partial^2}{c_0^2\partial t^2}\int_V q(\vec{y},t_e)\frac{y_i y_j}{2}dV_y + ... \end{aligned} \tag{128}$$

where $t_e = t - |\vec{x}|/c_0$ is the emission time. The first term corresponds to a concentration of the source into a monopole. The second term is the dipole correction. The third term is the quadrupole correction. It is easily verified that for a spatially limited source region in which $q = -\partial f_i/\partial x_i$, the monopole source term vanishes because the integral $\int_V(\partial f_i/\partial x_i)dV = \int_S(f_i n_i)dS = 0$ when S is a surface enclosing the source region on which $f_i = 0$. In that case the dipole becomes the leading order term.

It seems now quite obvious that non-linear convective terms and viscous stress correspond in the analogy of Lighthill to a quadrupole field ($\partial^2(\rho v_i v_j - \tau_{ij})/\partial x_i \partial x_j$), external forces to a dipole field ($-\partial f_i/\partial x_i$) and deviations from an isentropic flow correspond to a monopole field ($\partial^2((p'/c_0^2) - \rho')/\partial t^2$). A typical entropy fluctuation is found in unsteady combustion. The change in rate of the expansion of the gasses due to the unsteadiness of the combustion is clearly a monopole sound source. We should however be very careful. Entropy differences do not always result into monopole fields. A careful analysis by Morfey [72] and Obermeier [84] has shown that in a hot air jet in cold air the heat transfer does not result into a monopole sound source because it is not associated to a net volume change. A monopole field is only found when the gas in the jet has a different Poisson ratio γ than the surrounding gas. The problem of the interpretation of the source terms, is illustrated by considering an alternative formulation of Lighthill's analogy. Starting from the exact equation (55) we could had written a wave equation for the density perturbations ρ' rather than for the pressure perturbations p'. In order to do that we add on both sides of the equation the term $-c_0^2\partial^2\rho'/\partial x_i^2$. We would then had obtained the equally exact form of the analogy of Lighthill:

$$\frac{\partial^2\rho'}{\partial t^2} - c_0^2\frac{\partial^2\rho'}{\partial x_i^2} = \frac{\partial^2(\rho v_i v_j - \tau_{ij})}{\partial x_i \partial x_j} - \frac{\partial f_i}{\partial x_i} + \frac{\partial^2(p' - c_0^2\rho')}{\partial x_i^2} \tag{129}$$

in which the deviation from the isentropic behaviour has now a quadrupole character...!

We have reached the roots of "aero-acoustics". As long as we consider analogies as exact equations any variable can be used to describe the acoustical field. They are all equivalent. However then the analogy is simply a reformulation of the exact conservation law which must be completed with all the other equations discussed in section (2). It does not provide new information by itself. We use the analogies to introduce approximations. In that case we see that depending of the type of application considered a certain variable will provide a better basis for an intuitive approach than another. Clearly, when considering sound production by unsteady combustion, we should use p' rather than ρ'. When considering the sound produced by bubbly liquid the density fluctuations ρ' will provide more insight than the pressure fluctuations p'. We will see later that when we consider the sound produced by vortices the fluctuation in total enthalpy B' has some advantages as aero-acoustical variable.

4.8 Doppler effect

We can use the Green's function formalism to determine the effect of the movement of a source on the radiated acoustical field. We consider a point source (a monopole):

$$q(\vec{x},t) = Q(t)\delta(\vec{x} - \vec{x}_s(t)) \tag{130}$$

where $\vec{x}_s(t)$ is the position of the source. For free field conditions we have:

$$p'(\vec{x},t) = \int_{-\infty}^{t^+} \int_V \frac{Q(\tau)\delta(\vec{y} - \vec{x}_s(\tau))\delta(\tau - t_e)}{4\pi|\vec{x} - \vec{y}|} dV_y d\tau \tag{131}$$

with $t_e = t - |\vec{x} - \vec{y}|/c_0$. After carrying the spatial integration we find:

$$p'(\vec{x},t) = \int_{-\infty}^{t^+} \frac{Q(\tau)\delta(t - \tau - \frac{|\vec{x} - \vec{x}_s(\tau)|}{c_0})}{4\pi|\vec{x} - \vec{x}_s(\tau)|} d\tau \ . \tag{132}$$

This is an integral of the type:

$$\int_{-\infty}^{\infty} F(\tau)\delta(H(\tau))d\tau = \frac{F(t_e)}{|\frac{dH}{d\tau}|_{\tau=t_e}} \tag{133}$$

where $\tau = t_e$ correspond to roots of $H(\tau) = 0$ [6]. We assume for simplicity only a single root. The factor $|dH/d\tau|$ is due to the change of variable from τ to $H(\tau)$ needed to apply the property of the delta function (110). The absolute value corresponds to the change in sign of the boundaries of the integral when $dH/d\tau < 0$. In the particular case considered we have:

$$H(\tau) = t - \tau - \frac{|\vec{x} - \vec{x}_s(\tau)|}{c_0} \tag{134}$$

so that:

$$\frac{dH}{d\tau} = -1 + \frac{(x_i - x_{si})}{c_0|\vec{x} - \vec{x}_s|}\frac{dx_{si}}{d\tau} \tag{135}$$

[6] With $F(\tau) = Q(\tau)/(4\pi|\vec{x} - \vec{x}_s(\tau)|)$

or:

$$\frac{dH}{d\tau} = -1 + M_r \tag{136}$$

where M_r is the ratio of the component of the instantaneous velocity in the direction of the observer to the speed of sound: the relative Mach number. We can therefore write for the acoustic field:

$$p'(\vec{x}, t) = \frac{Q(t_e)}{4\pi r|1 - M_r(t_e)|} \tag{137}$$

where the emission time t_e is the solution of the equation:

$$c_0(t - t_e) = |\vec{x} - \vec{x}_s(t_e)| \tag{138}$$

and $r = |\vec{x} - \vec{x}_s(t_e)|$.
It can be shown that for subsonic flows, this equation has a single root. When the source moves supersonically along a curved path multiple solution can occur. In particular for a curved path all the sound emitted along the path can reach the listener at a focal point at the same time, this leads to the occurrence of super "bangs" of aircrafts [54].

The factor $|1 - M_r|^{-1}$ is called the Doppler effect. For a monopole sound source we see that the amplitude of the sound reaching the listener is multiplied by the Doppler factor. The frequency heard by the listener corresponds to $d\omega t_e/dt$. From equation (138) we find:

$$c_0(1 - \frac{dt_e}{dt}) = -\frac{(x_i - x_{si}(t_e))}{|\vec{x} - \vec{x}_s(t_e)|}\frac{dx_s}{dt_e}\frac{dt_e}{dt} \tag{139}$$

or:

$$\frac{dt_e}{dt} = \frac{1}{1 - M_r(t_e)} \tag{140}$$

we see that for a source with a constant frequency ω the listener will hear a frequency multiplied by a Doppler factor.

Considering a compact object of volume V the sound source corresponding to the time dependence of V and its path $x_s(t)$ is the monopole:

$$q\left(\vec{x}, t\right) = \frac{\partial^2}{\partial t^2} V \delta\left(\vec{x} - \vec{x}_s(t)\right) \ .$$

The corresponding acoustical field is given by taking $Q = V$ and taking the second derivative of (137):

$$p'\left(\vec{x}, t\right) = \frac{\partial^2}{\partial t^2}\left(\frac{V(t_e)}{4\pi r|1 - M_r(t_e)|}\right)$$

which implies that for Mach numbers close to unity, the movement of an object with a fixed volume V produces sound. In the far field approximation for $M_r < 1$ we have:

$$p'(\vec{x}, t) = \frac{V}{4\pi r(1 - M_r)^4}\left\{\frac{d^2 M_r}{dt_e^2} + \frac{\left(\frac{(dM_r)}{dt_e}\right)^2}{|1 - M_r|}\right\} \ .$$

We call this thickness sound.

Another example is a moving point force:

$$f_i = F_i(t)\delta(\vec{x} - \vec{x}_s(t)) \tag{141}$$

which correspond to the source:

$$q = -\frac{\partial f_i}{\partial x_i} \tag{142}$$

and the acoustical field:

$$p'(\vec{x},t) = -\int_{-\infty}^{t^+}\int_V \frac{\partial F_i(\tau)\delta(\vec{y} - \vec{x}_s(\tau))}{\partial y_i}\frac{\delta(t - \tau - \frac{|\vec{x}-\vec{y}|}{c_0})}{4\pi|\vec{x} - \vec{y}|}dV_y d\tau \ . \tag{143}$$

Partial integration and using the symmetry property of the Green's function (114) and integrating over space yields:

$$p'(\vec{x},t) = -\frac{\partial}{\partial x_i}\int_{-\infty}^{t^+} F_i(\tau)\frac{\delta(t - \tau - \frac{|\vec{x}-\vec{x}_s(\tau)|}{c_0}}{4\pi|\vec{x} - \vec{x}_s(\tau)|}d\tau \tag{144}$$

or:

$$p'(x,t) = -\frac{\partial}{\partial x_i}\left(\frac{F_i(t_e)}{4\pi r|1 - M_r(t_e)|}\right) \ . \tag{145}$$

In the far field approximation we obtain:

$$p'(\vec{x},t) = +\frac{x_i - x_{is}(t_e)}{|\vec{x} - \vec{x}_s(t_e)|}\frac{\partial}{c_0\partial t}\left[\frac{F_i(t_e)}{4\pi|\vec{x} - \vec{x}_s(t_e)| \cdot |1 - M_r(t_e)|}\right] \tag{146}$$

which involves higher powers of the Doppler factor dt_e/dt. Even when a source is moving at a uniform velocity, the Doppler effect can be quite complex depending on the nature of the source. An example is the sound radiation of a pulsating sphere moving at a uniform velocity. Dowling [28] finds a Doppler factor for the amplitude of the radiated sound $(1 - M_r)^{-7/2}$!

In free jets, sound is produced by the interaction of vortices which are convected with the main flow. This results into a significant increase of radiated power in the streamwise direction compared to the upstream direction.

4.9 Influence of walls

Walls have a considerable effect on the radiation of sound. Before we consider the acoustics of internal flows (next section), we discuss as an introduction the effect of plane walls. We start by considering the radiation of a monopole sound source placed at a distance h from an infinitely extended rigid impermeable wall with outer normal $\vec{n}$. In the acoustical

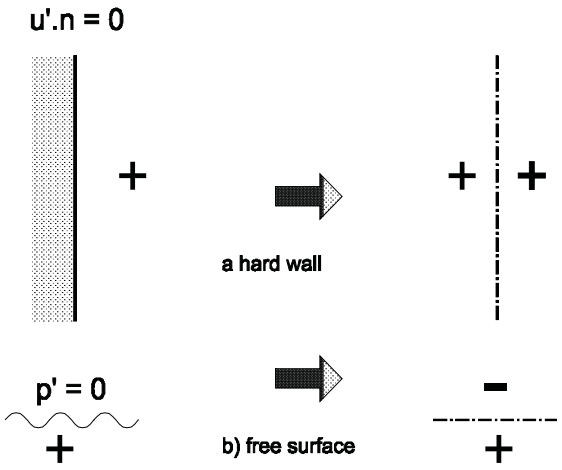

Figure 10: *Method of images applied to a monopole and a rigid wall. A rigid wall doubles the radiated power when* $k_0 h << 1$.

approximation the flow is inviscid, which implies that while the normal component $\vec{v} \cdot \vec{n}$ vanishes at the wall the tangential component is arbitrary. Such a flow can easily be constructed by using the method of images. We replace the actual problem with wall by the flow induced in free space by the monopole plus its image in the wall (figure 10). By reason of symmetry, in the plane of the wall the normal velocity component will vanish. If we now consider a listener in the far field, he will hear a superposition of the direct wave and the reflected wave (coming from the image). If the distance h is small compared to the wave-length ($k_0 h << 1$) there will be a constructive interference and the pressure $p'(\vec{x}, t)$ will be twice the pressure found without wall. As the intensity radiated scales as $< |\vec{I}| > \sim < |p'|^2 >$ the power radiated $P = \int_S \vec{I} \cdot \vec{n} dS$ will increase by a factor two. The intensity is increased by a factor four but we radiate in half the universe, instead of the whole free space. The increase in radiated power indicates clearly that the acoustical power generated by a source is not only determined by the source but also by the radiation impedance which it experiences. The work W performed by a volume injection at the rate $\frac{dV}{dt}$ depends on the pressure build-up around the injection point: $W = \int p' dV$. For an harmonic time dependence we have:

$$< P >= \frac{\omega}{2\pi} \int_0^T p' \frac{dV}{dt} dt \ . \tag{147}$$

The pressure generated by the image doubles the acoustical pressure around the source and therefore the power generated by the source. The presence of the wall makes it easier to compress the air as it is easier to catch a fish swimming close to the bottom of the river then far from the bottom. We leave as an exercise to the reader to calculate the effect of placing a monopole sound source in a 90^o corner between two rigid walls (figure (11)). Further reduction of the radiation angle to increase the radiated power is what we

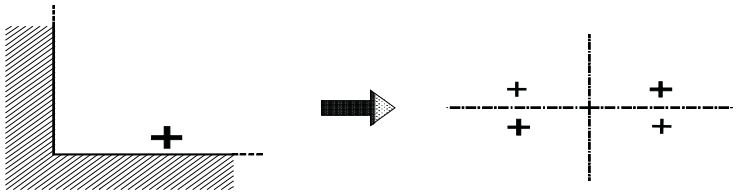

Figure 11: *Monopole in a corner.*

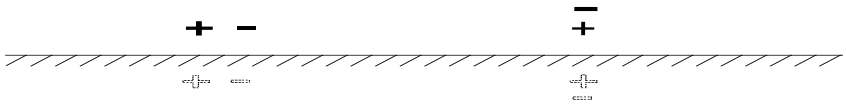

Figure 12: *Effect of a wall on dipole radiation depends on its orientation.*

do when we place our hands around our mouth (forming a horn) to shout more efficiently. The extreme case of shouting in a tube will be discussed in the next section.

Of course the impedance which a source needs in order to be efficient, depends on the nature of the source. If we consider a dipole close to a rigid wall, we have to distinguish the case of a dipole normal to the wall from the case of a dipole parallel to the wall. As shown in figure (12) the dipole normal to the wall will form with its image a quadrupole. It will therefore have a much weaker radiation than in free space. This is can be understood when we realize that such a dipole is generated by a point force $\vec{F}$. In order to perform work this force needs a fluid displacement $W = \int \vec{F} \cdot d\vec{x} = \int \vec{F} \cdot \vec{v} dt$. The acoustical power produced by a harmonic source is $< P >= (\omega/2\pi) \int \vec{F} \cdot \vec{v} dt$. As $\vec{v} \cdot \vec{n} = 0$ at the wall the dipole normal to the wall cannot radiate efficiently. The dipole placed parallel to the wall, will however see a doubling of the local flow velocity and this doubles the radiated power (figure (12)).

In a similar way when a monopole is placed close to a surface of constant pressure $p' = 0$, it will have trouble to radiate. This explains why we do not hear much when a fish comes to the surface and tries to speak to us.

4.10 Influence of a compact body on radiation

Sound production by turbulence in free space appears to have a quadrupole character corresponding to the source term $(\partial^2 \rho v_i v_j / \partial x_i \partial x_j)$ in the analogy of Lighthill (59). This is at low Mach numbers a very weak sound source. Usually the sound production is dominated by the effect of walls on the radiation. We can obtain a qualitative insight into this effect by considering a quadrupole sound source near a rigid compact cylinder. We can apply

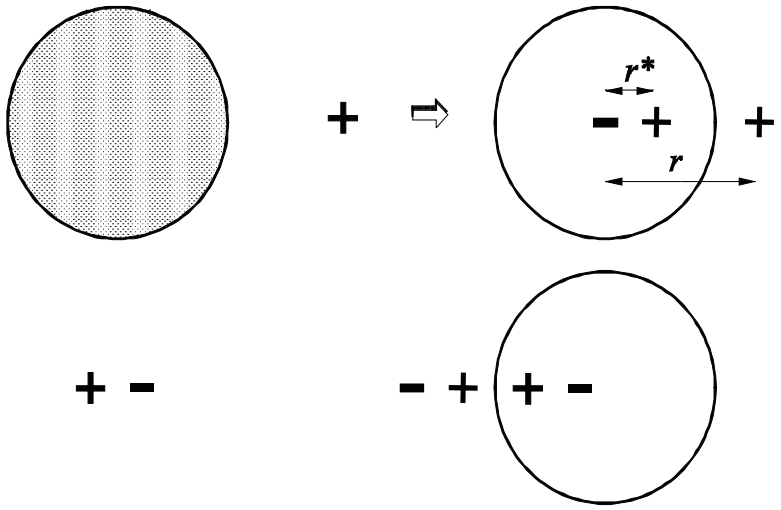

Figure 13: *Effect of a cylinder on the radiation of a monopole and of a quadrupole.*

the method of images to construct the resulting field. The acoustical flow field is locally incompressible and we can apply the circle theorem of Milne-Thomson [69]. As shown in figure 13 the image of a monopole sound source q placed at a distance r from the axis of a cylinder of radius R is an equal monopole q placed at the inverse point on the same radius as the original source, at a distance $r' = R^2/r$ from the axis. In order to satisfy the no-flow condition through the walls we have a second image of opposite strength $-q$ placed on the axis of the cylinder. In figure 13 we show an axial quadrupole consisting of a dipole near the surface and a dipole far away. The image of the first dipole will form with its original a quadrupole. The image of the second dipole will however be weak because of the effect of the inversion. Hence this second dipole will now radiate independently of the first.

This explains qualitatively the influence of wall curvature on sound radiation. We therefore understand why sharp edges strongly enhance turbulent sound radiation. This occurs for example at the trailing edge of a wing profile (wind turbines, aircrafts, ventilators, ...) or at our teeth (fricative sound production in speech).

We now propose a more formal approach [24] to understand this result. We start from the analogy of Lighthill (129) in which we neglected external forces $f_i = 0$:

$$\frac{1}{c_0^2}\frac{\partial^2 \rho'}{\partial t^2} - \frac{\partial^2 \rho'}{\partial x_i^2} = \frac{1}{c_0^2}\frac{\partial^2 T_{ij}}{\partial x_i \partial x_j} \ . \tag{148}$$

with:

$$T_{ij} = \rho v_i v_j - \tau_{ij} + (p' - c_0^2 \rho')\delta_{ij} \ . \tag{149}$$

In the integral formulation (113) this becomes:

$$\begin{aligned} p' &= c_0^2 \rho' = \int_{-\infty}^{t^+} \int_V \frac{\partial^2 (T_{ij})}{\partial y_i \partial y_j} G(\vec{x}, t | \vec{y}, \tau) dV_y d\tau \\ &- c_0^2 \int_{-\infty}^{t^+} \int_S \left[\rho' \frac{\partial G}{\partial y_i} - G \frac{\partial \rho'}{\partial y_i} \right] n_i dS_y d\tau \ . \end{aligned} \tag{150}$$

We made use here of the fact that at the listener position $p' = c_0^2 \rho'$.
The partial derivatives in the volume integral can be moved from the source to the Green's function by partial derivation:

$$\begin{aligned} p' &= \int_{-\infty}^{t^+} \int_V \frac{\partial^2 G}{\partial y_i \partial y_j} (T_{ij}) dV_y d\tau \\ &+ \int_{-\infty}^{t^+} \int_S [G \frac{\partial (T_{ij})}{\partial y_i} n_j - (T_{ij}) \frac{\partial G}{\partial y_j} n_i] dS_y d\tau \\ &- c_0^2 \int_{-\infty}^{t^+} \int_S [\rho' \frac{\partial G}{\partial y_i} - G \frac{\partial \rho'}{\partial y_i}] n_i dS_y d\tau \ . \end{aligned} \tag{151}$$

Using the definition $P_{ij} = p\delta_{ij} - \tau_{ij}$ and the momentum conservation law (13) we find:

$$\begin{aligned} p' &= \int_{-\infty}^{t^+} \int_V (T_{ij}) \frac{\partial^2 G}{\partial y_i \partial y_j} dV_y d\tau \\ &- \int_{-\infty}^{t^+} \int_S G \frac{\partial \rho v_i}{\partial \tau} n_i dS_y d\tau \\ &- \int_{-\infty}^{t^+} \int_S (P_{ij} + \rho v_i v_j) \frac{\partial G}{\partial y_j} n_i dS_y d\tau \ . \end{aligned} \tag{152}$$

By means of partial integration, we now move the partial derivative with respect to τ from $(\partial \rho v_i / \partial \tau)$ to the Green's function. We use the symmetry relationship $\partial G / \partial \tau = -\partial G / \partial t$ (listening later is equivalent to shooting earlier). As the integral is carried out with τ as variable we can move the time derivative $\frac{\partial}{\partial t}$ out of the integral. In the particular case of the free space Green's function G_0 we can also use the relationship $\partial G_0 / \partial y_i = -\partial G_0 / \partial x_i$. We can then move those space derivatives out of the integral. We can also carry out the time integration by making use of the delta function in $G_0 = \delta(\tau - t_e)/(4\pi r)$. Using the far field approximation $\partial / \partial x_i = -\partial / c_0 \partial t$ we find the result of Curle:

$$\begin{aligned} p'(\vec{x}, t) &= \frac{x_i x_j}{4\pi |\vec{x}|^2 c_0^2} \frac{\partial^2}{\partial t^2} \int_V \left[\frac{T_{ij}}{r} \right]_{\tau = t_e} dV_y \\ &- \frac{1}{4\pi} \frac{\partial}{\partial t} \int_S \left[\frac{\rho v_i}{r} \right]_{\tau = t_e} n_i dS_y \\ &- \frac{x_j}{4\pi |\vec{x}| c_0} \frac{\partial}{\partial t} \int_S \left[\frac{P_{ij} + \rho v_i v_j}{r} \right]_{\tau = t_e} n_i dS_y \ . \end{aligned} \tag{153}$$

When we limit ourselves to a fixed rigid body $v_i = 0$ on the surface S so that we have:

$$\begin{aligned} p'(\vec{x}, t) &= \frac{x_i x_j}{4\pi |\vec{x}|^2 c_0^2} \frac{\partial^2}{\partial t^2} \int_V \left[\frac{T_{ij}}{r} \right]_{\tau = t_e} dV_y \\ &- \frac{x_j}{4\pi |\vec{x}| c_0} \frac{\partial}{\partial t} \int_S \left[\frac{P_{ij}}{r} \right]_{\tau = t_e} n_i dS_y \ . \end{aligned} \tag{154}$$

The first integral is the sound production of the flow as it would be in the absence of the body. We see that indeed the presence of the body introduces a dipole source. This should

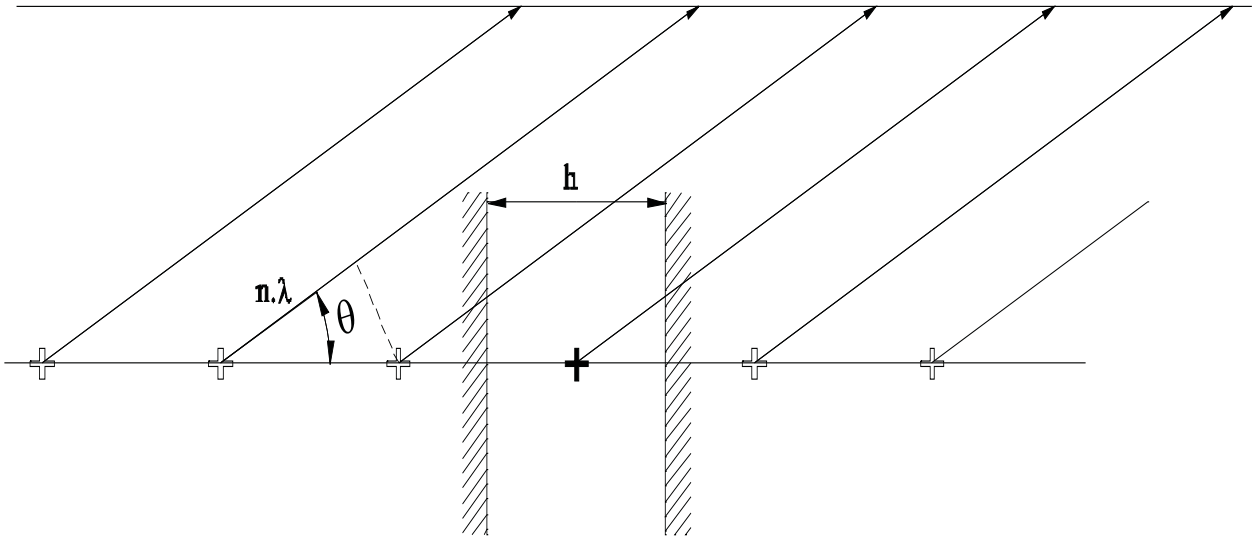

Figure 14: *Monopole source placed between two parallel rigid walls radiated in critical direction θ such that $k_0 h \cos\theta = 2\pi n$ $(n = 0, 1, 2...)$.*

be associated with a force. For a compact body we can neglect the variation of the emission time t_e over the surface an we have:

$$\begin{aligned} p'(\vec{x},t) &\simeq \frac{x_i x_j}{4\pi|\vec{x}|^3 c_0^2}\frac{\partial^2}{\partial t^2}\int_V [T_{ij}]_{\tau=t_e} dV_y \\ &- \frac{x_j}{4\pi|\vec{x}|^2 c_0}\frac{\partial F_j(t_e)}{\partial t} \end{aligned} \tag{155}$$

where $F_j = \int_S [P_{ij}]_{\tau=t_e} n_i dS_y$ is the instantaneous force which the fluid exert on the body.

5 Waves in pipes

5.1 Pipe modes

The method of images introduced in section 4.9 can also be used to understand the behaviour of a monopole source placed within a duct. As we see from figure 14 the images of a source placed on the symmetry axis of a channel, between two rigid walls, is an infinite row of images placed a distance h from each other (where h is the channel height).

In the far field waves from the source array (original source and its images) will add. We now consider a harmonically oscillating source. If there is a phase difference between waves from two successive sources in the array the amplitude of the sum will remain of the order of the amplitude emitted by a single source. If however we consider directions in which the difference in emission time Δt_e between two successive sources is an integer number $n = 0, 1, 2, ...$ of oscillation periods $2\pi/\omega$ there will be constructive interference.

All the waves add up in phase. This corresponds to directions at angles θ (with the array) satisfying the condition:

$$k_0 h \cos\theta = 2\pi n \ . \tag{156}$$

Each direction is a mode of propagation of waves through the channel. When $n = 0$ we find plane waves travelling in the direction of the pipe axis. For plane waves we recover a radiation impedance equal to the characteristic impedance $\rho_0 c_0$ of the fluid, which is independent of the frequency (compare to free space equation (101)). We will see that at low frequencies this plane wave mode is the only possible mode of propagation. In that case a volume injection $G(t) = dV/dt$ at a point in an infinite pipe of cross-sectional area S, we will observe two waves of amplitude $p'(x_1, t) = \rho_0 c_0 G(t \pm (x_1/c_0))/(2S)$ travelling respectively up and downstream of the pipe.

For higher order modes there is a critical frequency f_c, the cut-off frequency, below which propagation will not occur. For $n = 1$ obviously no non-zero value of θ can be found from equation (156) when the distance h between two consecutive sources in the array is smaller than the acoustical wave-length $\lambda = c_0/f = 2\pi/k_0$. Similar cut-off frequencies f_c are found for higher order modes $h > nc_0/f_c$. At the cut-off frequency we have a transversal resonance of the pipe.

Below the cut-off frequency f_c for the first transversal mode the radiation behaviour of a source is independent of its position within a cross-section of the pipe. At higher frequencies the position becomes important because the impedance which the source experiences depends on its position in the transversal standing wave. For example if we place the source close to one of the walls the array of sources will be formed by double sources spaced a distance $2h$ from each other (figure 15). The first higher order propagating mode corresponds to a resonance frequency $f_c = c_0/(2h)$ in the case of a source near the wall, while it was $f_c = c_0/h$ when the source was placed on the axis of the channel. The transverse standing wave at $f = f_c$ has a pressure node on the pipe axis. Hence on the axis $p' = 0$ and a volume injection cannot perform any work! (See equation (147)).

The effect of the impedance becomes dramatic for dipoles placed in a pipe. A dipole placed in an infinite pipe in the direction of the pipe axis will radiate very effectively. Below the first cut-off frequency only the plane wave mode can be excited. A point force $\vec{F}(t) = (F_1(t), 0, 0)$ will induce a pressure discontinuity $\Delta p = F_1(t)/S$ which will radiate as two plane waves $p'(\vec{x}, t) = \pm F(t \pm (x_1/c_0))/(2S)$. This should be compared to equation (108) for radiation in free space. We see now that in a pipe the dipole is not by definition a weaker sound source than the monopole source in contrast with the result which we found in free space. Example of unsteady pressure forces in duct systems which are directed in the direction of the axis, is the force on the blades of a ventilator as a result of interaction of those blades with the system of bars supporting the ventilator. If the distance between blades and support is to small, this will be a very strong source of sound. Also the direction of the flow will have an effect on this interaction. The interaction is stronger

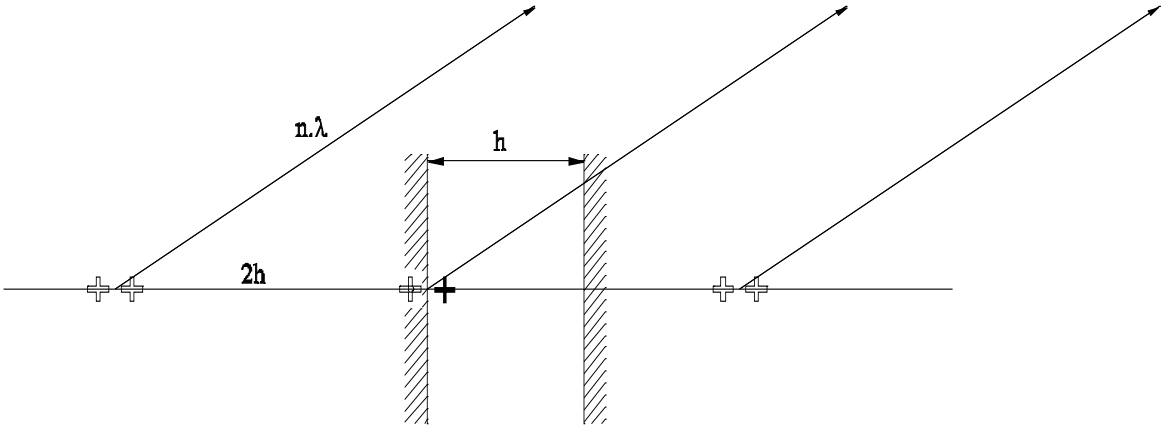

Figure 15: *A source near the wall of a channel forms an array of image sources with distance* $2h$*. The cut-off frequency for the first higher order propagation mode is now* $f_c = c_0/(2h)$

when the ventilator is downstream of the support and cuts through the wake of the support. Therefore silent ventilators which can be reversed are difficult to build. When the bars supporting the ventilator are placed radially the interaction between a blade and a bar will be abrupt and this will generate high frequencies for which we are quite sensitive. A suitable design of the support can considerably smooth out this interaction and move the sound production to lower frequencies (figure 16). Of course when performance is an issue a stator cannot be avoided. In such a case the ratio of number of stator and rotor blades can be chosen to move sound production to lower frequencies, avoiding at least radiation of higher order modes (Tyler and Sofrin [98]). This is used in aircraft motors.

When the dipole acts in the direction normal to the pipe axis it will not radiate below the first cut-off frequency. When a cylinder of diameter D is placed in a pipe flow with a uniform velocity U, unsteady vortex shedding with a characteristic frequency of about $f_{Karman} = 0.2U/D$ is observed. The vortex shedding corresponds to a fluctuating lift force, normal to the flow direction. For $f_{Karman} < f_c$ this will not radiate sound. Sound is only due to fluctuations in the drag force of the cylinder, which is more than one order of magnitude lower than the fluctuating lift force [8].

The results obtained above can also be found by seeking for solutions of the homogeneous wave equation (64) in a pipe of rectangular cross-section $S = h_2 h_3$. A solution is found by the method of separation of variables. We assume a solution of the type:

$$p'(\vec{x}, t) = H_1(x_1) H_2(x_2) H_3(x_3) \exp[i\omega t] \ . \tag{157}$$

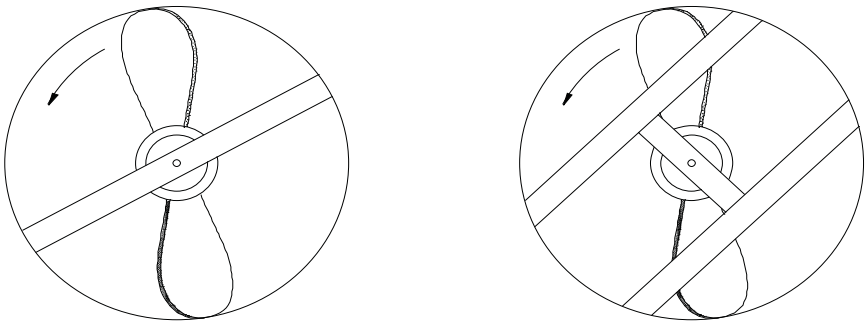

Figure 16: *The sound production due to the interaction between a ventilator and supporting bars is due to the change in aero-dynamics force on the blades when it passes through the wake of the bars. For radial support this interaction is abrupt and produces higher harmonics for which we are quite sensitive. The noise can be reduced by a proper design by which the interaction is smoothed out in time.*

Substitution in the wave equation yields:

$$k_0^2 + \frac{H_1^{"}}{H_1} + \frac{H_2^{"}}{H_2} + \frac{H_3^{"}}{H_3} = 0 \tag{158}$$

with $k_0 = \omega/c_0$. Which can only be satisfied if:

$$\frac{H_i^{"}}{H_i} = -\alpha_i^2 \tag{159}$$

where the α_i 's are constants. We have further the boundary conditions:

$$\begin{cases} \left(\frac{\partial p'}{\partial x_2}\right)_{x_2=0} = \left(\frac{\partial p'}{\partial x_2}\right)_{x_2=h_2} = 0 \\ \left(\frac{\partial p'}{\partial x_3}\right)_{x_3=0} = \left(\frac{\partial p'}{\partial x_3}\right)_{x_3=h_3} = 0 \end{cases} \tag{160}$$

at the walls of the pipe. Solutions for H_2 and H_3 satisfying those conditions are:

$$H_2 = \cos\left(\frac{n_2\pi}{h_2}x_2\right) \tag{161}$$

and:

$$H_3 = \cos\left(\frac{n_3\pi}{h_3}x_3\right) \tag{162}$$

with $n_2 = 0, 1, 2, ...$ and $n_3 = 0, 1, 2, ...$ The full solution is:

$$p'(\vec{x}, t) = \cos\left(\frac{n_2\pi}{h_2}x_2\right)\cos\left(\frac{n_3\pi}{h_3}x_3\right)\exp[i(\omega t \pm k_{n_2n_3}x_1)] \tag{163}$$

with:

$$k_{n_2n_3} = \sqrt{k_0^2 - (\frac{n_2\pi}{h_2})^2 - (\frac{n_3\pi}{h_3})^2}\ . \tag{164}$$

When $k_{n_2 n_3}$ is real we have propagating modes. When $k_{n_2 n_3}$ is imaginary, the mode is not propagating and its amplitude decreases exponentially with the distance from the source. A non propagating mode is also called evanescent, because its amplitude decreases with the distance from the source. Consider a relatively high frequency such as half of the cut-off frequency for the first non-planar mode:

$$\omega = \frac{1}{2}\left(\frac{\pi}{h}c_0\right); (h = h_2 = h_3) \ .$$

In such a case it is a reasonable approximation to state $k_{10} = i\left(\frac{\pi}{h}\right)$. Hence over a distance of one pipe width the amplitude of the (10) mode decays by a factor e^{π} which corresponds to 25 dB (91).

5.2 One dimensional Green's function for infinite pipe

We consider an infinite pipe with a uniform rectangular cross-section $S = h_2 h_3$. Below the cut off frequency for propagation of higher order modes the far field of the sound field generated by a spatially limited sound source is a plane wave $p'(x_1, t)$ which satisfies the one-dimensional wave equation:

$$\frac{1}{c_0^2}\frac{\partial^2 p'}{\partial t^2} - \frac{\partial^2 p'}{\partial x_1^2} = 0 \ . \tag{165}$$

The corresponding far field approximation of the "tailored" Green's function G can now be deduced by averaging equation (111) over the cross-section:

$$\frac{1}{c_0^2}\frac{\partial^2 g_0}{\partial t^2} - \frac{\partial^2 g_0}{\partial x_1^2} = \delta(x_1 - y_1)\delta(t - \tau) \tag{166}$$

where we define g_0 as:

$$g_0(x_1, t|y_1, \tau) = \int_{-h_2/2}^{h_2/2}\int_{-h_3/2}^{h_3/2} G(\vec{x}, t|\vec{y}, \tau)dx_2 dx_3 = SG(\vec{x}, t|\vec{y}, \tau) \ . \tag{167}$$

We made use of the fact that the Green's function G does not depend on the position of the observer within a cross-section of the pipe, because we assumed that only plane waves propagate (see previous section). The one-dimensional Green's function $g_0(x_1, t|y_1, \tau)$ satisfies the solution of d'Alembert and consists for reasons of symmetry of a wave $F(t-(x_1-y_1)/c_0)$ for $x_1 > y_1$ and a wave $F(t + (x_1 - y_1)/c_0)$ for $x_1 < y_1$. This can be written also in the form $F(t - |x_1 - y_1|/c_0)$. Integrating equation (166) over the compact ($\epsilon k << 1$) source region yields the boundary condition:

$$-(\frac{\partial g_0}{\partial x_1})_{x_1=y_1+\epsilon} + (\frac{\partial g_0}{\partial x_1})_{x_1=y_1-\epsilon} = \frac{2}{c_0}(\frac{\partial g_0}{\partial t})_{x_1=y_1+\epsilon} = \delta(t - \tau) \tag{168}$$

which is satisfied by:

$$g_0(x_1, t|y_1, \tau) = \frac{c_0}{2}H(t - \tau - \frac{|x_1 - y_1|}{c_0}) \tag{169}$$

where $H(t-\tau) = \int_{-\infty}^{t} \delta(t'-\tau)dt'$ is the Heaviside step function which is zero for $\tau > t$ and 1 for $\tau < t$. The Heaviside-function character of this one-dimensional Green's function g_0 can be understood by using the method of images which is illustrated in figure 17.

For an emission time between $t_e = t - r/c_0$ and $t_e + dt_e = t - (r + dr)/c_0$ at fixed obser-

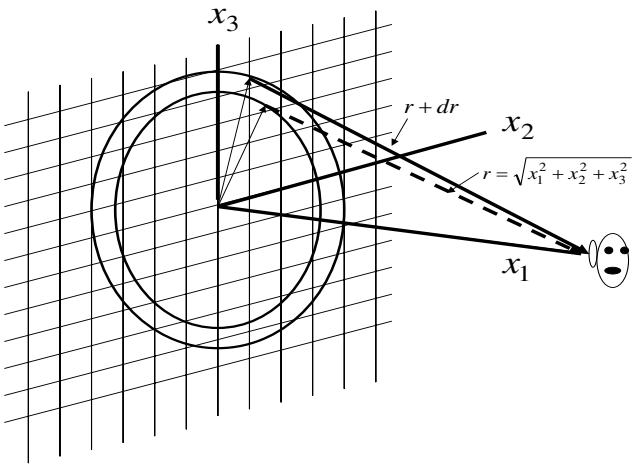

Figure 17: *Use of the method of images to explain the Heaviside-function character of the far field one-dimensional Green's function g_0. The images form an array of images. For an emission time between $t_e = t - r/c_0$ and $t_e + dt_e = t - (r + dr)/c_0$ at fixed observation time t and fixed listener position $(x_1, 0, 0)$, the number of images which emit a pulse scales as $\pi d(x_2^2 + x_3^2) = 2\pi r dr = 2\pi c_0 r dt_e$. As G_0 scales as r^{-1} the increase in number of images exactly compensates the increase in number of images.*

vation time t and fixed listener position $(x_1, 0, 0)$, the number of images which contribute to g_0 scales as $\pi d(x_2^2 + x_3^2) = \pi d(x_1^2 + x_2^2 + x_3^2) = 2\pi r dr$, with $r^2 = x_1^2 + x_2^2 + x_3^2$. Each pulse corresponds to the free space Green's function G_0 which scales as r^{-1} (equation (122)). This decrease of pulse amplitude with the distance r exactly compensates the increase in number of pulses within a certain interval dt_e.

5.3 Reflections at pipe discontinuities at low frequencies.

We have seen in section 5.1 that at low frequencies only plane waves propagate through a pipe of uniform cross section. We now consider the wave reflection which occurs in a quiescent fluid at pipe discontinuities: the change in pipe diameter and the pipe bifurcation.

We consider first a change in cross-section from S_I to S_{II} as shown in figure 18.

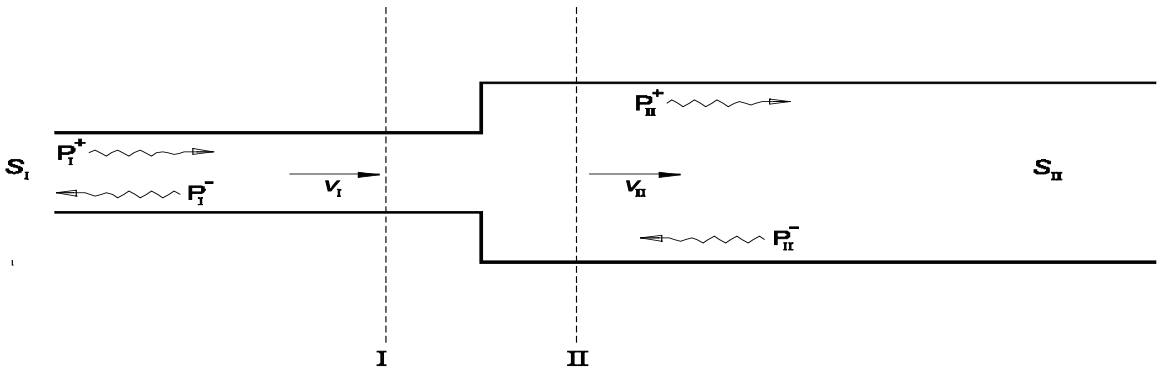

Figure 18: *Plane wave reflection at a change in cross-section.*

We assume at the cross-sections I and II a uniform flow and hence plane waves only. This occurs typically at distances of the order of a few times the pipe width from the discontinuity. In the limit $k_0 h \to 0$ evanescent modes generated at the discontinuity have decayed at least by a factor e^{π} (see section 5.1). We distinguish two type of plane waves: the incoming waves $p_I^+(t - x_1/c_0)$ and $p_{II}^-(t + x_1/c_0)$, converging towards the discontinuity, and the outgoing waves: $p_I^-(t + x_1/c_0)$ and $p_{II}^+(t - x_1/c_0)$. The corresponding flow velocities (equation (69)) $\rho_0 c_0 v_I = (p_I^+ - p_I^-)$ an $\rho_0 c_0 v_{II} = (p_{II}^+ - p_{II}^-)$ are related by the integral conservation law:

$$\frac{d}{dt}\int_V \rho dV + \int_S \rho \vec{v} \cdot \vec{n} dS = 0 \ . \tag{170}$$

The order of magnitude of the ratio of the volume integral to the fluxes in the surface integral is kh for a pipe width h and a wave number k_0. For sufficiently low frequencies the volume integral taken between plane I and II is negligible compared to the convective terms. Furthermore as the velocities are small compared to the speed of sound c_0, $\rho' << \rho_0$ and the surface integral simplifies to:

$$S_I v_I - S_{II} v_{II} = 0 \ . \tag{171}$$

The acoustical flow is inviscid and irrotational we can therefore complement this equation with the equation of Bernoulli (52) which in linearized form for a quiescent reference state becomes:

$$\frac{\partial(\varphi_{II} - \varphi_I)}{\partial t} + \frac{(p'_{II} - p'_I)}{\rho_0} = 0 \tag{172}$$

in which:

$$\varphi_{II} - \varphi_I = \int_I^{II} \vec{v} \cdot d\vec{x} \sim v_I h_I \ . \tag{173}$$

We see that the ratio of the inertial term $\partial\varphi/\partial t$ to the individual pressure terms is of the order of kh. Hence the equation of Bernoulli reduces in the low frequency limit to:

$$p'_I = p'_{II} \ . \tag{174}$$

The same equation can also be deduced [51] from the energy conservation law (82), but the present result is more general because it also holds between any pair of branches at a pipe bifurcation (which we will discuss later).

The equations (171) and (174) can be written in terms of amplitudes of individual waves $p_i^{\pm}$. This set of homogeneous equations can be written as the matrix transformation of vector (p_I^+, p_{II}^-) into (p_I^-, p_{II}^+). The corresponding transformation is called the scattering matrix. This is a very convenient notation allowing to calculate the acoustical response of complex networks [83].

Let us now consider the reflection of a wave p_I^+ at a pipe discontinuity in an infinite pipe. In such a case $p_{II}^- = 0$ and we find after some algebra the reflection coefficient:

$$\frac{p_I^-}{p_I^+} = \frac{S_I - S_{II}}{S_I + S_{II}} \tag{175}$$

and the transmission coefficient:

$$\frac{p_{II}^+}{p_I^+} = \frac{2S_I}{S_I + S_{II}} \ . \tag{176}$$

Looking at the limit $(S_I/S_{II}) \to \infty$ we find the behaviour of a hard wall $p_I^- = p_I^+$. Note that the transmitted wave amplitude is $p_{II}^+ = 2p_I^+$ does not vanish but corresponds to a negligible acoustical energy flux. Making stepwise convergence with $S_I >> S_{II}$ in a pipe results into an increase of the transmitted wave amplitude by a factor 2 at each contraction. This can result into high amplitudes. This effect is observed in organ pipe flow supply systems [**?**].

In the opposite limit $S_I/S_{II} \to 0$ we find the ideal open pipe termination behaviour with $p_I^- = -p_I^+$ and $p_{II}^+ = 0$. All the acoustical energy is reflected and the wave undergoes a phase jump of π upon reflection.

We now consider the acoustical behaviour of a pipe bifurcation as shown in figure 19.

We consider a compact junction $k_0 h << 1$ between N pipes noted with the index $i = I, II, III, ...N$. The mass conservation law (170) becomes:

$$\Sigma_{i=I}^N S_i v_i n_i = 0 \tag{177}$$

where n_i is the unit vector in the outwards direction (looking from the controle volume V around the junction) and the Bernoulli equation (172) yields:

$$p'_I = p'_{II} = ... = p'_N \ . \tag{178}$$

We have in principe $2N$ unknowns corresponding to the incoming and outgoing waves in each pipes respectively p_i^+ and p_i^-. It is in the general case most convenient to define the

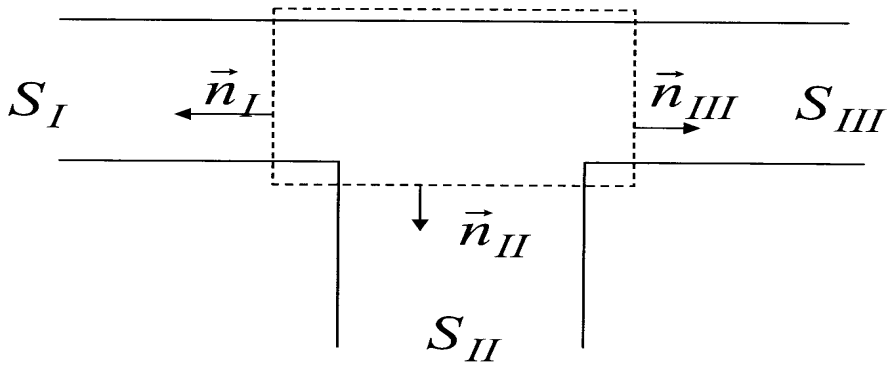

Figure 19: *Pipe bifurcation.*

(+) direction as outwards and the (−) direction as inwards. In that case we simply have $n_i = 1$. We then find in terms of the amplitudes of the waves the set of N equations:

$$\Sigma_{i=I}^{N} S_i(p_i^+ - p_i^-) = 0 \tag{179}$$

and:

$$(p_I^+ + p_I^-) = (p_{II}^+ + p_{II}^-) = ... = (p_N^+ + p_N^-) \ . \tag{180}$$

In order to determine the acoustical field we need N additional boundary conditions. Those can be either a specification of an incoming wave amplitude or a boundary condition in terms of the impedance $\hat{p}_i/\hat{v}_i$ for harmonic waves [7].

As an example we consider now the acoustical behaviour of a closed pipe segment placed along an infinite pipe of cross-sectional area S_I as shown in figure 20.

The side branch length is L_{II} and its cross-sectional area is S_{II}. We launch a wave $p_I^-(t + x_I/c_0)$ towards the junction and assume that $p_{III}^-(t + x_{III}/c_0) = 0$ because the pipe is infinitely long. At the closed pipe termination we have the reflection condition $p_{II}^+(t - L_{II}/c_0) = p_{II}^-(t + L_{II}/c_0)$. To obtain more explicitly results we now assume harmonic waves so that we have:

$$p_i' = p_i^+ \exp[i(\omega t - kx_i)] + p_i^- \exp[i(\omega t + kx_i)] \tag{181}$$

where the positive x_i direction is away from the junction. We therefore find (equation (178)):

$$p_I^+ + p_I^- = p_{II}^+ + p_{II}^- = p_{III}^+ \tag{182}$$

[7] For non-harmonic waves the impedance condition corresponds to a convolution integral in the time and is therefore much more complex.

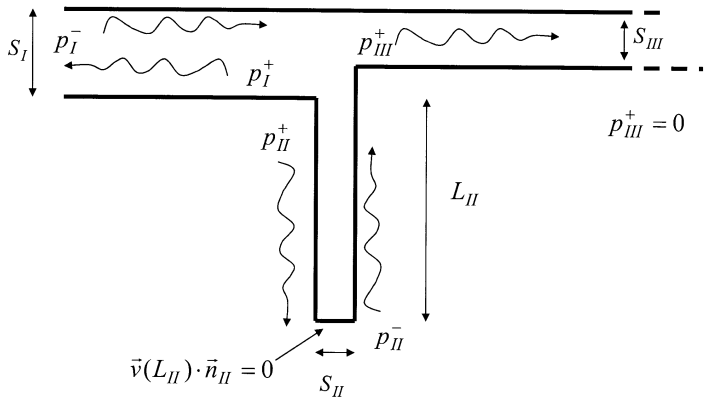

Figure 20: *Reflection of waves at a closed pipe segment.*

and (equation (177)):

$$S_I(p_I^+ - p_I^-) + S_{II}(p_{II}^+ - p_{II}^-) + S_{III}(p_{III}^+) = 0 \tag{183}$$

which complemented with:

$$p_{II}^+ \exp[-ik_0 L_{II}] = p_{II}^- \exp[ik_0 L_{II}] \tag{184}$$

form a complete set of 4 equations with 4 unknown $(p_I^+, p_{II}^+, p_{II}^-, p_{III}^+)$ for a given p_I^-. In the particular case that:

$$2(\frac{\omega}{c_0})L_{II} = (2n+1)\pi, \quad (n = 0, 1, 2, ...) \tag{185}$$

or $4L_{II} = (2n+1)\lambda$ which corresponds to:

$$p_{II}^+ + p_{II}^- = 0 \tag{186}$$

the closed side branch imposes a zero pressure at the junction and we automatically find from equation (182) that the junction acts as an ideal open pipe termination $p_I^- = -p_I^+$. Such a tuned closed pipe branch is therefore a perfect reflector. This is often used to prevent transmission of pulsations trough the gas outlet of a combustion engine with a steady rotational speed. The reflection is very efficient but is only effective when the pipe is very well tuned. In practice one therefore prefers to use another type of side-cavity, which we call a Helmholtz resonator. We will discuss this in detail later. A more accurate description of the reflection of waves at a closed side branch is found by taking into account visco-thermal damping of waves in the side branch. This can be done by using the complex wave number $k = (\omega/c_0) - (i-1)\alpha$ where the damping coefficient α is given by equation (93). In that case for the condition (185) about a fraction $2\alpha L_{II}$ of the incident wave p_I^- will be transmitted because p_{II}^+ is not exactly equal to p_{II}^-.

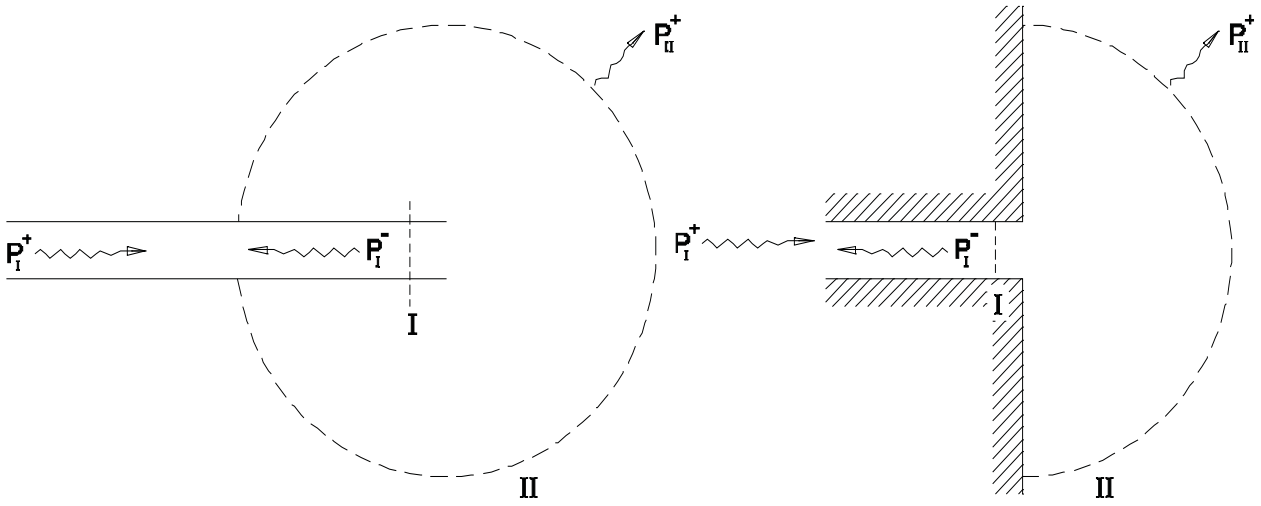

Figure 21: *Unflanged (A) and flanged (B) open pipe terminations.*

We would like to stress your attention to the fact that we avoided to call the side-branch a resonator. A resonator is a system within which waves are captured. In the absence of friction and radiation a steady oscillation is observed. Those steady oscillations are due to initial conditions and occur at the natural frequencies of the system which correspond to what we further will call modes or resonances. In the case of a pipe segment closed at one end and terminated by an ideal open end (free space) at the other we have a resonator with resonance frequencies satisfying condition (185). The waves form a stationary wave pattern in such a resonator which keep on oscillating without damping. However when the pipe segment is placed as side branch along an infinite pipe as in figure 20, a wave p_{II}^- reaching the junction will see a pipe expansion from S_{II} to $2S_I$ which results into a transmission of a fraction $[2S_{II}/(S_{II}+2S_I)]^2$ of the energy. If $S_I = S_{II}$ we see that each reflection results into a loss of a fraction $4/9$ of the wave energy. Hence the "resonator" is almost strongly damped, due to radiation losses!

5.4 The open pipe termination in quiescent fluid

The sound transfer between an internal flow and a listener, outside of the system, is either transmitted through wall vibrations or through an opening such as an open pipe termination. We neglect in our discussion wall vibrations. We now consider the radiation of sound from an open pipe termination of radius a into free space. We limit our discussion to the low frequency limit $k_0 a << 1$. We first consider the case of a thin-walled pipe as shown in figure 21. When the pipe termination is placed in a wall we call it "flanged". By opposition the thin walled pipe termination is called "unflanged". We want to calculated the impedance Z_p experienced by the internal acoustical field at the open pipe termination $x_I = 0$.

The oscillating volume flux at the pipe outlet, which is induced by the acoustical field

$\hat{p}_I$ within the pipe, will act in first approximation as a monopole sound source on the external fluid (II). We therefore expect that at some distance r from the pipe termination the acoustical field will be dominated by spherical outgoing waves:

$$\hat{p}_{II} = \frac{A}{r} \exp[-ik_0 r] \ . \tag{187}$$

In the pipe we have plane waves:

$$\hat{p}_I = p_I^+ \exp[-ik_0 x_I] + p_I^- \exp[ik_0 x_I] \ . \tag{188}$$

The corresponding velocities are respectively (equation (97)):

$$\hat{v}_{II} = \frac{\hat{p}_{II}}{\rho_0 c_0} \left(1 + \frac{1}{ik_0 r}\right) \tag{189}$$

and (equation (69)):

$$\hat{v}_I = \frac{1}{\rho_0 c_0} (p_I^+ \exp[-ik_0 x_I] - p_I^- \exp[ik_0 x_I]) \ . \tag{190}$$

As $k_0 a << 1$ we can find a distance $R >> a$ in the near-field $k_0 R << 1$ such that the flow is still locally incompressible for $r < R$ but already spherical symmetric. By conservation of mass in the volume delimited by $x_I = 0$ and $r = R$ we have for an unflanged pipe termination:

$$\hat{v}_{II} = \frac{S_I \hat{v}_I}{4\pi R^2} \tag{191}$$

This equation can be complemented with the time average of the energy equation (90) which combined with equation (89) gives:

$$< I_I > S_I = \frac{1}{2} \hat{v}_I \hat{v}_I^* Re[Z_p] S_I = \frac{1}{2} \hat{v}_{II}(R) \hat{v}_{II}^*(R) Re[Z(R)] 4\pi R^2 =< I_{II} > S_{II}. \tag{192}$$

which using equation (101) $Re[Z(R)] \simeq \rho_0 c_0 (k_0 R)^2$ becomes:

$$Re[Z_p] = \rho_0 c_0 \frac{k_0^2 S_I}{4\pi} \ . \tag{193}$$

For a circular pipe cross-section $S_I = \pi a^2$ we find the well known low frequency approximation of the result of Levine and Schwinger [66] $Re[Z_p]/(\rho_0 c_0) \simeq (k_0 a)^2/4$. It should be obvious from the discussion of section 4.9 that a flanged open pipe termination has a real part of the impedance which is twice as large as that for an unflanged open pipe termination. Furthermore due to the inertia of the flow in the near field of the pipe exit we expect an imaginary part of Z_p similar to that obtained for a compact sphere in equation (101):

$$Z_p \simeq \rho_0 c_0 [\frac{(k_0 a)^2}{4} + ik_0 \delta_p] \tag{194}$$

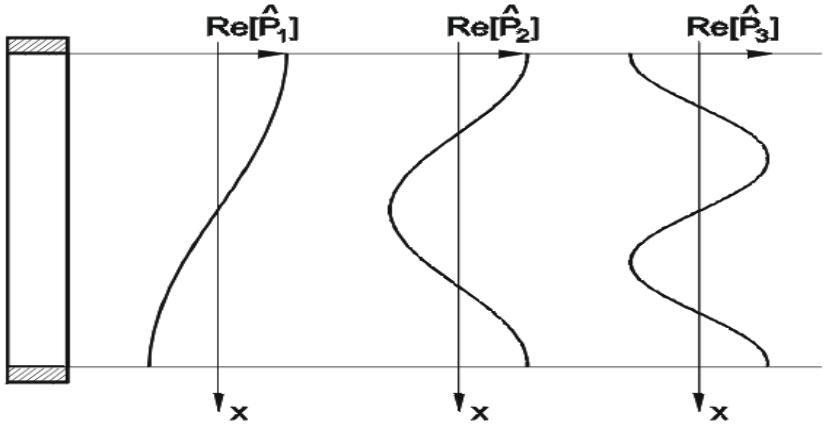

Figure 22: *Simple resonators in pipe systems and modes.*

in which δ_p is of the order of the pipe radius a. This imaginary part corresponds to a phase shift $2k_0\delta_p$ (factor $\exp[2ik_0\delta_p]$) between the incident wave p_I^+ and the reflected wave p_I^-. This would occur if we assume an ideal open pipe termination at $x_I = \delta_p$. We therefore call δ_p the end-correction of the pipe. For an unflanged pipe we have $\delta_p = 0.61a$ while for a flanged pipe a value $\delta_p = 0.82a$ is commonly used [79]. Please note that flow has a dramatic influence on this end correction ([97], [89]), [**?**].

5.5 Simple resonators in pipe systems

When a system is acoustically closed and we neglect visco-thermal losses, an initial perturbation will excite steady acoustical oscillations at frequencies corresponding to so-called modes of the system. Such systems which we call resonators are very important for internal flows. They can dramatically affect the radiation impedance of a sound source. Furthermore the acoustical energy can accumulate so that feedback from the acoustical field to the flow generating the acoustical field can become very important. In contrast to flows in free space we therefore often will observe self-sustained oscillation of the flow in a pipe system. Coupling of the main flow with the acoustical field which it generates is often the feedback mechanism. Typical examples of such behaviour are: human whistling, reed-oscillations in woodwind instruments, the membrane oscillation in a claxon,... It is therefore important to gain some insight into acoustical resonance behaviour.

The most simple resonator is a pipe segment of length L closed at both ends $x = 0$ and $x = L$ (figure 22).

In the absence of sources the plane wave solution (67) corresponds to the pressure field:

$$\hat{p} = p^+ \exp[-ik_0 x] + p^- \exp[ik_0 x] \tag{195}$$

with the corresponding velocity field:

$$\hat{v} = \frac{1}{\rho_0 c_0}(p^+ \exp[-ik_0 x] - p^- \exp[ik_0 x]) \ . \tag{196}$$

The boundary conditions at the pipe terminations $\hat{v}(0) = \hat{v}(L) = 0$ yields a homogeneous system of two equations for the amplitudes $p^{\pm}$:

$$p^+ - p^- = 0 \tag{197}$$

$$p^+ \exp[-ik_0 L] - p^- \exp[ik_0 L] = 0 \tag{198}$$

which can only have a non-trivial solution if:

$$2k_0 L = 2\pi n, \quad (n = 1, 2, 3, ...) \ . \tag{199}$$

The solutions $\omega_n = n\pi(c_0/L)$ correspond to the wel known standing wave patterns with $L = n(\lambda/2)$ which already appeared as transversal resonances in equation (161). The pressure distribution $\hat{p}$ can be written as a sum of contribution of the modes:

$$\hat{p} = \Sigma_{n=1}^{\infty} A_n \cos(\frac{n\pi x}{L}) \tag{200}$$

in which the amplitude of the modes is found by multiplying equation (200) by $\cos(\frac{m\pi x}{L})$ and integrating over the length of the pipe. Using the fact that $\frac{1}{L}\int_0^L \cos(\frac{n\pi x}{L})\cos(\frac{m\pi x}{L})dx = \frac{\delta_{mn}}{2}$ with $\delta_{nn} = 1$ $(n = m)$ and $\delta_{nm} = 0$ $(m \neq n)$, one finds:

$$A_n = \frac{2}{L}\int_0^L \hat{p}\cos(\frac{n\pi x}{L})dx. \tag{201}$$

Once the amplitudes A_n have been determined at a given initial time the further evolution of the solution in time is given by:

$$p'(x,t) = \Sigma_{n=1}^{\infty} A_n \cos(k_n x)\exp[i(\omega_n t)] \tag{202}$$

with $\omega_n = n\pi c_0/L$ and $k_n = \omega_n/c_0$.

The tailored Green's function $g(x,t|y,\tau)$ of this resonator is found by solving the equation:

$$\frac{1}{c_0^2}\frac{\partial^2 g}{\partial t^2} - \frac{\partial^2 g}{\partial x^2} = \delta(x-y)\delta(t-\tau) \ . \tag{203}$$

We assume the Fourier transform $\hat{g}$ to be given by a mode expansion such as equation (200). Substitution into the Fourier transform of equation (203) yields:

$$-k_0^2\hat{g} - \frac{d^2\hat{g}}{dx^2} = \frac{1}{2\pi}\delta(x-y)\exp[-i\omega\tau] \tag{204}$$

and:

$$\Sigma_{n=1}^{\infty}(k_0^2 - k_n^2)A_n\cos(k_n x) = -\frac{1}{2\pi}\delta(x-y)\exp[-i\omega\tau] \ . \tag{205}$$

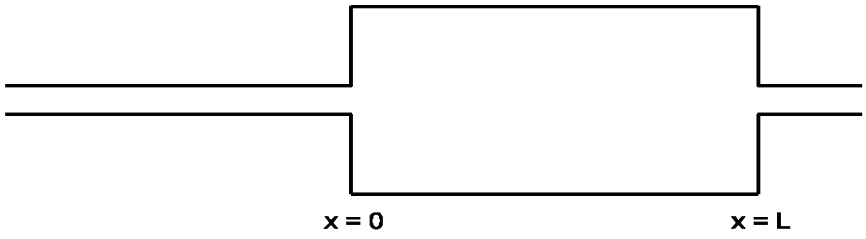

Figure 23: *A simple expansion chamber.*

Multiplying by $\cos(k_m x)$ and integrating over $0 < x < L$ yields:

$$\hat{g} = \Sigma_{n=1}^{\infty} \frac{2c_0^2 \cos(k_n x)\cos(k_n y)\exp[-i\omega\tau]}{2\pi L(\omega_n^2 - \omega^2)}. \tag{206}$$

We see that when we force the oscillations at a frequency ω which corresponds to the eigen-frequency ω_n of a mode the amplitude becomes infinite. This corresponds to a resonance. The inverse Fourier transform of this is:

$$g(x,t|y,\tau) = \Sigma_{n=1}^{\infty} \frac{2c_0 \cos(k_n x)\cos(k_n y)}{n\pi} H(t-\tau)\sin(\omega_n(t-\tau)). \tag{207}$$

We note that this Green's function does satisfy both the causality conditions [8] and the reciprocity principle (114). Furthermore we see that when the pipe is excited at a resonance frequency ω_n the corresponding mode will increase indefinitely unless we take losses into account. The first type of losses are the linear losses such as visco-thermal losses. They corresponds to complex values of the eigen-frequencies ω_n. The second type of losses are non-linear saturation mechanism. We will introduce those in section 5.8 when we discuss self-sustained oscillations.

Closed pipe segments are not common in industrial applications. However, pipe systems behaving approximately as closed pipes can be found. An example is an expansion chamber as shown in figure 23.

When such an expansion chamber is placed just upstream of the tail-pipe of an exhaust (figure 23), one observes in addition to the resonances corresponding to the standing waves in the expansion chamber, resonances due to the open-open tube character of the tail pipe and a low frequency resonance in which the fluid in the tail pipe is acting as an incompressible mass and the volume of the chamber as a spring. We call this low frequency resonance a Helmholtz resonance. We will discuss this in more detail in the next section, where we will consider the effects of flow on this resonance.

[8] $g(x,t) = 0$ and $\frac{\partial g}{\partial t} = 0$ for $t < \tau$.

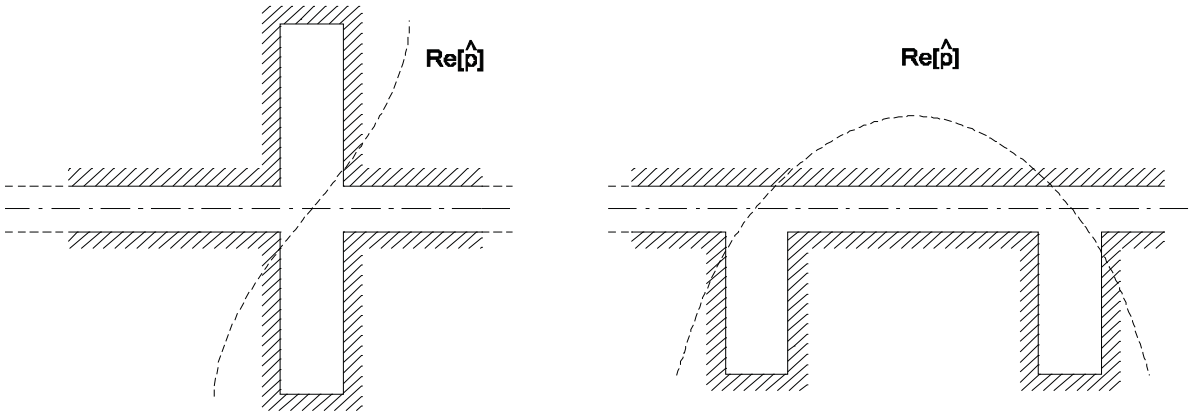

Figure 24: *Closed side branch resonators.*

Before leaving this subject we would like to introduce two other type of resonators which are common in pipe systems: the closed side branch resonator and the Parker-mode resonator.

In section 5.3 we have seen that a closed side branch of length L is a perfect reflector for critical frequencies corresponding to $L = (2n+1)\lambda/4$. The closed side branch imposes an ideal open end behaviour $p' = 0$ at the junction between the side branch and the main pipe. We insisted furthermore on the fact that when the cross-section areas of the main pipe and of the side branch were not very different, the closed side branch is not a resonator by itself. However when two closed side branches of length $L_I = (2n+1)\lambda/4 \;\; (n = 0, 1, 2, ..)$ and $L_{II} = (2m+1)\lambda/4 \;\; (m = 0, 1, 2...)$ are placed at distance $L_{III} = j\lambda/2 \;\; (j = 0, 1, 2, ...)$ from each other one obtains an almost perfect resonator (see figure 24).

Dramatic flow induced pulsation can be observed in such closed side branch resonators. For a main flow velocity U_0, pulsations amplitudes of the order of $p' \simeq \rho_0 c_0 U_0$ have been observed. In natural gas transport systems with $\rho_0 = 50$ kg m^{-3}, $c_0 = 400$ m s^{-1} and $U_0 = 20$ m s^{-1} this corresponds to $p' \simeq 4$ bar! This is 7% of the static pressure. For such high pressure levels one observes the formation of shock waves in the closed side branches [63]. This non-linear wave propagation phenomenon results into a generation of higher order harmonics of the resonance frequencies. The even harmonics are very efficiently radiated out of the resonator, because they correspond to standing waves pattern with a pressure anti-node at the junction of the side branch with the main pipe. This can become an important amplitude limiting mechanism in such resonances.

We now discuss resonances in open pipe segments.

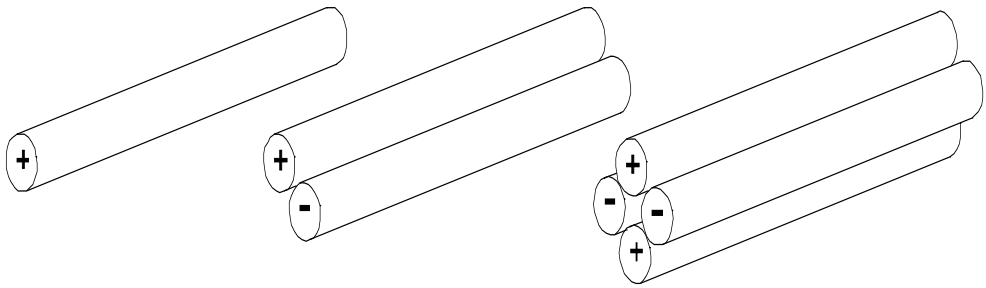

Figure 25: *Resonators formed by bundels of open pipe segments.*

In the previous section we have considered the radiation impedance of an open pipe termination. The real part of this impedance was proportional to the square of the ratio of the pipe radius to the acoustical wave length $Re[Z_p]/(\rho_0 c_0) = (k_0 a)^2/4 = (\pi a/\lambda)^2$ (equation (194)). The first resonance mode of an open-open pipe resonator of length L corresponds to $\lambda = 2L$. Hence for a resonator such as a flute with $a = 0.8$ cm and $L = 80$ cm we have low radiation losses $Re[Z_p]/(\rho_0 c_0) = O(10^{-3})$. We see from equation (93) that at the fundamental frequency the visco-thermal losses for a round trip of the wave $2\alpha L = O(10^{-1})$ are much larger than radiation losses. Fortunately musical sound is determined by the range of frequency 1 kHz $< f <$ 4 kHz for which radiation is quite efficient.

When the ratio a/L of pipe radius to pipe length increases, the radiation losses can become dominant because the radiation losses increase as $(a/L)^2$. If however we consider the twin-pipe configuration (figure 25) the two pipes can oscillate in opposite phase. The pipe terminations radiate then as dipoles. This reduces the radiation losses by a factor $(a/L)^2$ compared to the single pipe (equation (108)). A bundel of four pipes has an oscillation mode which radiates as a quadrupole which reduces the losses by a factor $(a/L)^4$. In a large scale grid one can observe oscillation modes corresponding to octupoles or even higher order combinations. This explains that a grid with cell radius smaller than the grid thickness can display spectacular resonances [105].

The most extreme case is found when a splitter plate is placed in a pipe as shown in figure 26. When the plate length L is larger than the pipe width h, the resonance $\lambda = 2L$ corresponds to a frequency below the cut-off for propagation of higher order modes. In such a case a dipole normal to the pipe axis does not radiate (section 5.1). When the upper and lower part of the pipe segment (separated by the splitter plate) oscillate in opposite phases, there will be no radiation losses. Vortex shedding at the trailing edge of the splitter plate can then induce very strong self-sustained pulsations. We call this a Parker-mode, because similar oscillations where observed for the first time, by Parker, in cascades of turbine blades [114].

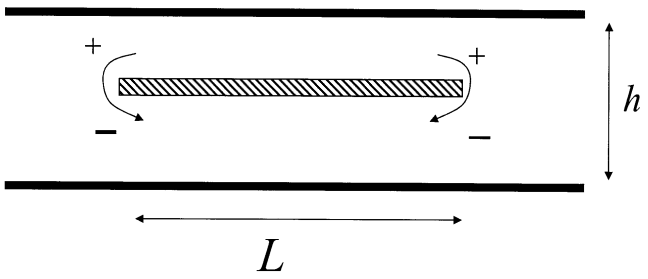

Figure 26: *The Parker-mode in a pipe with splitter plate.*

5.6 Helmholtz resonator

Resonating pipe segments have typically a length comparable to the acoustical wave-length. This can be inconvenient when we want to build resonators for low frequencies. A compact resonator is the Helmholtz resonator, which is a bottle. It is the equivalent in acoustics to the mass-spring system in mechanical vibrations (figure 27). Consider a bottle of Bordeaux wine with a volume V and a neck of length L with a uniform cross-section S. As the flow is compact and the neck is open we can neglect in first approximation the compressibility of the air in the neck. The mass M is given by:

$$M = \rho_0 S L \ . \tag{208}$$

When we move this mass outwards over a distance Δx the volume of the air in the bottle increases by $\Delta V = S\Delta x$. This expansion causes a change of pressure Δp in the bottle which corresponds to a restoring force $F = S\Delta p$ on the mass. Assuming an adiabatic expansion gives: $\Delta p = c_0^2 \Delta\rho = -c_0^2 \rho_0 (\Delta V/V)$ [9]. This linear relationship between the restoring force and the displacement corresponds to a stiffness K_s of the spring given by:

$$K_s = \frac{\rho_0 c_0^2 S^2}{V} \ . \tag{209}$$

The resonance frequency ω_0 of the system is:

$$\omega_0 = \sqrt{\frac{K_s}{M}} = c_0 \sqrt{\frac{S}{VL}} \ . \tag{210}$$

In this approximation we neglected the inertia of the flow outside the neck. It is obvious that there is some contribution of this flow to the inertia. We can take this into account by means of "end-corrections" δ as defined for the open pipe termination in section 5.4. We should then replace L in equation (210) by an effective length $L_{eff} = L + 2\delta$ ($\delta \simeq 0.8\sqrt{S/\pi}$).

[9] We used here the conservation of mass $\rho V = const.$

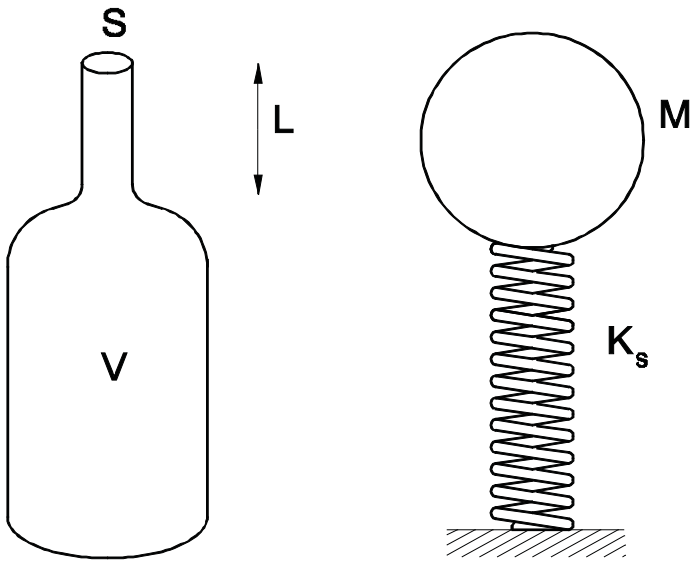

Figure 27: *The Helmholtz resonator behaves as an ideal acoustical mass-spring system. The inertia of the flow is concentrated in the neck. The compressibility is concentrated in the body of the bottle. The wave propagation effects are negligible.*

With this correction we can calculate the resonance frequency of a thin-walled container with a wall perforation surface S. [10]

In the case of Bourgogne wine or cider (figure 28), the bottle has a neck cross-section $S(x)$ which varies smoothly from the bottle cross-section S_{in} to the neck outlet cross-section S_{out}. In order to calculate the inertia of the acoustical flow we can use a one-dimensional incompressible flow approximation [23]. The mass conservation law becomes:

$$v(x)S(x) = v_{out}S_{out} \ . \tag{211}$$

The equation of Bernoulli (52) is for an incompressible flow:

$$\rho_0 \frac{\partial \varphi}{\partial t} + \frac{1}{2}\rho_0 v^2 + p = g(t) \tag{212}$$

where $\varphi = \int v dx$. Combining the mass conservation with the linearized Bernoulli equation in the absence of main flow, we find:

$$\rho_0 L_{eff} \frac{dv'_{out}}{dt} + p'_{out} = p'_{in} \tag{213}$$

where:

$$L_{eff} = \int_{in}^{out} \frac{S_{out}}{S(x)} dx \ . \tag{214}$$

[10] Note that if we replace a single hole by N small well separated perforations with a total surface S we have $\delta = \sqrt{S/(N\pi)}$.

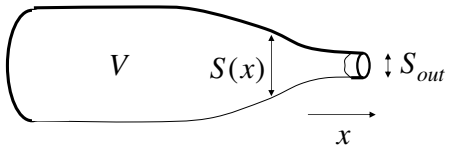

Figure 28: *A bottle of Bourgogne.*

We neglected the flow velocity in the body of the bottle. Equation (214) can be complemented with the integral mass conservation law applied to the volume V of the bottle, assuming a uniform density $\rho'_{in} = p'_{in}/c_0^2$:

$$\frac{V}{c_0^2}\frac{dp'_{in}}{dt} = -\rho_0 S_{out} v'_{out} \ . \tag{215}$$

Elimination of p'_{in} yields:

$$\frac{V L_{eff}}{S_{out} c_0^2}\frac{d^2 v'_{out}}{dt^2} + v'_{out} = -\frac{V}{\rho_0 S_{out} c_0^2}\frac{dp'_{out}}{dt} \ . \tag{216}$$

We recover essentially the same result as obtained for the bottle of Bordeaux with a different definition (214) of the effective length L_{eff}.

We finally consider the influence of a mean flow through the resonator such as we have in a muffler. We consider a muffler of volume V with a tail pipe of length L and uniform cross section area S. We assume a mean flow velocity U_0 through the tail pipe.
The equation of Bernoulli for compressible flow (52) becomes in linearized form:

$$\frac{\partial \varphi}{\partial t} + \frac{p'}{\rho_0} + v' U_0 = g(t) \ . \tag{217}$$

From the body of the muffler to the open end of the tail pipe yields:

$$L\frac{dv'_{out}}{dt} + \frac{p'_{out}}{\rho_0} + v'_{out} U_0 = \frac{p'_{in}}{\rho_0} \tag{218}$$

where we neglect the flow velocity in the muffler. The mass conservation law including flow effects becomes:

$$\frac{V}{c_0^2}\frac{dp'_{in}}{dt} = -\rho_0 S_{out} v'_{out} - \frac{p'_{out}}{c_0^2} S_{out} U_0 \ . \tag{219}$$

Elimination of p'_{in} yields:

$$\begin{aligned} &\left(\tfrac{LV}{S_{out}c_0^2}\right)\tfrac{d^2 v'_{out}}{dt^2} + \left(\tfrac{VU_0}{c_0^2 S_{out}}\right)\tfrac{dv'_{out}}{dt} + v'_{out} \\ &= -\tfrac{p'_{out}}{\rho_0 c_0^2} U_0 - \tfrac{V}{\rho_0 c_0^2 S_{out}}\left(\tfrac{dp'_{out}}{dt}\right) \ . \end{aligned} \tag{220}$$

The surprise in equation (220) comes from the fact that when we assume that there is a main flow velocity U_0 through the neck, as we do have in the tail-pipe of a car muffler, we see that there is a damping. We did not assume any visco-thermal losses in the resonator nor did take radiation into account but we do have a damping. The origin of this term is that we assumed that the pressure p'_{out} at the outlet is equal to the pressure outside the system. By assuming that the pressure at the outlet is equal to the pressure outside the resonator we actually assume that there is a free jet formed by flow separation at the pipe outlet. In this free jet the kinetic energy of the flow is dissipated by turbulence. The flow in such a jet is not a potential flow. The pressure remains constant as the velocity decreases. This is in contradiction with the equation of Bernoulli. We will discuss this more in detail when we consider the theory of vortex-sound.

5.7 Bubble resonance

We consider the response of a small isolated spherical bubble of radius a to homogeneous pressure fluctuations $p'_i = \hat{p}e^{i\omega t}$ due to an incoming low frequency acoustic wave. We assume the gas bubble to have a uniform internal pressure $p'_b = \hat{p}_b e^{i\omega t}$. Due to the excitation the bubble radius will oscillate harmonically: $a = a_0 + \hat{a}e^{i\omega t}$. This result into the radiation of a spherical wave with pressure $p'_r = \hat{p}_r e^{i\omega t}$ at the surface of the bubble. Assuming that there is no mass exchange nor heat transfer between the bubble and its surroundings we have:

$$\frac{\hat{\rho}_b}{\rho_b} = -3\frac{\hat{a}}{a_0} \tag{221}$$

and

$$\hat{\rho}_b = \frac{\hat{p}_b}{c_b^2} \ . \tag{222}$$

Neglecting the influence of surface tension we have from the momentum balance on the surface of the bubble:

$$\hat{p}_b = \hat{p}_i + \hat{p}_r \ . \tag{223}$$

We have furthermore at the bubble surface (97):

$$\hat{v}_r = i\omega\hat{a} = \frac{\hat{p}_r}{\rho_l c_l}\left(1 + \frac{1}{\frac{i\omega a_0}{c_l}}\right) . \tag{224}$$

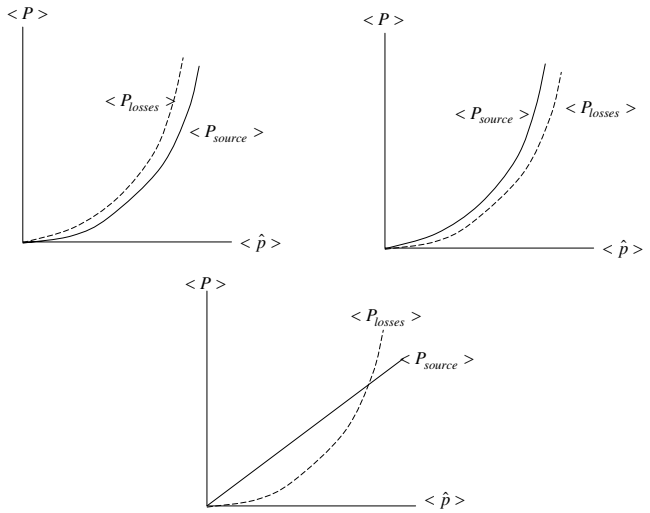

Figure 29: *Self-sustained oscillations are due to a feedback loop. In a linear system if the source is proportional to the pulsation amplitude* $q \sim \hat{p}$*, the power* $< P_{source} >$ *generated by the source will scale with* $|\hat{p}|^2$*. Linear losses* $< P_{losses} >$ *will also scale with* $|\hat{p}|^2$*. The system can either be unstable* $< P_{source} > \; > \; < P_{losses} >$*, stable* $< P_{source} > \; < \; < P_{losses} >$ *or neutrally stable* $< P_{source} > \; = \; < P_{losses} >$*. The pulsation amplitude predicted by linear theory is either infinite, zero or undetermined. As non-linear saturation mechanism must occur to allow the stabilization of the oscillation at a finite well defined amplitude.*

where ρ_l and c_l are respectively the density and the speed of sound of the liquid surrounding the bubble. The amplitude of the radiated wave $\hat{p}_r$ is given by:

$$\hat{p}_r = + \frac{\hat{p}_i}{\left[1 - \frac{\rho_l a_0^2 \omega^2}{3\rho_b c_b^2} + i\left(\frac{\omega a_0}{c_l}\right)\right]} \left(\frac{\rho_l a_0^2 \omega^2}{3\rho_b c_b^2}\right) \; .$$

We observe a resonance for:

$$\left(\frac{\omega_0 a_0}{c_b}\right) = \sqrt{\frac{3\rho_b}{\rho_l}} \; .$$

For air at atmospheric conditions $3\rho_b/\rho_l = 4 \times 10^{-3}$ so that indeed the bubble is compact and our assumption of a uniform internal pressure is reasonable for $\omega \leq \omega_0$. The resonance frequency ω_0 is called the Minnaert frequency.

5.8 Self-sustained oscillations

Oscillations at defined frequencies ω can occur as a result of a feedback from the acoustical field to the source (figure 29). Accumulation of acoustical energy in a resonator enhances this feedback.

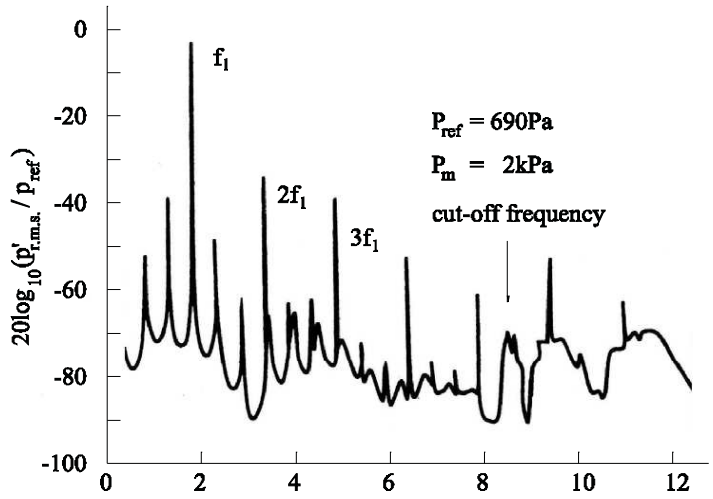

Figure 30: *Spectrum of the pressure measured within a small organ pipe which has been overblown twice. The pipe oscillates at a frequency close to the third pipe resonance. The self-sustained oscillation results into a line spectrum. The continuous back ground is the broad band noise which is modulated by the pipe resonances.*

Linear theory cannot predict a finite oscillation amplitude as found in most self-sustained oscillations. A non-linear saturation mechanism must occur to stabilize the system at a finite oscillation amplitude. When this occurs, the system will have a fundamental oscillation frequency ω_0 which by definition is real (stable oscillation). Higher harmonics of the fundamental frequency $n\omega_0$ will also be generated by the non-linearity of the system. We will find a line spectrum. Please note that in general the eigen-frequencies ω_n of the pipe modes will not form an harmonic series ($\omega_n \neq n\omega_0$).

This is clearly demonstrated by the spectrum of the pressure fluctuations measured in a small organ pipe shown in figure 30. We observe a line spectrum forming a perfectly harmonic series which corresponds to the self-sustained oscillation of the system. We also see the response of the pipe to broad-band turbulence noise. This continuous spectrum is modulated by the pipe resonances. The first resonances are quite sharp. As the frequency increases the resonances become broader. As we approach the first transversal resonance frequency at $8,2$ kHz the radiation losses of longitudinal oscillation modes become so important that we can hardly distinguish any resonance peaks. We still clearly see the lines of multiples of the fundamental frequency.

At the cut-off frequency we observe a strong increase in amplitude of the turbulence noise due to the first transversal resonance of the pipe. We further see that the oscillation frequency ω_0 is close to the third resonance frequency ω_3 of the system. The pipe has

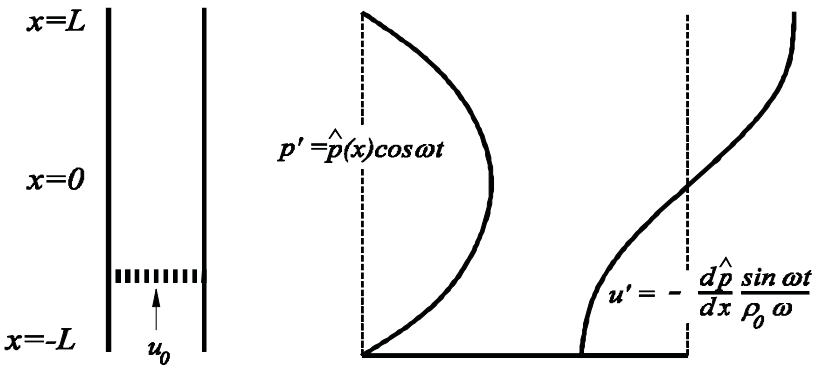

Figure 31: *De Rijke tube: a vertical open pipe segment with a hot grid placed at a quarter of the pipe length above the bottom end.*

been overblown two times. We also observe that the second harmonic $2\omega_0$ does not fit the sixth resonance of the pipe ω_6. The difference between the line spectrum and the pipe resonances become more and more important until above the cut-off frequency we cannot see any relationship between the resonance frequencies and the multiples of ω_0.

An interesting example of self-sustained oscillation is the whistling of the Rijke-tube (figure 31). This phenomenon discovered by de Rijke (1948) was analyzed by Rayleigh [95]. We follow the line of his discussion. This is a vertical open pipe of length $2L$ in which a grid with wire thickness d has been placed at $x = -L/2$, where we take $x = 0$ in the middle of the pipe.

The grid is hot, which induces a vertical convective flow with a velocity U_0. We assume the flow to be uniform. In reality the gas above the grid is hotter than below and therefore the flow has to be accelerated as it passes through the grid. We will neglect such effects and assume a uniform main flow temperature and corresponding velocity of sound c_0 in the pipe. When the grid is sufficiently hot and the tube is well designed a loud whistling sound is emitted [11]. The frequency of the sound corresponds quite accurately to the resonance frequency $\omega_0 = 2\pi c_0/(4L)$. When the grid is placed at the upper half of the pipe $x > 0$ or in the middle of the pipe $x = 0$, no sound is emitted. Higher order modes can in principle be excited but this appears to be difficult as a result of the large visco-thermal and radiation losses. If only the fundamental frequency ω_0 is excited we can approximate the acoustic pressure field in the pipe by:

$$p' = \hat{p}\cos(\frac{\pi x}{2L})\cos(\omega_0 t) \ . \tag{225}$$

[11] For a tube length $L = 30$ cm the pipe cross-sectional radius should be $a \simeq 1$ cm. The grid should be made of wire with a diameter d in the range 0.3 mm $< d <$ 0.7 mm with a mesh size comparable to the wire diameter.

The corresponding velocity v' is found by using the momentum equation (61):

$$v' = \frac{\hat{p}}{\rho_0 c_0} \sin(\frac{\pi x}{2L}) \sin(\omega_0 t) \ . \tag{226}$$

We see that when the pressure in the pipe reaches a maximum or a minimum the velocity vanishes. When the pressure is decreasing $0 < \omega_0 t < \pi$ the acoustical velocity in the upper part $x > 0$ of the pipe is positive and it is negative in the lower part $x < 0$. Fluid is leaving the pipe. For $\pi < \omega_0 t < 2\pi$ fluid is entering the pipe and we have the opposite behaviour.

We expect that the sound source which is driving the oscillation is an unsteady heat transfer from the grid to the surrounding gas. The gas expands upon heating which leads to a volume source (monopole). This corresponds to the entropy term in the analogy of Lighthill (equation (59)):

$$\frac{1}{c_0^2}\frac{\partial^2 p'}{\partial t^2} - \frac{\partial^2 p'}{\partial x^2} = \frac{\partial^2}{\partial t^2}(\frac{p'}{c_0^2} - \rho') \tag{227}$$

Neglecting convective effects we can also write the constitutive equation (22) in the linearized form $p' = c_0^2 \rho' + (\frac{\partial p}{\partial s})_\rho s'$. Using the corresponding linear approximation $\rho_0 T_0 (\partial s'/\partial t) = -\nabla \cdot \vec{q}$ of the entropy equation (37) we find:

$$\frac{1}{c_0^2}\frac{\partial^2 p'}{\partial t^2} - \frac{\partial^2 p'}{\partial x^2} = -\frac{(\frac{\partial p}{\partial s})_\rho}{T_0 \rho_0 c_0^2}\frac{\partial}{\partial t}\nabla \cdot \vec{q} \ . \tag{228}$$

If we integrate the source over a volume V enclosing the grid we find:

$$\int_V \nabla \cdot \vec{q} dV = \int_S \vec{q} \cdot \vec{n} dS \tag{229}$$

where S is the surface of the grid and $\vec{n}$ its outer normal unit vector. The unsteady heat flux from the grid $\vec{q}$ is a source of sound. We can also identify this source to a volume injection term $\partial(Q_m/\rho_0)/\partial t$ as introduced in equation (79). We use further $\partial(Q_m/\rho_0)/\partial t$ as a shorthand notation for this source.

In order to proceed we must now provide a model for the heat transfer from the grid to the gas. A very simple model is to assume that the heat is transfered through thermal boundary layers of thickness δ_T and to assume a linear temperature profile. The concept of boundary layer applies when the Peclet number $\rho c_p U_0 d/K$ based on the grid wire diameter d is much larger than unity. This appears to be a reasonable approximation in a Rijke tube. Following Fourier's law (34), we find for the heat flux towards the gas, at the surface of the grid:

$$q_w = \vec{q} \cdot \vec{n} = K \frac{T_w - T}{\delta_T} \ . \tag{230}$$

where T_w is the grid temperature which we assume to be constant and $T = T_0 + T'$ is the gas temperature outside the boundary layer. We neglect the effect of variations in the heat

conductivity K.

When the grid is placed in the middle of the pipe at $x = 0$, the acoustical velocity v' vanishes. We therefore see that q_w can only fluctuate as a result of the isentropic temperature fluctuations $T' = (\gamma - 1)p'/\gamma$ due to the acoustical pressure fluctuations. As T' and p' are in phase we see from equation (230) that the heat flux q_w decreases when p' increases. The power $< P_{source} >$ generated by the source during an oscillation period is:

$$< P_{source} >= \frac{\omega_0}{2\pi} \int_V \int_0^{2\pi/\omega_0} p' \frac{Q_m}{\rho_0} dt dV \tag{231}$$

where we integrated over a volume enclosing the grid. As the variation in p' is opposite to that of Q_m the power generated by the source will be negative. Fluctuations will be damped by the heat transfer. This corresponds to Rayleigh's explanation why we do not observe any whistling when the grid is placed in the middle of the tube.

If fluctuation in heat transfer should drive the oscillations they should be induced by acoustical velocity fluctuations v'. The largest fluctuations are found at the pipe terminations $x = -L$ and $x = L$. However the acoustical pressure p' vanishes there so that from equation (231) we see that no power can be generated at those positions (pressure nodes).

Clearly the position $x = -L/2$ is a compromise for which there is both a significant fluctuation of pressure p' and of velocity v'. Why should then the sound be produced only when the grid is at $x = -L/2$ and not at $x = L/2$? In order to find this out we ask ourselves how the flow influences the thermal boundary layer thickness δ_T. In first approximation δ_T is determined by the diffusion of heat during a time corresponding to the convection time [12] $3d/U_0$ of fluid along the grid (wire diameter d). For a laminar boundary layer assuming a quasi-steady response, we find:

$$\delta_T \simeq 4\sqrt{\frac{Kd}{\rho_0 c_p \left(U_0 + u'\right)}} \tag{232}$$

which linearized would imply that the fluctuations of Q_m/ρ_0 would be proportional to v': $\delta_T \sim \sqrt{\frac{Kd}{\rho_0 c_p U_0}} \left(1 - \frac{u'}{2U_0} + ...\right)$. As the fluctuations p' and v' are $\pi/2$ out of phase the integral over a period of oscillation of the power (231) will vanish [13]. Hence an oscillation is only possible as a result of a phase delay between the heat transfer fluctuations and the velocity fluctuations. Such a phase delay is provided by the memory time of the boundary layer which corresponds roughly to the convection time $\tau \simeq 3d/U_0$ of a particle in the boundary layer of a grid wire. As shown in figure 32 we see that for $x < 0$ the optimal phase shift is $\omega_0 \tau = \pi/2$ so that the system will oscillate at the critical velocity U_0 determined by:

$$\frac{d\omega_0}{U_0} \simeq \frac{\pi}{6} \ . \tag{233}$$

[12] The velocity at which perturbations are convected in a laminar boundary layer is of the order of $U_0/3$

[13] $\int_0^{2\pi/\omega_0} \sin(\omega_0 t) \cos(\omega_0 t) dt = 0$.

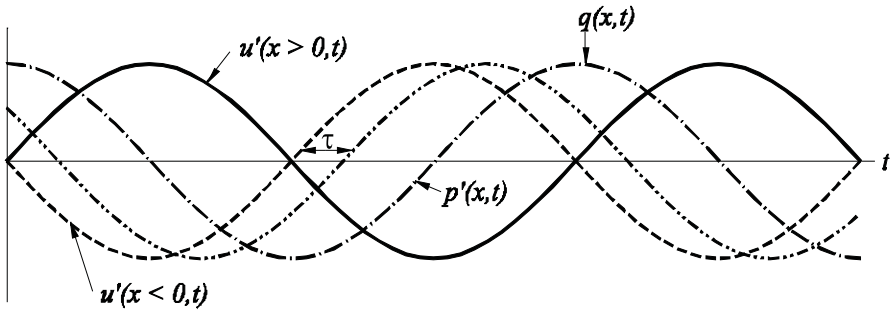

Figure 32: *Phase of heat flux, pressure and velocity fluctuations in a Rijke tube.*

In a Rijke-tube the flow velocity is determined by the tube length and the grid temperature (natural convection), this puts a constrain to the design of the pipe. This constrain can be removed by using forced convection. Indeed, it is easier to drive the pipe when it is placed horizontally and we blow through it.

When the grid is placed in the upper part of the pipe we need a much larger phase shift $\omega_0\tau = 3\pi/2$ which corresponds to lower flow velocities. Low velocities correspond to thicker thermal boundary layers δ_T. While oscillations could occur, in practice we do not observe them because the heat transfer is reduced by the thick boundary layers.

The non-linear amplitude limiting mechanism which determines the oscillation amplitude appears to be the blocking of the heat transfer when hot air from the wake of the grid wire is driven back to the grid. We expect this to occur when acoustical particle displacements become comparable to the grid wire diameter d. Hence the pulsation amplitude can be estimated from:

$$\frac{v'}{\omega_0 d} \simeq 1 \ . \tag{234}$$

The amplitude predicted by this simple formula agrees very wel with experimental results. This confirms that we have identified the correct non-linearity. This saturation mechanism was identified by Heckl [39]. Rayleigh describes this effect as the driving mechanism rather than as the amplitude limiting effect.

The condition of a positive time average source power $< P_{source} >$ which is necessary to initiate self-sustained oscillations is called the "Rayleigh" criterion. Like in this example instabilities are very often due to a time delay. This time delay can for example be the convection time of fuel from a reservoir to a flame. Analysis such as presented here can be very helpful to find cures for undesired oscillations.

5.9 The clarinet

The clarinet has a cylindrical bore of length L and cross-section S terminated by a small exponentional horn (figure 33).

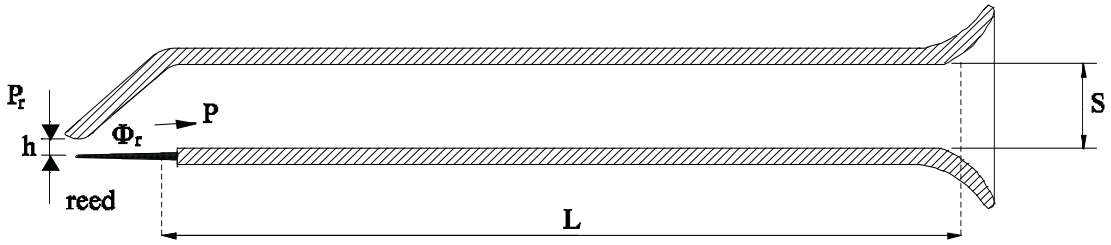

Figure 33: *The clarinet*

The mouth piece is closed by a thin slide of reed which can oscillate. Reed is a special kind of cane similar to bamboo. The reed opening h is controlled by the pressure difference $(p_m - p)$ between the mouth of the player p_m and the pipe inlet p. Assuming the reed oscillation to be controlled by a single degree of freedom we have the equation of motion:

$$M_r \frac{d^2h}{dt^2} + R_r \frac{dh}{dt} + K_r(h - h_r) = -S_r(p_m - p) \tag{235}$$

where M_r is the mass of the reed, R_r is its damping coefficient, K_r is the reed stiffness, h_r the opening of the reed channel at rest and S_r is an effective reed surface. This equation of motion (235) is only valid in a limited range of oscillation. Only positive values of the reed opening h are possible. Furthermore due to the curvature of the wall against which the reed is presses (lay), the stiffness K_r and the mass M_r will be functions of the opening h. We ignore such effects. The flow of air Φ_r through the reed channel can be estimated by assuming a frictionless, quasi-steady and incompressible flow with formation of a free jet of thickness h and width w in the mouthpiece of the pipe [42]:

$$\Phi_r = hw\sqrt{\frac{2|p_m - p|}{\rho_0}}\text{sign}(p_m - p) \ . \tag{236}$$

This induces a flow velocity v at the pipe inlet which is given by:

$$v = \frac{\Phi_r}{S} \tag{237}$$

where S is the cross-sectional aera of the pipe.
The most simple approach to understand the oscillation of the system is to assume a quasi-steady behaviour of the reed. In such a case the equation of motion reduces to:

$$h = h_r - \frac{S_r(p_m - p)}{K_r} \ . \tag{238}$$

Substitution in equation (236) gives the expression:

$$\Phi_r = w(h_r - \frac{S_r(p_m - p)}{K_r})\sqrt{\frac{2|p_m - p|}{\rho_0}}\text{sign}(p_m - p) \ . \tag{239}$$

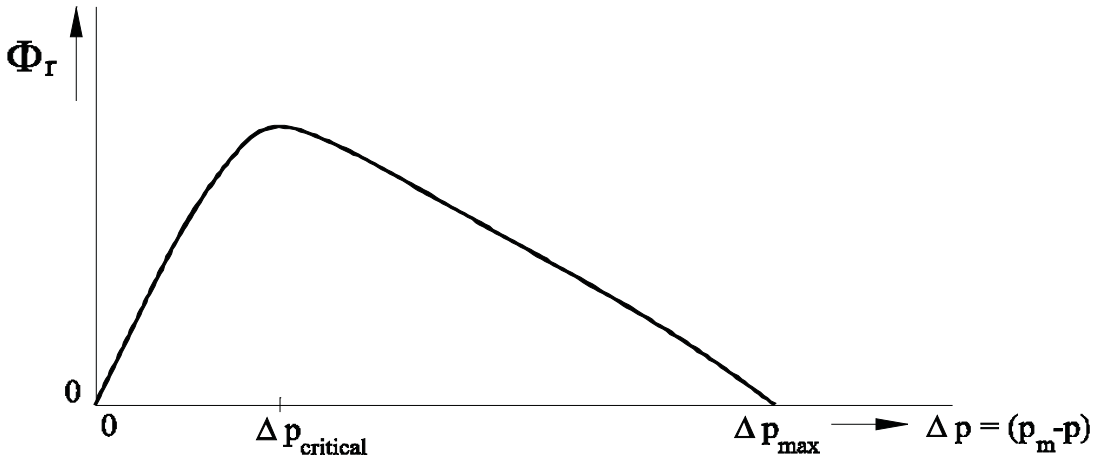

Figure 34: *Quasi-steady flow characteristic of a clarinet.*

In figure 34 we show this relationship between Φ_r and $(p_m - p)$. Obviously when $(p_m - p) = 0$ there is no flow. Furthermore when $(p_m - p) = \Delta p_{max} = h_r K_r / S_r$ the reed closes completely and the flow is stopped. Between those two zero's the flow has a maximum value at a critical value $(p_m - p) = \Delta p_{max}/3 = \Delta p_{critical}$.

It is obvious from figure 34 that $d\Phi_r/dp > 0$ for $(p_m - p) > \Delta p_{critical}$ while $d\Phi_r/dp < 0$ for $(p_m - p) < \Delta p_{critical}$. For small amplitude harmonic perturbations p' and Φ'_r, the acoustical power $< P_r >$ generated by the flow injection is given by:

$$< P_r >= \frac{\omega}{2\pi} \int_0^{2\pi/\omega} p' \Phi'_r dt = \frac{\omega}{2\pi} \int_0^{2\pi/\omega} (p')^2 \frac{d\Phi_r}{dp} dt \ . \tag{240}$$

Hence we see that the reed flow can only drive acoustical oscillations in the pipe for blowing pressures p_m larger than the critical value $\Delta p_{critical}$ for which $\frac{d\Phi_r}{dp} > 0$. The condition (240) corresponds to the Rayleigh criterion. This corresponds to the experimental fact that there is a blowing pressure threshold below which the clarinet does not oscillate.

A more sophisticated analysis including non-linear effects is provided by Kergomard [13]. The theory of Kergomard is summarized by Fletcher and Rossing [33]. Saturation of the amplitude of oscillation occurs when the amplitude of p' becomes comparable to the blowing pressure $p_m (p' \simeq p_m)$.

Self-sustained oscillations are often discussed in terms of linear stability theory [116] which predicts the pressure threshold for p_m above which oscillation will occur and the frequency ω of the oscillation. Often such a theory is much more complex than a non-linear theory. Furthermore it does not predict a finite oscillation amplitude and linearization involves often the introduction of non-physical assumptions.

6 Vortex-sound theory

6.1 Paradox of D'Alembert and flow separation

In the previous section we have used the analogy of Lighthill as a definition of aero-acoustical sound sources. Those sources were deviations of the actual flow from the ideal (linear, inviscid and isentropic) acoustical behaviour of the uniform stagnant fluid (surrounding the listener). While this is often a reasonable reference state it is not always applicable. For example when we consider a pipe flow, the flow region will be extended. Following Lighthill the sources of sound will not be concentrated into a small region as we do observe in practice.

An alternative is to use a potential flow as reference. We illustrate this by considering a constriction in a pipe such as our vocal folds. Oscillation of the folds produce what we call voiced sound by modulating the volume flow which enters in the vocal tract. By articulating we change the acoustical resonances of the vocal tract which modifies the spectrum of the radiated sound. The typical Strouhal number $St = fD/U_0$ based on the oscillation frequency $f \simeq 10^2$ Hz, the thickness of the folds $D \simeq 10^{-2}$m and the flow velocity at the glottis $U_0 \simeq 30$ m s^{-1} is $St \simeq 3 \times 10^{-2}$. We therefore expect that the flow will be quasi-steady and that the fluid displacement by the movement of the folds will not be a major source of sound. The Reynolds number $Re = DU_0/\nu$ is of the order of 10^4, so that we expect that friction will be limited to thin boundary layers of thickness $\delta/D \sim Re^{-1/2}$ ($\nu = 1.5 \times 10^{-5}$ m^2 s^{-1}). The Mach number $M = U_0/c_0$ is low so that steady flow compressibility can be neglected $M^2 \sim 10^{-2}$. Those are arguments to use a frictionless (potential) flow theory and to assume the flow to be locally incompressible and quasi-steady. We also assume a one dimensional flow. In such a case the mass conservation law becomes:

$$U(x)S(x) = U_0 S_0 \tag{241}$$

where S is the duct cross-section at position x. If we assume the cross-section S_I upstream of the folds to be equal to the cross section S_{II} downstream of the folds, we find $U_I = U_{II}$. Substitution of this result into the equation of Bernoulli for steady, frictionless incompressible flows:

$$\frac{1}{2}\rho_0 U_I^2 + p_I = \frac{1}{2}\rho_0 U_{II}^2 + p_{II} \tag{242}$$

yields the surprising result that there is no pressure difference across our vocal folds $p_I = p_{II}$. Hence the vocal folds do not affect the flow. This is the equivalent of the paradox of d'Alembert which shows that a body placed into a steady uniform potential flow does not experience any force. We have a voiceless flow model. The key idea of the analogy of Howe is that all potential flows are actually voiceless. He therefore proposes to use a potential flow as reference in the aeroacoustical analogy. We will discuss this later in more detail. We now first try to understand how nature allows us to make sound by oscillation of our vocal folds.

It is important to realize that when the irrotational-flow (potential) approximation is assumed to be uniformly valid the flow becomes quite unrealistic. Flow control is the result of the occurrence of flow separation. A potential-flow approximation involves a tangential slip velocity of the fluid at solid walls. This is not a correct model for an actual flow. Experience shows that the fluid sticks to the wall. At high Reynolds numbers there is a thin transition region near the wall in which the flow velocity drops rapidly from its value u_∞ dictated by the potential flow approximation to the wall velocity (figure 35). We call this a viscous boundary-layer. As illustrated in figure 35 by comparing a typical boundary-layer velocity profile with the velocity distribution in a solid body rotation, it is obvious that a boundary-layer flow involves rotation of the fluid particles.

The fluid velocity in the *thin* boundary layer is directed mainly along the wall. It can be shown from the momentum conservation law that in such a "quasi-parallel" flow the gradient of pressure $\vec{n} \cdot \nabla p$ normal to the flow direction is negligible. The fluid particles in the boundary layer are therefore driven by the same pressure gradient as the fluid particles in the main potential flow u_∞. In a steady diverging incompressible flow, the velocity decreases $U(x)S(x) = U_0 S_0$. Within the main flow the pressure will increase as predicted by Bernoulli $\frac{1}{2}\rho_0 U(x)^2 + p(x) = \frac{1}{2}\rho_0 U_0^2 + p_0$. The fluid particles in the main flow climb up the adverse pressure gradient by using their kinetic energy. At the wall the fluid particles do not have much kinetic energy, but they feel the same adverse pressure gradient. This means that in an adverse pressure gradient (opposite to the main flow) the fluid near the wall would flow in a direction opposite to the main flow. This backflow is somewhat retarded by the viscous drag by the main flow on the fluid in the boundary layer. The fluid particles in the bulk of the flow drag the fluid in the boundary layers up the pressure gradient. Backflow does occur when the diffusion time δ_v^2/ν of momentum through the boundary layer (of thickness δ_v) reaches a critical fraction of the main flow acceleration time $-(du_\infty/dx)^{-1}$. At the "limit" of the backflow the fluid of the boundary layer separates from the wall and is injected into bulk of the flow (figure 36).

This boundary layer separation implies an injection of vorticity into the main flow, associated with the rotation of fluid particles from the boundary layer. At high Reynolds numbers the fluid from the boundary layers remains for a long time distinct from the surrounding fluid and forms a transition surface between a high and a low-velocity region (separated flow region). The separation "surface" is called a shear layer. Shear layers are unstable and tend to roll-up into structures in which the vorticity is concentrated. We call these structures "vortices". A region of high velocity bounded by shear layers is what we call a "free jet". Free jets are quite unstable and tend to break down into vortex rings which are eventually dissipated by a three-dimensional instability which we call turbulence. Turbulence involves a stretching of vortical structures which induces a rapid transfer of energy from large scale structures down to scales which are so small that viscous dissipation becomes dominant. It is important to realize that, because of the dissipation, the Bernoulli equation is certainly not valid in such a turbulent region.

The three steps:

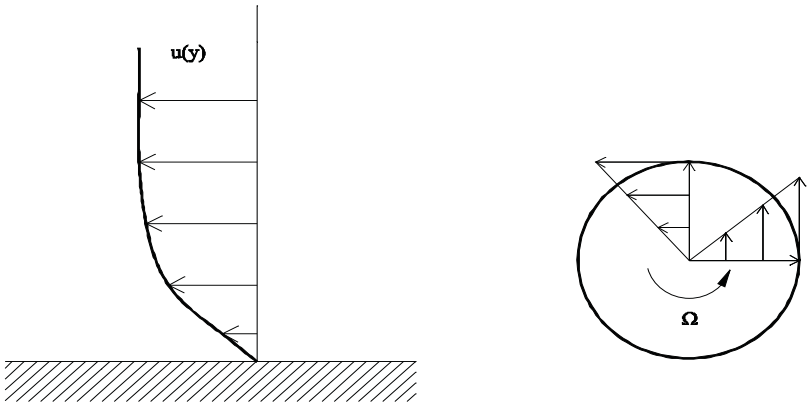

Figure 35: *Boundary layer velocity profile compared to solid body rotation* ($\omega_z = (\partial v/\partial x) - (\partial u/\partial y) = 2\Omega$).

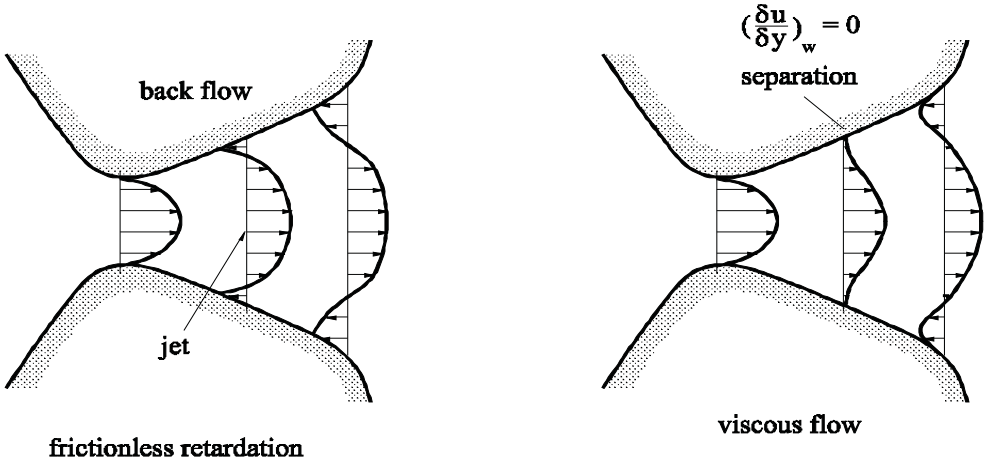

Figure 36: *Flow separation due to an adverse pressure gradient in: a) In a non-uniform frictionless retarded flow we observe back-flow at the wall in the divergent part of the channel. b) In a viscous flow the separation is retarded by the viscous drag of the fluid near the wall by the main flow.*

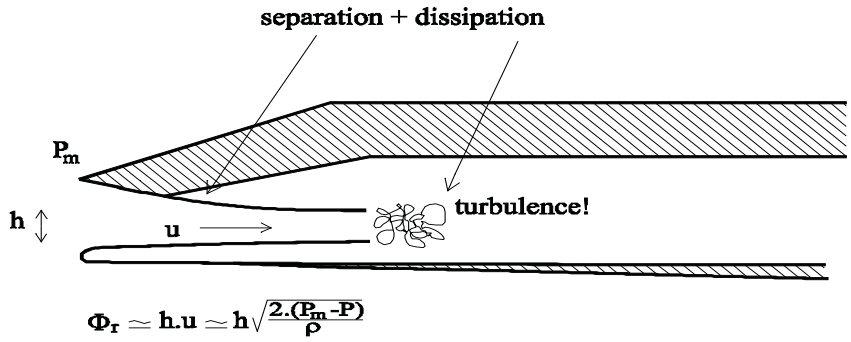

Figure 37: *Flow control by a valve (clarinet reed) involving free jet formation and turbulent dissipation. The velocity in the jet is estimated by applying the equation of Bernoulli from the player's mouth to the jet. We assume a uniform pressure in the mouthpiece.*

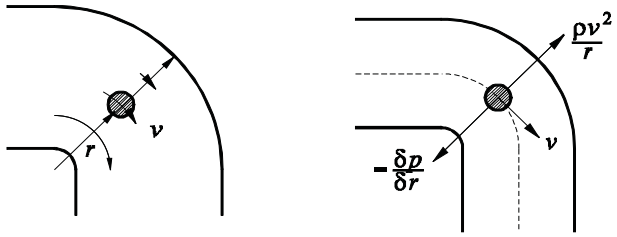

Figure 38: *In a potential flow the streamlines bend as a result of the normal pressure gradient which compensates the centrifugal force on the fluid particle. At a sharp edge this centrifugal force is infinite. The pressure at the edge becomes infinitely low. Following the law of Bernoulli* $\frac{1}{2}\rho_0 v^2 + p =$ *constant, the velocity becomes infinitely large.*

- boundary layer separation
- evolution of the vorticity distribution and
- turbulent dissipation

are the keys to flow control by reeds and therefore to sound production in most wind instruments (figure 37).

We note that flow separation becomes easy to describe within the framework of a frictionless limit if we confine ourselves to sharp edges (rather than smooth surfaces). Near a sharp edge potential flow velocities become infinitely large (figure 38). The gradient $(\partial p/\partial r)$ of pressure necessary to compensate the centrifugal acceleration U^2/R and to make the flow turn around the corner implies a infinitely low pressure at the sharp edge ($R \to 0$). Applying Bernoulli ($p + \frac{1}{2}\rho_0 u^2 =$ const) we see that the velocity becomes infinitely large at the edge. As the velocity gradients also become very large we cannot neglect viscous forces even if the viscosity is small (High Reynolds numbers). By introducing within the flow a vorticity in the form of a shear layer attached to the edge we can compensate this

singular behaviour and obtain a finite velocity at the edge. Imposing a finite velocity appears to correspond to a shear layer leaving the edge tangentially at the upstream side of the edge. This is a very good description of the actual flow separation which is observed in experiments. The condition of the tangential flow separation at a sharp edge, is called, within the framework of a frictionless theory, a "Kutta" condition [19].

6.2 Vortex-sound analogy

In the previous section we have suggested that potential flows are silent. The velocity in a potential flow is the gradient of a scalar potential $\vec{v} = \nabla\varphi$. Such a flow has not rotation because $\vec{\omega} = \nabla \times \nabla\varphi = 0$. We have seen in the previous section that deviation from potential flow behaviour is due to injection of rotational fluid from the viscous boundary layers into the main flow. This occurs as a result of flow separation due to adverse pressure gradients. The vorticity $\vec{\omega}$ is a measure for the rotation of fluid particles. The magnitude $|\vec{\omega}|$ of the vorticity is twice the angular velocity of the fluid particle. We expect from the previous section that vorticity is a source of sound.

This can be established formally by considering the analogy of Howe which defines the acoustical flow as the unsteady irrotational component of the total flow. Given a velocity field $\vec{v}$ we can use the decomposition of Helmholtz to separate the flow into a rotational and an irrotational part:

$$\vec{v} = \nabla\varphi + \nabla \times \vec{\psi} \tag{243}$$

where φ is a scalar potential and $\vec{\psi}$ is a vector stream function. The vorticity is given by $\vec{\omega} = \nabla \times \nabla \times \vec{\psi}$. Furthermore the effect of compressibility are taken into account by the potential component of the flow $\nabla \cdot \vec{v} = \nabla^2\varphi$. As we know that the acoustic field should be a compressible and unsteady flow, we define the acoustical flow velocity $\vec{u}$ as:

$$\vec{u} = \nabla\varphi' \tag{244}$$

where $\varphi' = \varphi - \varphi_0$ is the deviation of φ from the steady component φ_0 of the potential.

An explicit relationship between vorticity and sound production is obtained by starting from the equation of motion for a homentropic flow (Crocco's equation):

$$\frac{\partial\vec{v}}{\partial t} = -\nabla B - (\vec{\omega} \times \vec{v}) + \frac{\vec{f}}{\rho} \, . \tag{245}$$

We further introduce the notation:

$$\vec{f_c} = -\rho(\vec{\omega} \times \vec{v}) \tag{246}$$

for the density of the Coriolis force experienced by an observer moving with the flow. We see that $\vec{f_c}$ acts as an external force on a potential flow. As $B = i + |\vec{v}|^2/2$ is a constant

in a steady potential flow it looks promising to use the fluctuation $B' = i' + \vec{V}'\vec{v}_0$ as aero-acoustical variable ([51], [27], [78]). Taking the divergence of Crocco's equation subtracting the time derivative of the mass conservation law we obtain:

$$\frac{\partial}{\partial t}(\frac{1}{\rho}\frac{D\rho}{Dt}) - \nabla^2 B = -\nabla \cdot (\frac{\vec{f_c} + \vec{f}}{\rho}) \ . \tag{247}$$

In order to obtain a wave equation for B we now add on both sides of equation (247) the term $\frac{1}{c_0^2}\frac{D_0^2 B'}{Dt^2}$ and find:

$$\frac{1}{c_0^2}\frac{D_0^2 B'}{Dt^2} - \nabla^2 B' = -\nabla \cdot (\frac{\vec{f_c} + \vec{f}}{\rho}) + [\frac{1}{c_0^2}\frac{D_0^2 B'}{Dt^2} - \frac{\partial}{\partial t}(\frac{1}{c^2}\frac{Di}{Dt})] \tag{248}$$

in which we have made use of the equation:

$$\frac{D\rho}{Dt} = \frac{1}{c^2}\frac{Dp}{Dt} = \frac{\rho}{c^2}\frac{Di}{Dt} \ . \tag{249}$$

We define $B' = B - B_0$ as the deviation from the steady potential flow total enthalpy B_0 and c_0 the corresponding local speed of sound. Further we use the definition:

$$\frac{D_0}{Dt} = \frac{\partial}{\partial t} + (\nabla\varphi_0) \cdot \nabla. \tag{250}$$

We distinguish now two aero-acoustical sources of sound: the Coriolis force and a second term which we have put between brackets [...]. It is obvious that for very low Mach numbers $U_0/c_0 << 1$ this additional term vanishes. Deviations are expected to have in first approximation a monopole character and to scale with the volume of the source region. Howe [51] suggested if, we limit ourselves to small Mach number flows and to compact source regions, this sound source is negligible. This is confirmed by experience.

When convective effects are negligible $M << 1$ we can use Kirchhoff energy equation for a harmonic acoustical field and we obtain the equation for the power $< P_v >$ generated by vortices:

$$< P_v >= \int_V < \vec{f_c} \cdot \vec{u} > dV \tag{251}$$

which will be most useful to provide heuristic models of the interaction between vortices and acoustical flow.

The success of "Vortex-Sound" theory is due to the fact that vorticity is much more confined (limited in space) than the sound source of Lighthill. As shown by Powell [91], Möhring [70] and Schram [103] the formulation of the analogy in terms of vortex sound allow the reinforcement of momentum and energy conservation to our flow model. Furthermore as understood by Powell, it allows to use all the powerful methods of vortex dynamics. We give a short introduction to this subject in the next section.

6.3 Vortex dynamics

We now consider more general flows in which there is some vorticity ($\vec{\omega} \neq 0$). In the case of a frictionless homentropic flow we can, by taking the curl of Crocco's equation, deduce an equation which involves only the kinematic quantities [14] $\vec{v}$ and $\vec{\omega}$:

$$\frac{\partial \vec{\omega}}{\partial t} = -\nabla \times (\vec{\omega} \times \vec{v}) = -(\vec{v} \cdot \nabla)\vec{\omega} + (\vec{\omega} \cdot \nabla)\vec{v} \ , \tag{252}$$

or, using the mass-conservation law, we find:

$$\frac{D}{Dt}(\frac{\vec{\omega}}{\rho}) = [(\frac{\vec{\omega}}{\rho}) \cdot \nabla]\vec{v} \ . \tag{253}$$

This equation is a consequence of the absence of tangential (viscous) forces on the particles of fluid. Without tangential forces there is no torque and the impulse momentum of the particle should be conserved. The particle rotation increases as a result of a stretching $(\vec{\omega} \cdot \nabla \vec{v})$ in the direction of $\vec{\omega}$ because of the reduction of the moment of inertia of the particle by stretching. When there is no stretching the vorticity remains constant. We can therefore also expect that in more general situations where the flow is not irrotational, we can still deduce the flow from purely kinematic equations. The easiest case is that of an incompressible two-dimensional flow $\vec{v} = (v_1, v_2, 0)$ for which the vorticity $\vec{\omega} = (0, 0, \omega)$ of a fluid particle remains constant [15]:

$$\frac{D\vec{\omega}}{Dt} = 0 \ . \tag{254}$$

Vorticity "dynamics" based on this equation enables the expert in fluid dynamics to make an "intuitive" prediction of the flow [101]. Some numerical methods like the vortex blob method [62], are based on this two-dimensional frictionless flow approximation.

As an example of the use of point vortex models we consider a pair of two line vortices with opposite circulations Γ and $-\Gamma$. The circulation which corresponds to the strength of the vortex is the integral of $\vec{v}$ along a contour C enclosing the vortex:

$$\Gamma = \oint_c \vec{v} \cdot d\vec{s} = \int_S \vec{\omega} \cdot \vec{n} dS \ .$$

Using Stokes theorem this can be written as the integral of the "flux" of vorticity $\vec{\omega}$ through a surface S sustained by C. For the case of a line vortex we expect a circular flow pattern with tangential velocity v_θ around the vortex line. The circulation can then be written as: $\Gamma = 2\pi r v_\theta$, where r is the distance to the vortex line. This means that the vortex induces a velocity field: $v_\theta = \frac{\Gamma}{2\pi r}$. The radial velocity $v_r = 0$ vanishes because we assume that

[14] $\nabla \times \nabla B = 0$ and we assume that $\nabla \times (\vec{f}/\rho) = 0$ because $\vec{f} = 0$.

[15] In a three-dimensional flow the vorticity of a particle changes as a result of the stretching of a fluid particle, which induces an increase of angular velocity by conservation of angular momentum. Since in an incompressible two dimensional flow the particles are not stretched in the direction of $(0, 0, \omega)$, the vorticity of a fluid particle remains constant.

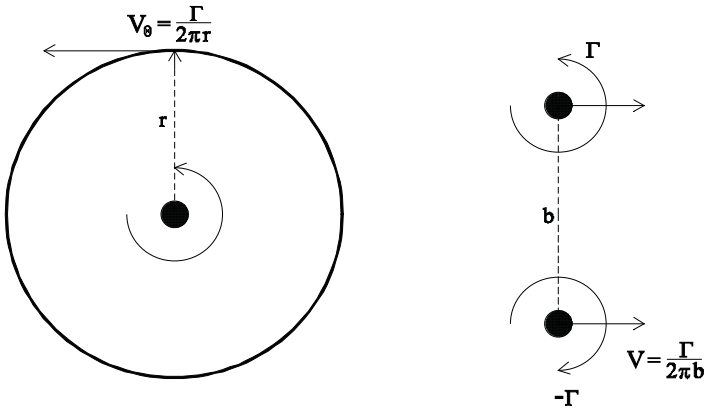

Figure 39: *a) Flow pattern around a line vortex and b) movement of a pair of line vortices.*

there is no source of volume in the flow. As vorticity moves with the local flow velocity in an incompressible two-dimensional flow ($D\omega_z/Dt = 0$) a pair of vortices with opposite circulations (Γ and $-\Gamma$) will move with a velocity ($\Gamma/2\pi b$), where b is the distance between the vortices. A pair of vortices with the same circulation will turn around the midpoint of the line segment joining their cores. This type of vortex motion is discussed in detail by Saffman [101].

Using point vortices and applying the images method it is a simple matter to predict the interaction of vortices with rigid walls. Furthermore, study of the perturbation of an infinite row of point vortices unables us to comprehend the instability of so-called shear layers (see next section) and the formation of large coherent vortical structures which we call "vortices".

6.4 Dipole character of vortex sound

It is a puzzling fact that in Powell's analogy we have obtained an approximation of Lighthill's quadrupole $\partial^2 \rho v_i v_j / \partial x_i \partial x_j$ which has a dipole character $-\nabla \cdot \vec{f_c}$. We discuss this "paradox" in the present section.

A key property of vorticity is that its elementary form is a dipole. There are no sources of vorticity. This can easily be verified from the definition $\vec{\omega} = \nabla \times \vec{v}$ which implies that the vorticity field is divergence-free: $\nabla \cdot \vec{\omega} = 0$. Vorticity lines $\vec{s}(\vec{x}, t)$ defined by $\vec{\omega} \times d\vec{s} = 0$ are consequently closed-curved [16]. The most elementary form of vorticity distribution is therefore a vortex ring. In a simplified model we can concentrate the vorticity in a torus of

[16] In frictionless theory the effect of the vorticity in the boundary layers is taken into account by images of the "vorticity" field in the wall. Vortex lines ending on a wall form a closed curve together with their images.

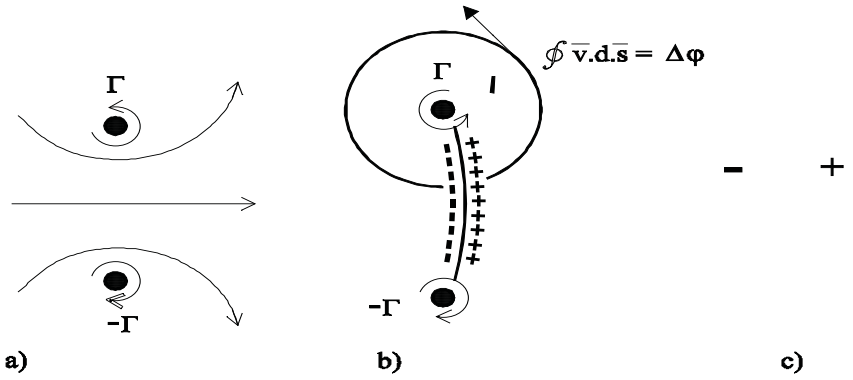

Figure 40: *Dipole character of a vortex ring [94].*

limited thickness. In practice this core thickness is determined by viscous forces. Outside this core we have a potential flow. For any curve C which does not enclose the core the circulation $\oint_c \vec{v} \cdot d\vec{s}$ is zero. Any curve enclosing the core has a circulation:

$$\Gamma = \oint_c \vec{v} \cdot d\vec{s} = \int_s \vec{\omega} \cdot \vec{n} dS \ , \tag{255}$$

independent of the choice of the contour C, as long as it encloses the core. The surface S in this equation is an arbitrary surface sustained by the contour C.

In many examples of applications of vortex-sound theory the vorticity $\vec{\omega}$ is concentrated in a line vortex corresponding to the limit of a infinitely thin core. It is important to realize that this model introduces spurious effects. In a two-dimensional flow a system of four (or more) line vortices show a chaotic behaviour due to the singularity of the velocity at the vortex line. Furthermore a line vortex ring cannot exist in a three-dimensional flow because the curvature of a line vortex implies an infinitely large self-induced velocity. The finite thickness of the viscous core is essential [4].

In view of the fact that we implicitly always assume a finite viscous core [94], we further discuss the flow induced by a vortex ring formed by a closed vortex line. Taking the circulation around the vortex core we find that the potential φ is not single-valued. Assuming an integration from a point A towards a point B placed on both sides of a control surface S_Γ sustained by the vortex ring (figure 40) we find a jump $\Delta\varphi$ of the potential at S_Γ:

$$\Delta\varphi = \int_A^B \vec{v} \cdot d\vec{s} = \oint_C \vec{v} \cdot d\vec{s} = \Gamma \ , \tag{256}$$

corresponding to the circulation of the vortex line. As explained by Prandtl [94], a discontinuity $\Delta\varphi$ on the surface S_Γ can be considered as induced by a uniform layer of dipoles with a strength Γ per unit area on S_Γ. This dipole layer is the limit (for $Q \to \infty$ and $\delta \to 0$) of a layer of sources with total strength Q separated by a distance δ from a layer of

sinks of equal strength. This signifies a large uniform flow in the interface between the two layers. The momentum associated with this dipole distribution is $(Q\delta) = |\rho_0 \Gamma \int_S \vec{n} dS_\Gamma|$.

Applying a force $\vec{F}$ for a certain time on the flow implies the production of a momentum $\int \vec{F} dt$ which corresponds to the creation of a vortex structure of dipole strength $\rho_0 \Gamma \int_S \vec{n} dS_\Gamma = \int \vec{F} dt$. When the product of the circulation Γ times the surface S_Γ changes, there is a force acting on the flow [17]. It is therefore not surprising that a study of the evolution of the vorticity in a flow field provides information on the forces acting on the flow.

An example of this is the flow through a glottis. Due to boundary layer separation, a free jet is formed in the diverging part of the glottis (section 6.1). Because of turbulent mixing the vorticity in the shear layers delimiting the jet is annihilated further downstream (figure 36). The jet between the separation point and the turbulent mixing region forms a vorticity distribution which induces a pressure difference $\Delta p = \frac{1}{2} \rho U_j^2$ across the glottis, U_j being the flow velocity in the jet. In terms of vortex sound the deviation between the jet flow and a potential flow is a source of sound. This source of sound is a dipole corresponding to the force $S_j \Delta p$, S_j is the jet's cross-sectional area. This representation is equivalent to the more classical model in which the volume flux $(S_j U_j)$ is assumed to act as a volume source for the downstream part of the acoustic system (vocal tract). The advantage of the vortex-sound interpretation of the flow is that it not only enables us to understand the quasi-stationary jet flow but could also be used to formulate a model of an essentially non-stationary sound-production mechanism. For example the impingement of the modulated vorticity of the jet on the false vocal cords can result in whistling as discussed in a double-diaphragm configuration by Rayleigh [95], Bouasse [10], Wilson and Beavers [115] and Stokes & Welsh ([107], [47]).
When no net force is acting on the flow as is the case when considering a turbulent free jet, there is no net dipole and, as explained by Lighthill [68], the sound is produced by a quadrupole. If we observe an acoustical dipole there is a force involved in the sound production.

If we consider the sound production of vortices in free field conditions we can write the analogy of Howe [51] in the form:

$$B' = - \int_{-\infty}^{t^+} \int_V G_0(\vec{x}, t | \vec{y}, \tau) \nabla \cdot (\vec{\omega} \times \vec{v}) dV_y d\tau \ . \tag{257}$$

By partial integration and making use of the symmetry of the free space Green's function $\nabla_x G_0 = -\nabla_y G_0$ we find:

$$B' = -\nabla_x \cdot \int_{-\infty}^{t^+} \int_V G_0(\vec{x}, t | \vec{y}, \tau) (\vec{\omega} \times \vec{v}) dV_y d\tau \ . \tag{258}$$

[17] Applying the steady Bernoulli equation across the surface S_Γ we see that a time-dependence of the circulation $\Gamma = \Delta\varphi$ corresponds to a pressure jump $\Delta p = -\rho_0 (\partial\Gamma / \partial t)$. $\int \Delta p \vec{n} dS_\Gamma$ corresponds to the force $\vec{F}$ acting on the flow which causes the variation in Γ.

Using a multipole expansion around $\vec{y} = 0$ and noting the leading order term (dipole) should vanish in the absence of external forces we have:

$$\begin{aligned} B' &= -\nabla_x \cdot \int_{-\infty}^{t^+} \int_V G_0(\vec{x}, t|0, \tau)(\vec{\omega} \times \vec{v}) dV_y d\tau \\ &- \nabla_x \cdot \int_{-\infty}^{t^+} \int_V (\nabla_y G_0)_{\vec{y}=0} \cdot \vec{y}(\vec{\omega} \times \vec{v}) dV_y d\tau \end{aligned} \tag{259}$$

which yields in the far field approximation and using the delta function in G_0 to carry out the time integration:

$$B' = -\frac{x_i x_j}{4\pi |\vec{x}|^3 c_0^2} \frac{\partial^2}{\partial t^2} [\int_V y_i (\vec{\omega} \times \vec{v})_j dV_y]_{\tau = t_e} \tag{260}$$

with $t_e = t - |\vec{x}|/c_0$. This is Powell's result. For a compact source region we neglect the variation of t_e over the jet ([91], [20], [22]). For jet of circular cross section the Strouhal number $St_D = fD/U_0$ based on the dimension of the vortical region D is of order unity. The condition of compactness $Dk2\pi \left(\frac{Df}{U_0}\right) \left(\frac{U_0}{c_0}\right) << 1$ also implies $U_0/c_0 << 1$. In the case of planar free jets, however, it appears [6] that the Strouhal number $St_h = hf/U_0$ based on the jet thickness h is of the order of $St_h \simeq 3 \times 10^{-2}$.

Using his formula Powell [91] predicted the sound production of two co-rotating vortex lines (2-D flow).

Möhring ([71], [20]) has proposed for low Mach numbers $\frac{U_0}{c_0} \ll 1$ compact vortical flows $k_0 D << 1$ in free space an alternative formulation of equation (260) which can have some numerical advantages:

$$p' = \frac{\rho_0}{12\pi c_0^2 |\vec{x}|^3} \frac{\partial^3}{\partial t^3} [\int_V x_i y_i y_j (\vec{\omega} \times \vec{x})_j dV_y]_{\tau = t_e} \ . \tag{261}$$

As explained by Schram [103], the difference between Powell's and Möring's formulation is due to a difference in reinforcement of momentum and energy conservation in the flow. For circular symmetrical flows an additional reinforcement of the energy conservation results into a very robust formulation. Using this formulation Möhring [71] was able to describe the sound production of leap-frogging circular vortex rings by means of a highly simplified locally 2-D flow model.

6.5 Grazing flow along a Helmholtz resonator

An empty bottle, the open window of a car, a harbour,... (Fig. 41) are examples of Helmholtz resonators which "whistle" when exposed to a grazing flow along the opening. Such oscillations have been described by Elder [30] in terms of a model analogous to Fletcher's jet drive in flue instruments. Howe [49], Möhring [70], Crighton [21], ... have

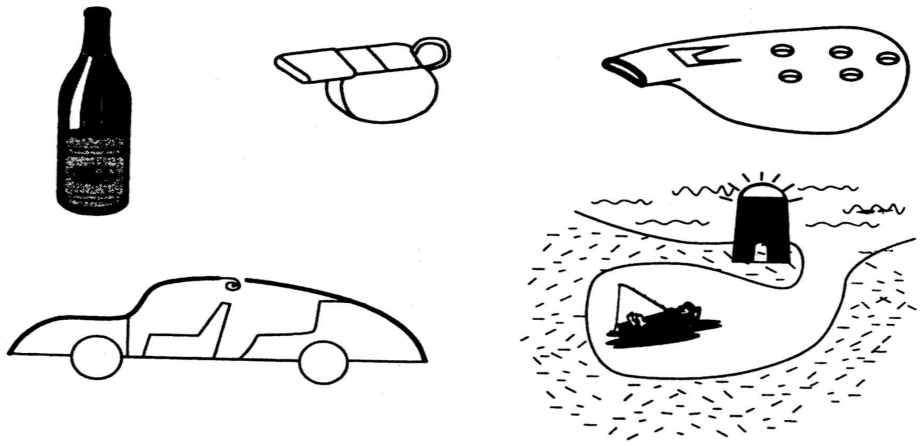

Figure 41: *Some Helmholtz resonators.*

developed linear models to predict the conditions of stability of such flows described in terms of thin shear layers.

We present here a modification of the simple *non-linear* model proposed by Nelson [81] for a study of flow pulsations in a muffler. The model appears to describe qualitatively the self-sustained flow pulsations in pipe systems with closed side branches [11], [88]. This simple model is a prototype of a vortex-sound theory.

We start our discussion by considering the non-oscillating grazing flow across an orifice of a resonator. The flow separates at the upstream edge of the orifice to form a shear layer separating the main flow U_∞ outside the resonator from the "stagnant" fluid in the resonator. We further assume a rectangular orifice of width W in the direction of the flow (x-axis) and depth H normal to the main flow (z-axis). The circulation $\Delta\Gamma$ of an element of length Δx of the shear layer can be calculated by taking the circulation along a path enclosing the element (Fig. 42). We find:

$$\Delta\Gamma = \oint_{\Delta S} \omega_z dS = \oint_C \vec{v} \cdot d\vec{s} = -U_\infty \Delta x \ . \tag{262}$$

The fluid in the shear layer is convected with a velocity U_c which is a compromise between U_∞ and the low velocity in the resonator:

$$U_c \simeq U_\infty/2 \ . \tag{263}$$

This entails a rate of flow of vorticity along the upstream edge at the origin of the shear layer of:

$$\frac{d\Gamma}{dt} = \frac{d\Gamma}{dx} U_c = -U_\infty U_c \ . \tag{264}$$

Nelson [81] assumes that this rate of vorticity shedding is not modified by the pulsations. The perturbation of the shear layer by the transversal acoustic field is assumed to trigger

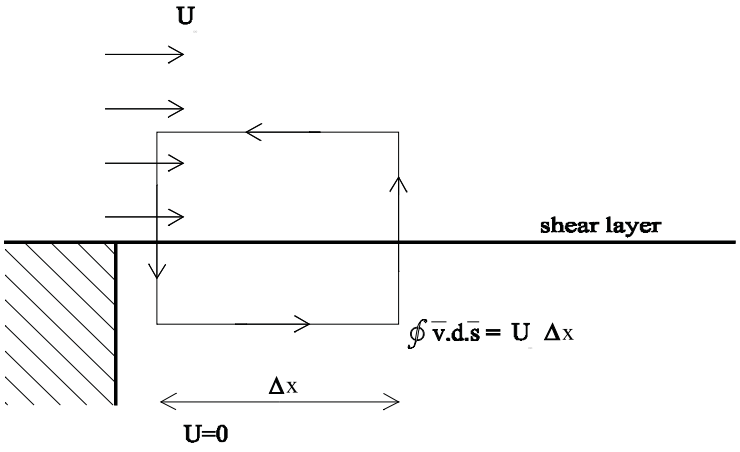

Figure 42: *Nelson's model of vortex shedding.*

a concentration of the vorticity into discrete line vortices rather than a modification of the rate of vorticity shedding at the upstream edge of the orifice $d\Gamma/dt$. This model was found by Bruggeman [11] to be valid under conditions of moderately large acoustic amplitudes:

$$10^{-2} \leq u'_a/U_\infty \leq 10^{-1} \ . \tag{265}$$

These amplitudes are strong enough to induce a saturation of the shear layer instability leading to the formation of discrete vortical structures (figure 44) and yet weak enough for the flow separation at the upstream edge to be controlled by the steady mean flow.

The vortices are formed each time period T at: $t = nT + \tau_c$. Nelson [81] and Bruggeman [11] both found that t corresponds to the instant at which the acoustic flux changes direction from outwards to inwards of the resonator [18]. For harmonic oscillations this corresponds to a minimum of the pressure in the resonator. According to this model the circulation of the vortex increases linearly with time during the first period of its life. In Nelson's model we assume that the vortex is convected along the plane of the unperturbed shear layer ($y = 0$) with a uniform velocity $U_\Gamma \simeq 0.4U_\infty$:

$$\omega_z = -(t - nT - \tau_c)U_\infty U_c \delta(x - x_\Gamma)\delta(y - y_\Gamma) \ , \tag{266}$$

for $t - \tau_c < (n+1)T$ where:

$$x_\Gamma = (t - nT - \tau_c)U_\Gamma \ , \tag{267}$$

and

$$y_\Gamma = 0 \ . \tag{268}$$

[18] This is only valid for moderate amplitudes. At large amplitudes the acoustic field induces a shift of the vortex shedding which is discussed by Peters [88] and Kriesels [63]. At low amplitudes the vortex shedding is not only controlled by acoustical perturbations of the shear layer. Hydrodynamic feedback also becomes significant resulting in other phase conditions for vortex shedding

Note that U_Γ differs from the local convection velocity U_c of vorticity near the upstream edge of the orifice. The velocity U_Γ corresponds to the convection of a large coherent vortical structure rather than to a distributed vorticity convected with the velocity U_c. After one period of oscillation the circulation saturates and we have a time-independent vorticity of the vortical structure:

$$\omega_z = -T(U_\infty U_c)\delta(x - x_\Gamma)\delta(y - y_\Gamma) \ , \tag{269}$$

for $t - \tau_c > (n+1)T$. For the sake of simplicity we approximate the acoustic velocity field $\vec{u}'_a$ through the orifice as a harmonic, spatially uniform [19] flow of amplitude $\hat{u}_m$:

$$\vec{u}'_a = (0, -\hat{u}_m \sin \omega_0 t, 0) \ , \tag{270}$$

with $\omega_0 = 2\pi/T$.

Substitution of this vortex model of the shear layer and of this simple acoustic field in Howe's energy corollary provides the rate of production $< P_s >$ of energy by the shear layer:

$$< P_s >= \rho_0 \hat{u}_m U_\infty U_c W H \frac{\cos(St_\Gamma)}{St_\Gamma} \ , \tag{271}$$

for:

$$St_\Gamma = \frac{W\omega_0}{U_\Gamma} > 2\pi \ , \tag{272}$$

and:

$$< P_s >= \rho_0 \hat{u}_m U_\infty U_c W H \frac{1}{2\pi} \left[\cos(St_\Gamma) - \frac{\sin St_\Gamma}{(St_\Gamma)} \right] \ , \tag{273}$$

for:

$$St_\Gamma < 2\pi \ . \tag{274}$$

The function $< P_s > /P_{ref} = 2\pi < P_s > / \frac{1}{2}\hat{u}_m \rho U_\infty U_c (HW)$ is shown in Fig.43.

We observe a series of critical velocities for maxima of $< P_s >$ corresponding to successive "hydrodynamic modes" of the shear layer. Flow visualizations of the first two hydrodynamic modes have been obtained by Nelson [81], Bruggeman [11] and Peters [88] (Fig. 44).

In principle the production of sound could be balanced by radiation and friction losses of the resonator. This would lead to rather unrealistically large pulsation amplitudes $\hat{u}_m/U_\infty$. A more realistic pulsation amplitude is obtained by assuming energy losses due to vortex shedding at the (sharp) downstream edge of the resonator. Two simple models are available to describe this vortex shedding:

- the quasi-steady approximation ([55], [26]) and

[19] The exact spatial distribution of the acoustic flow depends on the geometry of the orifice. If the edges of the orifice are sharp, the flow is certainly non-uniform [48], [112]. At the edges the velocity field is singular. The assumption of a spatially uniform acoustic field is reasonable when the edges of the cavity are rounded.

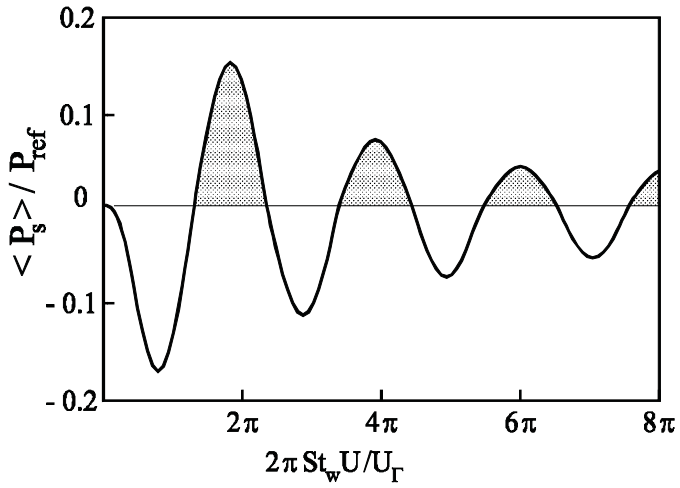

Figure 43: *Acoustical power $< P_s >$ produced by the shear layer as predicted by Nelson's model. The Strouhal number St_w is defined as $St_w = \omega_0 W/U_\infty$. When $< P_s >$ is positive, self-sustained oscillations can be sustained.*

Figure 44: *Visualization of vortical structures formed by acoustic perturbation of a shear layer at moderate amplitudes (second hydrodynamic mode).*

- the high Strouhal number approximation [48].

In the first model we assume a quasi-steady free jet formed at the orifice as a result of the transversal acoustic flow. We assume that this induces a pressure difference $\frac{1}{2}\rho_0 u_m^2$ across the orifice. Using this model we find a dissipated acoustic power:

$$< P_d >= - < \frac{1}{2}\rho_0 \hat{u}_m^3 (H \times W) > \ . \tag{275}$$

This simplified model corresponds to the assumption that the vortex shedding at the downstream edge of the orifice can be described as a separation of the transversal flow through the orifice driven by the acoustic oscillation. We assume that this phenomenon is independent of the shear-layer flow. We further assume that there is no recovery of the pressure in the free jet. These are rather crude assumptions. It is strange to use a unsteady model for the vorticity in the shear layer while we use here a quasi-stationary model for the vortex shedding at the downstream edge of the orifice.

The second model which seems more reasonable presupposes a local vortex shedding at the downstream edge of the orifice. We assume that the flow separates at the edge and that the vorticity can be concentrated in a single line vortex. The strength and position of the vortex are calculated by assuming a Kutta condition of finite flow velocity at the edge [48]. Within the framework of such a local model it is reasonable to assume that this vortex shedding is driven by the transversal flow independently of the shear-layer behaviour. For typical Strouhal numbers $St_a = \omega_1 W/\hat{u}_m = O(1)$, the acoustic energy absorption predicted by this model is of the same order of magnitude as that predicted by the quasi-stationary model discussed above. In his original paper Howe [48] takes into account the influence of the uniform grazing flow U_∞. For the present application it seems more appropriate to assume that the local vortex shedding is only induced by the acoustic flow through the orifice. We neglect the main flow U_∞ in the local description of the vortex shedding. If we furthermore assume that the acoustic velocity has a constant value during each half-period (alternating only in sign), the solution of the flow problem is self-similar and can be obtained analytically. Peters [88] finds the acoustic power produced by this type of vortex shedding to be: $< P_d >= -\left(\frac{9}{\pi}\right)^{5/3} \frac{1}{\sqrt{32}} \left(\frac{St_a}{2\pi}\right)^{1/3} \frac{1}{2}\rho_0 \hat{u}_m^3 WH$ for a rectangular edge (angle $\frac{\pi}{2}$). According to Howe's model $< P_d >$ scales with $\hat{u}_m^{8/3}$.

The balance of the power $< P_s > + < P_d >= 0$, can be used to calculate $(\hat{u}_m/U_\infty)$. It is typically found [63] that:

$$\hat{u}_m/U_\infty = 0(1) \ . \tag{276}$$

This result is independent of the type of vortex-shedding model used. As $< P_s >$ is proportional to $\hat{u}_m$ while $< P_d >$ scales with $\hat{u}_m^3$, it is obvious that $(\hat{u}_m/U_\infty)$ is not very sensitive to the details of the model. A more detailed discussion of three different models is provided by Dequand [25]. For rounded edges of the orifice Dequand [25] observes experimentally $\hat{u}_m/U_\infty \simeq 0,6$. For a cavity with sharp edges the amplitude decreases to $\hat{u}_m/U_\infty \simeq 0.1$.

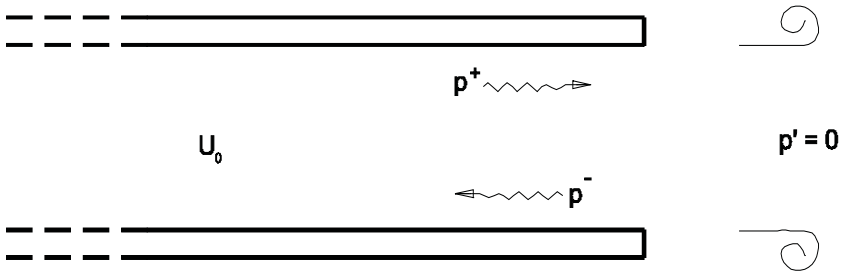

Figure 45: *Pipe termination with flow*

6.6 Low frequency behaviour of an open pipe termination

We consider a sharp-edged open pipe termination (figure 45).

We assume free space outside the pipe. Due to the presence of a subsonic main flow trough the pipe a free jet is formed in which the kinetic energy of the flow is dissipated. We assume a quasi-steady behaviour of the jet. In such a case the pressure in the jet will be equal to the pressure of its surroundings. If we assume a uniform main flow the linearized mass conservation law becomes:

$$(\frac{\partial}{\partial t} + U_0 \frac{\partial}{\partial x})\rho' + \rho_0 \frac{\partial v'}{\partial x} = 0 \ . \tag{277}$$

The corresponding momentum equation is:

$$\rho_0 (\frac{\partial}{\partial t} + U_0 \frac{\partial}{\partial x})v' + \frac{\partial p'}{\partial x} = 0 \ . \tag{278}$$

Elimination of v' and of $\rho' = p'/c_0^2$ yields the wave equation:

$$\frac{1}{c_0^2}(\frac{\partial}{\partial t} + U_0 \frac{\partial}{\partial x})^2 p' - \frac{\partial^2 p'}{\partial x^2} = 0 \ . \tag{279}$$

The corresponding solution is:

$$\hat{p} = p^+ \exp[-ik_0^+ x] + p^- \exp[ik_0^- x] \tag{280}$$

with:

$$k_0^\pm = \frac{\omega}{c_0 \pm U_0} \ . \tag{281}$$

Substitution in the momentum equation (278) yields:

$$\hat{v} = \frac{p^+ \exp[-ik_0^+ x] - p^- \exp[ik_0^- x]}{\rho_0 c_0} \tag{282}$$

If we neglect acoustical radiation we will have a zero acoustical pressure at the outlet $p'_{out} = 0$. If a pressure wave p^+ is traveling towards the pipe outlet a reflected wave p^- will be generated to satisfy this boundary condition. So we have:

$$p^+ + p^- = 0 \tag{283}$$

and a corresponding pressure reflection coefficient:

$$\frac{p^-}{p^+} = -1 \ . \tag{284}$$

In contrast with the case of an ideal open pipe termination this does not mean that there are no acoustical energy losses upon reflection. If we consider the fluctuations of total enthalpy B' we have in linearized approximation:

$$B' = \frac{p'}{\rho_0} + U_0 v' \tag{285}$$

so that:

$$B^{\pm} = \frac{p^{\pm}}{\rho_0}(1 \pm \frac{U_0}{c_0}) \ . \tag{286}$$

From equation (284) we find:

$$\frac{B^-}{B^+} = \frac{U_0 - c_0}{U_0 + c_0} \ . \tag{287}$$

This formula is in close agreement with experimental results at low Strouhal numbers $\omega a_0/U_0 < 1$ [89].

The absorption of acoustical energy corresponds to the absorption which we found in our discussion of the Helmholtz resonator (section 6.5). Using the vortex sound theory we can predict this behaviour by assuming (within an acoustical model) a discontinuity in the total enthalpy $\Delta B_{source} = -U_0 v'$ placed at the pipe termination. This aero-acoustical source corresponds to the deviation of the actual flow from the reference potential flow which we would have without the formation of a free jet. The acoustical energy absorption $- < (\rho' U_0 + \rho_0 v')\Delta B_{source} >$ can be expressed in terms of the real part of a radiation impedance $\frac{1}{2} Re[z]|v'|^2$. As $p' = 0$ and consequently $\rho' = 0$ we find [55]:

$$Re[z]/\rho_0 c_0 = M$$

The absorption of acoustical energy by the flow at the pipe termination can be used to design a non-reflecting pipe termination. This is what we call an anechoïc termination (without echo). For this purpose Bechert proposed to place an orifice with opening S_j at the end of a pipe with cross-section S_p (figure 46 [5]). Using a quasi-steady incompressible flow model we find the velocity U_j in the free jet:

$$\rho_j U_j S_j = \rho_p U_p S_p. \tag{288}$$

The equation of Bernoulli:

$$B_j = B_0 \tag{289}$$

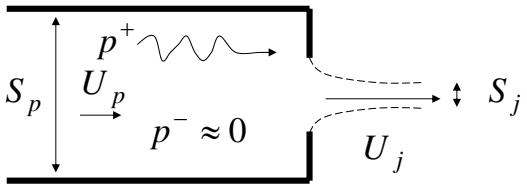

Figure 46: *Anechoïc pipe termination of Bechert.*

becomes in linearized form if we assume $p'_j = 0$:

$$\begin{array}{ll} \rho_0 v'_j S_j = & \rho'_p U_p S_p + \rho_0 v'_p S_p \\ v'_j U_j = & v'_p U_p + \frac{p'_p}{\rho_0} \end{array} \tag{290}$$

In these equations we have neglected terms of the second order in the Mach number U_j/c_0. We assume for example that the average density in the pipe is equal to the density in the jet. Substitution of $p' = c_0^2 \rho', p'_p = p^+ + p^-$ and $v'_p = (p^+ - p^-)/(\rho_0 c_0)$ yields:

$$\frac{p^-}{p^+} = \left(\frac{1 + M_p}{1 - M_p}\right) \left(\frac{1 - M_p \left(\frac{S_p}{S_j}\right)^2}{1 + M_p \left(\frac{S_p}{S_j}\right)^2}\right). \tag{291}$$

From this equation we see that at the critical Mach number given by:

$$\frac{U_0}{c_0} = \left(\frac{S_j}{S_p}\right)^2 \tag{292}$$

the reflection coefficient vanishes. Using a series of diaphragms one can extend the conditions for a reasonably anechoïc behaviour to a finite range of Mach numbers.
In the limit $S_j = S_p$ we recover the reflection coefficient at an open pipe termination given

by equation (284) $p^-/p^+ = -1$. In the opposite limit $S_j/S_p \to 0$ we have $p^-/p^+ = -1$ because $M_p = \left(\frac{S_j}{S_p}\right) M_j \to 0$ for $M_j << 1$. We recover the reflection coefficient at a closed pipe.

Another interesting limit case is the condition when the flow at the orifice is sonic $M_j = 1$. This condition corresponds to the highest Mach number than we can reach at the orifice for a steady isentropic flow. In such a case the flow at the orifice is chocked. If we assume a quasi-steady flow behaviour we have:

$$M_j = \frac{U_j}{c_j} = 1.$$

In quasi-steady approximation the Mach number M_p in the pipe is determined by the ratio S_p/S_j of the pipe cross-section to the orifice cross-section. For a caloric perfect gas with constant specific heat ratio γ we find:

$$\frac{S_p}{S_j} = \frac{1}{M_p} \left(\frac{1 + \frac{\gamma-1}{2} M_p^2}{\frac{\gamma+1}{2}} \right)^{\frac{\gamma+1}{2(\gamma+1)}}.$$

From the condition $M_j^2 = 1$ we therefore find $M_p = const$ which implies:

$$\frac{v_p'}{U_p} = -\frac{c_p'}{c_p} = 0$$

where c_p is the speed of sound in the pipe. For a caloric perfect gas, $p = \rho RT$ and $c = \sqrt{\gamma RT}$ assuming an isentropic flow $(p_p/p_{ref}) = (S_p/\rho_{ref})$ we have:

$$\frac{v_p'}{U_p} - \frac{\gamma - 1}{2\gamma} \frac{p_p'}{p_p} = 0.$$

Using $v_p' = (p^+ - p^-)/\rho_p c_p$ and $p_p' = p^+ + p^-$ we find:

$$\frac{p^-}{p^+} = \frac{1 - \left(\frac{\gamma-1}{2}\right) M_p}{1 + \left(\frac{\gamma-1}{2}\right) M_p} \quad \text{and} \quad \frac{B^-}{B^+} = \frac{(1 - M_p)}{1 + M_p} \frac{\left(1 - \left(\frac{\gamma-1}{2}\right) M_p\right)}{\left(1 + \left(\frac{\gamma-1}{2}\right) M_p\right)}.$$

For low Mach M_p we find:

$$\frac{S_p}{S_j} \simeq \frac{1 + \left(\frac{\gamma+1}{8}\right) M_p^2 + \ldots}{M_p \left(\frac{\gamma+1}{2}\right)^{\frac{\gamma+1}{2(\gamma-1)}}}.$$

For $M_p << 1$ we have:

$$M_p = \left(\frac{S_j}{S_p}\right) \frac{1}{\left(\frac{\gamma+1}{2}\right)^{\frac{\gamma+1}{2(\gamma-1)}}}.$$

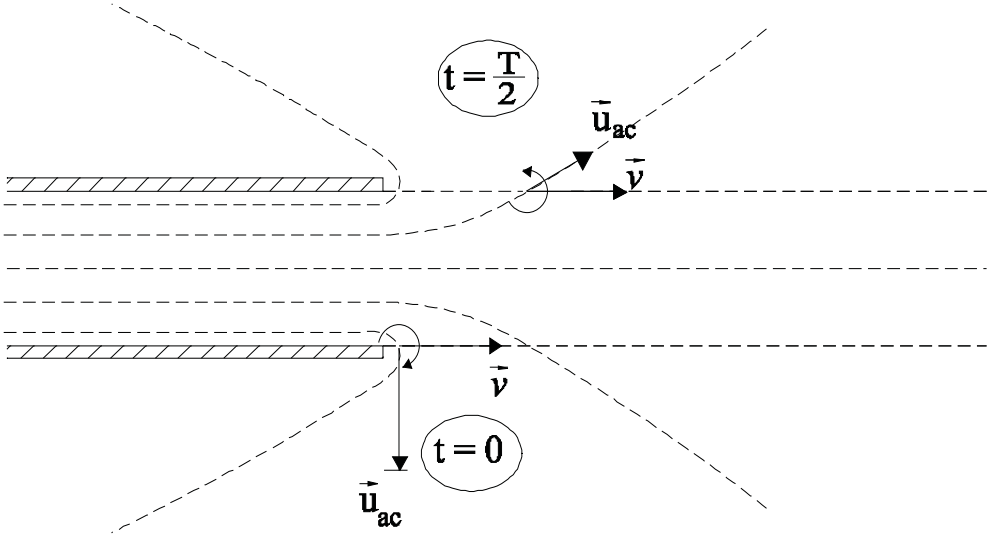

Figure 47: *A model for the flow at the outlet of a pipe with main flow. The acoustical field induces the breakdown of the shear-layer of the free jet into discreet vortices which are convected at a constant velocity in the direction along the pipe axis. The acoustic flow $\vec{u}_{ac}$ has a stream-line pattern corresponding to a potential flow. It has a singularity at the sharp edge of the pipe termination.*

We would like now to understand the absorption of sound in terms of a more detailed flow model. The acoustical velocity fluctuation induces a modulation of the vorticity in the shear layers of the free jet. As these shear-layers are unstable, the perturbation in the vorticity will grow as it is convected away with the flow. A linearized theory taking into account the dynamics of the shear-layers is very complex (Munt [77], Rienstra [98], Cargill [12], Howe [97]). A simple heuristic model can be obtained at moderately high amplitudes. For typical values $v'/U_0 \leq 10^{-2}$ the perturbations in the vorticity of the shear layers will trigger the formation of discreet vortical structures in which all the vorticity shed at the separation point is concentrated. A new vortex is formed each oscillation period when the acoustical velocity turns from pipe inwards to outwards. As the acoustical perturbations are not very large the circulation of the vortex growth linearly in time following Nelson's approximation: $d\Gamma/dt = -U_0^2/2$ (see section 6.5). Those vortices are convected roughly at a constant velocity $U_\Gamma \sim U_0/2$ in the direction of the pipe axis. We have furthermore an acoustical stream-line pattern corresponding to a potential flow (figure 47). It has therefore a singularity at the sharp edge where flow separation occurs.
In order to obtain more insight we now use the energy corrolary of Howe:

$$< P_v >= -\rho_0 \int_V < \vec{\omega} \times \vec{v}) \cdot \vec{u}_{ac} > dV. \tag{293}$$

We first consider the acoustical behaviour of the vortices just as they are formed close to the edge of the pipe termination. Due to its potential flow character the acoustical stream-lines near the edges of the pipe exit are normal to the pipe axis. They turn smoothly

around the corner. Due to the singularity at the edge the acoustical velocity will locally be very large compared to the instantaneous value of the fluctuating velocity v' imposed to the flow in the pipe. The cross product $(\omega \times \vec{v}) \cdot \vec{u}_{ac}$ will be large and positive. Which corresponds to an absorption of sound. This seems logical because there is formation of vortices due to acoustical perturbations. However after half an oscillation period the sign of $(\omega \times \vec{v}) \cdot \vec{u}_{ac}$ changes because the acoustical flow turns from pipe outwards to pipe inwards while the vorticity and the convective velocity $\vec{v}$ keep the same sign. There is therefore now a production of sound. This sound production will however be much weaker than the initial absorption because the vortex is now far from the edge singularity. The acoustical flow velocity decreases and its direction turns towards that of the convective velocity $\vec{v}$ (figure 47). This explains the net sound absorption after an oscillation period.

Now that we have seen that the absorption of sound at an open pipe termination is due to a balance between an initial absorption upon vortex shedding followed by a production of sound, we can try to shift the balance in favor of the production. Replacing the edges by round lips does reduce the singularity of the acoustical flow at the separation point. Furthermore the acoustical velocity is at the separation point almost directed along the pipe axis. Therefore the initial sound absorption becomes quite low. In order to produce sound in the second half of the oscillation period the vortices should not have travelled too far way from the opening. As they travel away the acoustical velocity amplitude decreases roughly with the square of the distance and the direction of the acoustical velocity turns towards the pipe axis. To avoid this we should blow at a critical speed such that the travel time of the vortices along the lips corresponds to about an half oscillation period. For a radius of curvature R_L of the lips we should have $2R_L f/U_0 \simeq 1/2$. This fits quite well with the experiments. When we try to whistle very hard we do not produce any sound. This explains the frustration of children trying to blow harder and harder when they try to whistle. Please note that this model explains that the sound production does not become more efficient when we introduce sharp edges in the flow. This contradicts the early heuristic models in which sound production was assumed to be due to collision of the shear-layers with sharp edges. A sharp edge placed downstream of the flow separation point can increase the sound production but this is not always the case. We have already seen in our discussion of the Helmholtz resonator that vortex shedding at this downstream edge is likely to be an amplitude limiting mechanism in self sustained oscillations. This also occurs in flue organ pipes [113], [31]

The heuristic model described above explains acoustically induced flow instability in diffusers [67].

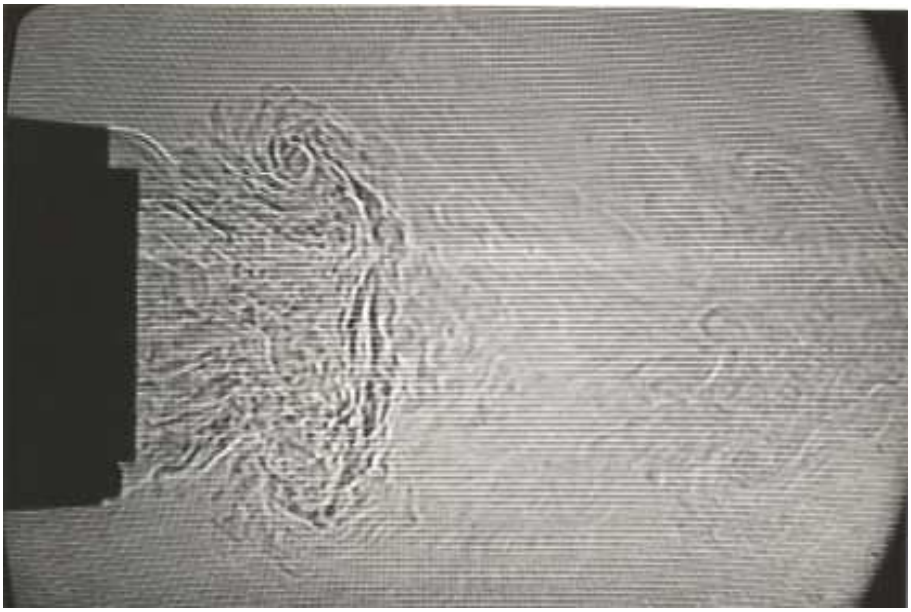

Figure 48: *Acoustically induced flow separation at a sharp edge of a clarinet pipe without horn.*

6.7 High amplitude response of resonators

Flow separation does not only occur as a result of a steady main flow. We consider now a case in which there is no time average main flow. When the amplitude of the acoustical particle displacement $\hat{u}_{ac}/\omega$ becomes comparable to the radius of curvature of an edge we can observe flow separation (figure 48 [26]). In a clarinet the horn will not only enhance the radiation of the musical sounds, it will also prevent flow separation to occurs in spite of the large acoustical displacements. For typical fortissimo blowing pressures $p_m = 3kPa$ the acoustical fluctuations in the pipe correspond to velocities at the pipe exit of the order of $p_m/(\rho_0 c_0) = 8m/s$. (The amplitude of acoustical pressures at the mouth piece reaches the level of the mouth pressure p_m.) For a low note $f = 140$ Hz this corresponds to particle displacement amplitudes $\frac{p_m}{\rho_0 c_0 \omega}$ of almost 1 cm. This is comparable to the pipe radius. At higher frequencies the tone holes are open, so that much of the acoustical flow has to pass through a rather narrow orifice. In spite of the lower acoustical particle displacement due to an increase of the frequency, the acoustical displacement reach the order of magnitude of the diameter of tone holes. If the tone holes are too narrow this causes a severe damping. In fact a thin walled clarinet will need narrower tone holes than a thick walled clarinet in order to achieve the same acoustical inertia. The result is that such a thin walled clarinet does not produce any sound([59],[79]).

One of the key improvement of Boehm in the design of the modern traverso flute was to enlarge the holes. In order to allow for this on a thin-walled pipe, chimneys are placed around the holes. Boehm believed that he had increased the radiation efficiency of his

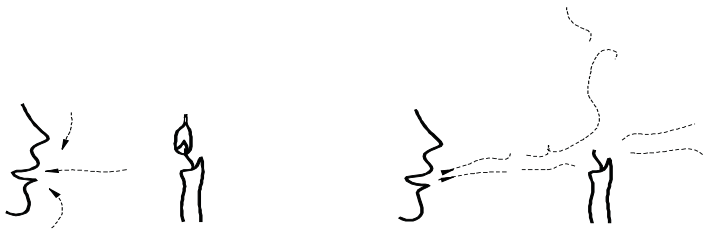

Figure 49: *Non-linearity of the flow at a tone hole. There is a jet formed by the outgoing flow. The incoming flow is potential. It decays with the square of the distance from the hole. You cannot blow a candle by aspiring air.*

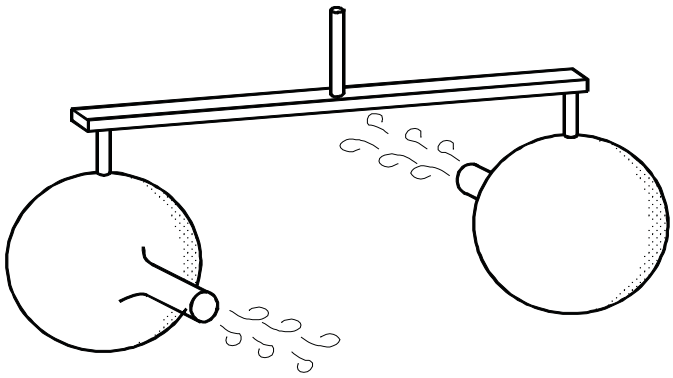

Figure 50: *A carrousel driven by Helmholtz resonators excited at large amplitudes.*

instrument by increasing the mouth-tone and the hole diameters. He did actually reduce losses due to vortex shedding. This allows high oscillation amplitudes in the pipe[31],[113].

Even with thick walls there is a strong vortex shedding at tone holes of a clarinet. When flow separation occurs we can easily feel the outflow because there is formation of a free jet. The inflow cannot be detected because it is a potential flow which decays very rapidly as we move away from the opening of the tone hole. Hence when we place a candle it will be blown away by the outgoing flow, but almost not affected by the inflow. Try to blow a candle out by aspiring air. You need strong lungs to achieve that (figure 49).

As the incoming air flow is not directive it is not associated with any momentum transfer. The outgoing flow form a free jet which carries a momentum flux $\rho S U^2$. This result into a net force on a Helmholtz resonator which is excited at large amplitudes. This effect can be used to make a carrousel turn ([10]) as shown in figure 50.

Similar non-linear flow separation is common in bass reflex ports of loudspeaker boxes [100]. A loudspeaker is placed in a box to avoid leakage of the acoustical flow around the edges of the loudspeaker. At low frequencies the air in a closed box is almost incom-

pressible. In order to allow for the radiation of low frequencies an opening is made in the box through a pipe segment called the bass reflex port. The Helmholtz resonance of this system is tuned to allow oscillation of the membrane down to about 50 Hz. When loud low frequency sounds are played with such a box flow separation is observed and one can not only blow a candle but even blow soap bubbles. The impulsive vortex shedding excites the resonances of the pipe segment which are around 1 kHz. This is experienced as noise. The effect of the vortex shedding can considerably reduced by rounding off the edges of the pipe segment. We should however round both the inner and outer side of the pipe segment. This is not always done in bass reflex ports! Furthermore one can drastically reduce the noise by placing a few perforations along the pipe segment. The jet flow generated by high amplitude oscillation of a Helmholtz resonator is called in the literature a synthetic jet. Such synthetic jets can be used for flow control or as a cooling device[36].

In other resonators like straight closed straight pipes high amplitudes can induce the formation of shock waves. In particular when both ends of the pipe are closed the formation of shock can occur at modest acoustical amplitudes if the quality factor of the resonator is high. When the pipe is open at one end the reflection at the open-end inverse the compression waves into expansion waves which have opposite non-linear wave steepening effects [26]. This implies that shock are only observed at very high amplitudes when the shock formation distance is shorter than the pipe length. This is common in brass instruments[44]. The typical brassy sound is due to shock wave generation in the pipe. In car muflers shock wave formation cause so called rasping sound.

7 Turbulent noise

7.1 Turbulence

Turbulence is a complex chaotic unsteady flow behaviour which appears when friction forces are too small compared to non-linear convective forces to stabilize the flow in regions of large shears rates such as boundary layers, shear-layers.... In general the ratio of non-linear convective forces $\rho(\vec{v}\cdot\nabla)\vec{v}$ and of viscous forces $\nabla\cdot\vec{\vec{\tau}}$ is estimated by using the Reynolds number defined by:

$$Re = \frac{U_0 D^2}{\nu_0 L} \tag{294}$$

where U_0 is a characteristic (main flow) velocity, D is a characteristic gradient length for the viscous force ($\nu_0\nabla^2\vec{v} \sim \nu_0 U_0/D^2$) and L is a gradient length for the convective force ($(\vec{v}\cdot\nabla)\vec{v} \sim U_0^2/L$).

Depending on the choice of D and L the Reynolds number is a measure either for the importance of dissipation in the flow or for the stability of the flow. In general in most shear flows when we take $L = D$ we obtain a measure for the stability of the flow. For example a pipe flow is in general likely to be turbulent if the Reynolds numbers based on

the diameter D of the pipe is larger than a critical value $Re_D = U_0 D/\nu_0 > 2300$. However the importance of dissipation in a pipe flow depends also on the length L of the pipe.

When the flow velocity varies smoothly over the characteristic length D we call the flow laminar, by opposition to turbulent. In general below the critical Reynolds number for the appearance of turbulence the dissipation becomes smaller with increasing Reynolds number. The higher Reynolds the more accurate the equation of Bernoulli becomes. Turbulence implies however a strong dissipation by transfer of energy from the large length scale D towards vortical length scales which have a characteristic Reynolds number of unity and dissipate the kinetic energy of the flow. This transfer occurs by a cascade of energy from large to small length scales by the stretching of vortical structures. Dissipation becomes essential in a turbulent flow and the equation of Bernoulli is certainly not valid.

Turbulence occurs in many systems which produce noise because noise production is often associated with large flow velocities or extended sources corresponding to large Reynolds numbers. Typical Reynolds numbers of an aircraft is $Re_D = 10^8$ based on the wing cross section cord length. Exception to this rule are musical instruments and biological systems [20]

Turbulence is important because it appears in most systems which are important sources of noise. In particular it is an intrinsic source of noise which remains when all other effects have been minimized. For example if we build a ventilation fan in a rigid channel, even if the fan is perfect and we avoid any interaction of the blades with the (mechanical) support of the fan, there will be an unsteadiness of the flow due to turbulence (incoming channel flow and boundary layer-trailing edge interaction). This results into a variable thrust (dipole) of the fan which generates propagating waves. Typically the sound will then be a broad band noise in contrast to the sound produced by the interaction of a fan with a support which generated harmonics of the rotation frequency.

An accurate prediction of the sound production by turbulent flows is quite difficult. In many cases even a numerical model is not accurate enough to predict the correct scaling rules for the production of sound in free field conditions. Analytical methods to determine the scaling rules and understand the elementary processes which control the sound production are still important tools. We illustrate this statement with the turbulent free jet.

[20] The evolution of recorders have produced instruments in which the flow is dominantly laminar which may be due to the optimization of the ratio of harmonic sound to broad band noise in this particular instrument. However the instrument work at the verge of turbulence, because otherwise the sound production would be too weak. In a similar way the blood-circulation works at the maximum Reynolds number just before the onset of turbulence. This corresponds to the minimum of viscous losses. When turbulence appears in such systems, its typical noise production is an indication for the practician for a defect of our body. We will also see that the appearance of turbulence is a significant problem when considering the scaling up of devices such as acoustical cooling machines. Again in such a case the optimum would be like in a biological system to remain just below the onset of turbulence.

7.2 Isothermal free jets

The prediction of the correct scaling rule for the production of sound by a free jet is a major succes of Lighthill's theory in understanding sound production by flows. As stressed by Powell[93] it is important to realize that Lighthill did *predict* this scaling rule, and that it is only after this prediction that experimental results could be classified and understood correctly. Theory was not just a confirmation of an excisting empirical scaling rule.

The steps in the procedure of Lighthill show an elegant blend of analytical methods and an optimal use of our empirical knowledge on the jet flows. Each step of the derivation is non-trivial and we therefore discuss them each separately:

a) Define an aero-acoustic sound source Q_a acting on a virtual fluid which is an extrapolation of the quiescent flow surrounding the observer:

$$\frac{\partial^2 \rho'}{\partial t^2} - c_0^2 \frac{\partial^2 \rho'}{\partial t^2} = Q_a \tag{295}$$

with:

$$Q_a = \frac{\partial^2 T_{ij}}{\partial x_i \partial x_j} \tag{296}$$

with:

$$T_{ij} = \rho v_i v_j - \tau_{ij} + \delta_{ij}(p - c_0^2 \rho) \tag{297}$$

as a result of an exact combination of conservation laws (59).

b) Assume that at low Mach numbers we can neglect friction and heat transfer:

$$T_{ij} \approx \rho_0 v_i v_j \tag{298}$$

where ρ_0 is the mean density. We neglect compressibility in the source region.

c) Formulate an integral equation using the Green's function G:

$$c_0^2 \rho' = \int_{-\infty}^{t^+} \int_V G \frac{\partial^2 T_{ij}}{\partial y_i \partial y_j} d\vec{y} d\tau \tag{299}$$

d) In free space we use the free space Green's function $G_0 = \frac{\delta(\tau - te)}{4\pi|\vec{x}-\vec{y}|}$ (122). We use partial integration to move the spatial derivative from the unknown T_{ij} towards the exactly known G_0 and use the symmetry of G_0 with respect to derivation (124) with respect to the observer and source positions $\vec{x}$ and $\vec{y}$ to obtain $\frac{\partial^2 G_0}{\partial y_i \partial y_j} = \frac{\partial^2 G_0}{\partial x_i \partial x_j}$. Move the differentiation out of the integral over $\vec{y}$ the source position:

$$c_0^2 \rho' = \frac{\partial^2}{\partial x_i \partial x_j} \int_{-\infty}^{t^+} \int_V T_{ij} G_0 d\vec{y} d\tau \tag{300}$$

e) Realize that in the far field approximation the sound field at the observers position has a characteristic gradient length which is imposed by the locally plane wave behaviour at this position:

$$\frac{\partial}{\partial x_i} \approx -\frac{1}{c_0}\frac{x_i}{|\vec{x}|}\frac{\partial}{\partial t} \tag{301}$$

f) Use the delta function in $G_0 = \frac{\delta(\tau - t_e)}{4\pi r}$ to carry out the time integration:

$$4\pi c_0^2 \rho' \approx \frac{x_i x_j}{|\vec{x}|^2 c_0^2}\frac{\partial^2}{\partial t^2}\int_V [\frac{T_{ij}}{|\vec{x}-\vec{y}||1-\frac{\partial t_e}{\partial \tau}|}]_{\tau=t_e} d\vec{y} \tag{302}$$

with $t_e = t - \frac{|\vec{x}-\vec{y}|}{c_0}$.

g) Assume that the source volume V in which $Q_a \neq 0$ is compact and neglect the variations in $|\vec{y}|$ around $\vec{y} = 0$. This is valid for subsonic jets because the characteristic time scale[21] is D/U_0 which implies that $\frac{D}{\lambda} \sim \frac{D}{Dc_0/U_0} = M_0$. In other words assume that the dominant frequencies correspond to the motion of vortical structures with a length scale corresponding to the width D of the jet. As a consequence of the compactness we have:

$$t_e \approx t - \frac{|\vec{x}|}{c_0} \tag{303}$$

and:

$$r = |\vec{x} - \vec{y}| \approx |\vec{x}| \tag{304}$$

h) Assume that the order of magnitude estimate of the Lighthill stress tensor is: $T_{ij} \sim \rho_0 U_0^2$.

i) Assume that because the velocity of the jet decreases as r^{-1} along the jet axis for $r > 5D$, the source region has a limited volume scaling following: $V \sim D^3$.

j) Assume that the sound is produced by interaction of vortical structures while they are convected with the jet velocity U_c which implies that:

$$\frac{\partial t_e}{\partial \tau} = \frac{U_c}{c_0}\cos\theta \tag{305}$$

where θ is the angle between the jet axis and the direction of the observer's position.

As final result we find:

$$4\pi c_0^2 \rho' \sim \frac{1}{c_0^2|\vec{x}|}[\frac{U_0}{D}\frac{\partial t_e}{\partial t}]^2 \frac{\rho_0 U_0^2 D^3}{|1 - M_c\cos\theta|} \tag{306}$$

or:

$$\frac{\rho'}{\rho_0} \sim \frac{D}{4\pi|\vec{x}|}\frac{M_0^4}{|1 - M_c\cos\theta|^3} \tag{307}$$

[21] $\frac{\partial}{\partial \tau} \sim \frac{U_0}{D}$

where $M_0 = U_0/c_0$ and $M_c = U_c/c_0$. Typically $U_c/U_0 \simeq 0,3$ [72].

The global agreement between the measure sound intensity $< I > \sim < (\rho')^2 >$ and the sound production of isothermal subsonic jets is so good that the deviations observed at low Mach numbers are referred to as "excess" sound. This excess sound has been clearly identified by Morfey [72] and other researchers as the results of unavoidable nozzle effects on the jet sound. It is indeed very difficult to measure pure isothermal jet noise. These effects scale with M_0^3 rather than M_0^4 for the true free jet noise and become therefore always dominant at very low Mach numbers.

A crucial result of Lighthill's analogy is that in hydro-acoustics for typical water jet velocities of $1m/s$ the sound production cannot be predicted from numerical flow calculation which show inaccuracies of the order of $M_0^4 \sim 10^{-10}$. An accuracy we cannot at the present time dream of. As typical accuracies of numerical calculations are of the order of 10^{-2}, the prediction of sound production is rather meaningless below $M_0 \approx 0.3$ for free field conditions. Direct numerical simulation of jet noise are therefore usually carried out at higher Mach numbers (around $M_0 = 0,9$). We will see that in confined flows the sound production is much less difficult because the sources become much more effective.

An interesting feature of the Lighthill scaling law is that in spite of the fact that it was explicitly derived for low subsonic flows, it does not performe to bad even at supersonic flow velocities if we avoid directions such that:$M_c \cos\theta = 1$ in which strong directional radiation occurs (coincidence angle). It should, however, be obvious that $< I >$ cannot keep increasing as M_0^8 because this would imply that the noise power would become larger than the kinetic energy $\frac{1}{2}\rho_0 U_0^3 \frac{\pi}{4} D^2$ in the jet flow. At high Mach numbers $< I >$ cannot increase faster than M_0^3. This appears a reasonably correct scaling rule for supersonic jets. At supersonic speeds the hypothesis of an isothermal flow becomes meaningless. An analysis including the influence of temperature difference in the flow has been proposed by Tam [108]. In supersonic jets one observes new sources of sound such as the interaction of vortices with shock waves in under or over-expanded free jets. At high speeds about 5% of the kinetic energy in the jet is radiated away as sound in free field conditions [37].

The usefulness of a scaling rule is illustrated by the sound production of civil aircraft engines. The thrust of a free jet scales with $\rho U_0^2 D^2$ and should be kept to a certain value to maintain an aircraft in the air. The power necessary to generate this thrust scales as $\rho_0 U_0^3 D^2$. Hence a large jet diameter implies an efficient engine, which is the main reason to use the so called "high by-pass" motor. The nice feature of the engine is that it is not only efficient but also silent. Indeed an increase of diameter by a factor two at constant thrust induces a reduction of flow velocity by a factor two and following Lighthill's scaling rule a reduction of the sound pressure level by $18dB$ (factor 8 in ρ'). At the present time due to additional measures in the construction of the engine (inlet wall covered by sound absorbing material...) result into a level of sound production which makes the flow noise around the air-craft as important as the engine noise.

Before leaving the subject, it is interesting to stress a last time the elegance of Lighthill's procedure by showing that a more simplified approach would have been quite useless [20]. If we for example simply assume that because we consider a low Mach number $M_0 \ll 1$,

we can neglect the retarded time effects over the source region we would have:

$$4\pi c_0^2 \rho' \sim \frac{1}{|\vec{x}|}\int_V [\frac{\partial^2 T_{ij}}{\partial y_i \partial y_j}] d\vec{y} = \frac{1}{|\vec{x}|}\int_S \frac{\partial T_{ij}}{\partial y_{j_i}} n_j dS = 0 \tag{308}$$

because the control surface S is taken outside the source region ($T_{ij} = 0$ on S). Hence we cannot find any sound production if we do not assume some retarded time variation over the source region. If we assume that the retarded time variations are of the order of $\Delta\vec{y}/c_0 \sim D/c_0$ we would then find:

$$\frac{\partial}{\partial y_i} \sim \frac{1}{D} \tag{309}$$

which would imply a monopole dependence of the sound production $< I > \sim M_0^4$. This is of course a dramatically overestimation of the sound production at low Mach numbers. For $M_0 = 0.1$ we would have an error of about $40dB$.

In the same way as we should appreciate the Lighthill's scaling law we should apply it only to isothermal free jets. Applications to confined jets or even to condensate vapor jets is rather meaningless. We will in the following sections indicate how the presence of walls modified the radiation of turbulence. Finally we will discuss the impact of a difference in speed of sound c in the source region and speed of sound c_0 at the position of the listener.

7.3 Low frequency behaviour of a jet in an infinite pipe

It is interesting now to investigate the behaviour of a small turbulent free jet confined in a pipe. As a result of the contribution of all the images, we expect that at low frequencies the sound intensity radiated by a confined jet will be much larger than that of a free jet. The theory of Lighthill using the infinite pipe low frequency Green's function has been used by Ffowcs Williams[35] to quantify this effect. We summarize here the results.

Assume a small jet of diameter D placed in a pipe of cross-sectional area S with axis along the x_1 coordinate in a cartesian system $\vec{x} = (x_1, x_2, x_3)$. Assume that the jet velocity U_0 is such that:

$$M_0 = U_0/c_0 \ll 1 \tag{310}$$

and:

$$He = \frac{M_0\sqrt{S}}{D} \ll 1 \tag{311}$$

which implies that the characteristic acoustical wave length of the sound generated by the large scale vortical structures in the jet is much larger than the pipe diameter. This allows us to assume plane waves propagation in the pipe. The corresponding one dimensional Green's function is given by equations (167) and (169):

$$G = \frac{c_0}{2S} H(t - \tau - \frac{|x_1 - y_1|}{c_0}) \tag{312}$$

and using the integral formulation of Lighthill's analogy:

$$p' = \int_{-\infty}^{t^+}\int_V G \frac{\partial^2 T_{ij}}{\partial y_i \partial y_j} d\vec{y} d\tau \ . \tag{313}$$

By partial integration we have:

$$p' = \int_{\infty}^{t^+} \int_V T_{11} \frac{\partial^2 G}{\partial y_1^2} d\vec{y} d\tau \tag{314}$$

where we used the fact that G is independent of y_2 and y_2. Furthermore we have:

$$\frac{\partial G}{\partial y_1} = \frac{1}{2S} \delta(t - \tau - \frac{|y_1 - x_1|}{c_0}) \frac{\partial |x_1 - y_1|}{\partial y_1} \tag{315}$$

where:

$$\frac{\partial |x_1 - y_1|}{\partial y_1} = -\text{sign}(x_1 - y_1) = -\frac{\partial |x_1 - y_1|}{\partial x_1} \tag{316}$$

we have also the symmetry property:

$$\frac{\partial G}{\partial x_1} = -\frac{\partial G}{\partial y_1} \tag{317}$$

as for the free space Green's function. This implies that:

$$p' = \frac{\partial}{\partial x_1} \int_{-\infty}^{t^+} \int_V \frac{1}{2S} T_{11} \delta(t - \tau - \frac{|x_1 - y_1|}{c_0}) \text{sign}(x_1 - y_1) d\vec{y} d\tau \ . \tag{318}$$

Assuming that:

$$T_{11} \sim \rho_0 U_0^2 \tag{319}$$

and using the far field approximation:

$$\frac{\partial}{\partial x_1} = -\text{sign}(x_1 - y_1) \frac{1}{c_0} \frac{\partial}{\partial t} \sim \frac{M_0}{D} \tag{320}$$

we find if we neglect the retarded time variation in the jet:

$$p' \sim \frac{M_0}{D} \frac{\rho_0 U_0^2 D^3}{2S} \tag{321}$$

or:

$$< I > \sim (\frac{\rho_0 M_0^3 D^2}{S})^2 \tag{322}$$

indeed a much stronger radiation than in free field conditions.

7.4 Low frequency turbulent sound production by a diaphragm.

The analogy of Curle discussed in section 4.9 can also be used in a pipe. We consider a low Mach number flow in a pipe with a discontinuity. Ignoring convective effects at the observer's position, we start our discussion from equation (152):

$$\begin{aligned} p' &= \int_{-\infty}^{t^+} \int_V (\rho v_i v_j - \tau_{ij}) \frac{\partial^2 G}{\partial y_i \partial y_j} dV_y d\tau \\ &- \int_{-\infty}^{t^+} \int_S G \frac{\partial \rho v_i}{\partial \tau} n_i dS_y d\tau \\ &- \int_{-\infty}^{t^+} \int_S (P_{ij} + \rho v_i v_j) \frac{\partial G}{\partial y_j} n_i dS_y d\tau \ . \end{aligned} \tag{323}$$

We now introduce the one dimensional low frequency Green's function:

$$G(\vec{x},t|\vec{y},\tau)=\frac{g_0(x_1,t|y_1,\tau)}{S}=\frac{c_0}{2S}H(t-\tau-\frac{|x_1-y_1|}{c_0}) \tag{324}$$

which has the following symmetry property:

$$\frac{\partial g_0}{\partial x_1}=-\frac{\partial g_0}{\partial y_1}=-\frac{1}{2}\mathrm{sign}(x_1-y_1)\delta(t_e-\tau) \tag{325}$$

with:

$$t_e=t-\frac{|x_1-y_1|}{c_0}\ . \tag{326}$$

Furthermore we have:

$$\frac{\partial g_0}{\partial \tau}=-\frac{c_0}{2}\delta(t_e-\tau)\ . \tag{327}$$

As G is independent of y_2 and y_3 we have:

$$\begin{aligned} Sp'(x_1,t) &= -\frac{\partial}{\partial x_1}\int_{-\infty}^{t^+}\int_V \frac{\partial g_0}{\partial y_1}T_{11}dV_y d\tau \\ &- \int_{-\infty}^{t^+}\int_S \frac{\partial g_0}{\partial y_1}[P_{1j}+\rho v_1 v_j]n_j dS_y d\tau \\ &- \int_{-\infty}^{t^+}\int_S g_0\frac{\partial \rho v_i}{\partial \tau}n_i dS_y d\tau\ . \end{aligned} \tag{328}$$

By partial integration in time and using causality [45] using the filter properties of the delta functions we find:

$$\begin{aligned} Sp'(x_1,t) &= -\frac{1}{2}\frac{\partial}{\partial x_1}\int_V [T_{11}]_{\tau=t_e}\mathrm{sign}(x_1-y_1)dV_y \\ &- \frac{1}{2}\int_S [P_{1j}+\rho v_1 v_j]_{\tau=t_e}\mathrm{sign}(x_1-y_1)n_j dS_y \\ &- \frac{c_0}{2}\int_S [\rho v_i]_{\tau=t_e}n_i dS_y\ . \end{aligned} \tag{329}$$

We now apply this to a diaphragm in a pipe as shown in figure 51.
As the observer is in a plane wave region we have:

$$\frac{\partial}{\partial x_1}=-\frac{1}{c_0}\mathrm{sign}(x_1-y_1)\frac{\partial}{\partial t}\ . \tag{330}$$

As the walls are rigid $v_i=0$ on S so that equation (329) reduces for $x_1>y_1$ to:

$$\begin{aligned} Sp' &= +\frac{1}{2c_0}\frac{\partial}{\partial t}\int_V [\rho v_1^2+p-c_0^2\rho']_{\tau=t_e}dV_y \\ &- \frac{1}{2}\int_S [P_{1j}]_{\tau=t_e}\mathrm{sign}(x_1-y_1)n_j dS_y\ . \end{aligned} \tag{331}$$

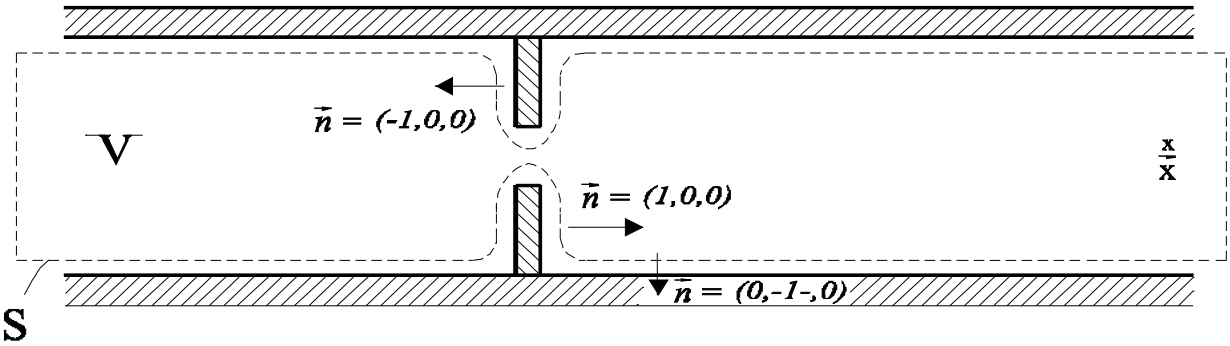

Figure 51: *Diaphragm in a pipe and definition of controle surface S and volume V.*

If we neglect the viscous effects at the pipe walls we have $P_{1j}n_j = p\delta_{1j}n_j = pn_1 = 0$ at those walls, because $n_1 = 0$. The surface integral reduces to the walls of the diaphragm. If we neglect variations of emission time t_e the surface integral $\int_S P_{ij}n_j dS$ corresponds simply to the instantaneous force of the flow on the diaphragm. We therefore expect a simple relationship between the sound production by a turbulent pipe flow at a pipe discontinuity and the pressure loss coefficient $C_D = 2\Delta p/(\rho_0 U_0^2)$. This contribution scales as $\rho_0 U_0^2$. The volume integral corresponds to the noise of turbulence as we find in a pipe without diaphragm which scale as M_0^3 and can therefore be neglected at low Mach numbers. It appears indeed that turbulent sound in pipes is mainly due to sources localized at pipe discontinuities. When we put our teeth in the flow we make much stronger fricative sounds (s, f,...) than when we blow with open mouth (h). The ideas described above have been used by Nelson and Morfey [80] to obtain correlation for sound production at slit shaped diaphragms and spoilers in rectangular ducts. The same idea has been used by Oldham [85] for circular ducts. Oldham [85] claims a general correlation for both types of diaphragms. Recent study on bends by Gijrath [38] and Nygard [83] show however that the pressure loss coefficient C_D is not sufficient to characterize the sound production at a discontinuity. This is due to the essential difference between turbulence in slit jet flows and circular jet flows which has been already discussed by Bjorno [6] and Verge [113]. The claim of Oldham [85] that Nelson [80] misinterpreted his own data is not verified. Indeed the difference at low frequencies between the normalized spectra for slits and circular diaphragm does corresponds to the differences observed by Bjorno [6] between circular and planar jets. While a circular jet of diameter D has a maximum of sound production at $Sr_D = fD/U_0 \simeq 1$ a planar jet of thickness h displays a maximum around $Sr_h = fh/U_0 \simeq 0.03$. The most unstable oscillation modes of a planar jet are flapping modes while those of a circular jet are helicoidal modes. Similarly the sound production of supersonic jets formed by slits studied by Hirschberg [43] (valve leakage) is quite different from the sound produced by supersonic jet from circular orifices in pipes studied by Reethof [96].

When considering turbulence noise in pipes, the transversal resonances of the pipe play an essential role. This has already been illustrated in the spectrum of an flue organ pipe shown in figure 30. Also in speech the first transversal mode of our vocal tract (around 3 kHz) is dominant in fricative sounds. A discussion of this effect is provided by Nelson [80].

In the above discussion we have ignored the effect of the main flow on the acoustical wave propagation. The Doppler effect is expected to favor downstream sound radiation. This has been observed by Åbom [**?**]. This will not only induce a Doppler effect but can also strongly influence the sound absorption. The absorption of sound by a turbulent pipe flow is discussed by Ronneberger [99] and Peters [89].

When we consider a flow of a liquid through a pipe, the main sound production mechanism is the sound radiated by gas bubbles. The acoustical resonances of bubbles are spectacular and their presence dramatically affects sound production [20], [117]. We will not treat this fascinating subject here.

7.5 Free jet in a bubbly liquid

We now consider the influence of a large difference between the local speed of sound c in the source region and the speed of sound c_0 at the position of the listener. An example of such a situation is the sound production of a bubbly liquid jet in a liquid surrounding. As discussed by Crighton [19], the relevant speed of sound c is the low frequency limit at which the bubbles of gas are in equilibrium with the liquid. The density ρ of the gas/liquid mixture is given by:

$$\rho = \beta\rho_g + (1-\beta)\rho_l$$

where ρ_g is the gas density, ρ_l is the liquid density and β the volume fraction of gas in the mixture. The compressibility of the mixture is given by:

$$\frac{1}{\rho c^2} = \frac{\beta}{\rho_g c_g^2} + \frac{(1-\beta)}{\rho_l c_l^2}$$

where c_g is the speed of sound in the gas and c_p is the speed of sound in the liquid. Eliminating ρ we find:

$$c^2 = \frac{1}{[\beta\rho_g + (1-\beta)\rho_l]\left[\frac{\beta}{\rho_g c_g^2} + \frac{(1-\beta)}{\rho_l c_l^2}\right]} \ .$$

For not too small or too large values of β because $\rho_g/\rho_l = 0(10^{-3})$ while $\rho_g c_g^2/(\rho_l c_l^2) = 0(10^{-4})$ we can use the approximation:

$$c^2 = c_g^2 \frac{\rho_g}{\rho_l \beta(1-\beta)} \ .$$

The compressibility is dominated by the gas phase while the inertia is determinded by the liquid. For an air-water mixture at atmospheric conditions $c_g = 340$ m/s, $\rho_g = 1,2$ kg/m^3,

$c_l = 1500$ m/s and $\rho_l = 10^3$ kg/m^3 we find for $\beta = 0,5$ a minimum value of the speed of sound $c \simeq 20$ m/s. Using equation (55) we obtain by substracting from both sides the term $c_0^2 \frac{\partial^2 \rho'}{\partial x_i^2}$, het analogy of Lighthill in the form:

$$\frac{\partial^2 \rho'}{\partial t^2} - c_0^2 \frac{\partial^2 \rho'}{\partial x_i^2} = \frac{\partial^2 \rho v_i v_j - \tau_{ij}}{\partial x_i \partial x_j} + \frac{\partial^2}{\partial x_i^2}\left(p' - c_0^2 \rho'\right) - \frac{\partial f_i}{\partial x_i}$$

where ρ' is used as aero-acoustical variable.

This form of the analogy stresses the source term

$$\frac{\partial^2}{\partial x_i^2}\left(p' - c_0^2 \rho'\right) = \frac{\partial^2}{\partial x_i} p' \left(1 - \left(\frac{c_0}{c}\right)^2\right)$$

which is due to the difference in inertia of the reference fluid and entropy patches in the source region. In the source region p' scales in the same way as $\rho v_i v_j$ as $\rho_0 U_0^2$. Hence the factor $\left(1 - \left(\frac{c_0}{c}\right)^2\right)$ represents an amplification factor of the source when comparing with an isothermal free jet. For an air-water mixture as discussed above $\left(\frac{c_0}{c}\right)^2 = 5 \times 10^3$ corresponding to an enhancement of the sound production by 74 dB compared to the sound production of an underwater pure water jet for a listener in pure water. When taking a shaver in a bath tub we indeed observe a dramatic reduction of sound production when the shower jet is submerged in the water avoiding air entrainment compared to the sound produced by the shower jet impinging on the surface of the water.

References

[1] Allam, S. and Åbom, M., Investigation of damping and radiation using full plane wave decomposition in ducts, J. Sound and Vibration 292 (2007) 727-743.

[2] Acheson, D.J., Elementary fluid dynamics, Clarendon Press, Oxford (1990).

[3] Anderson, A.B.C., Metastable jet-tone states of jets from sharp-edged, circular, pipe-like orifices, J. Acoust. Soc. Am. 27 (1955) 13-21.

[4] Batchelor, G.K., An introduction to fluid dynamics, Cambridge University Press, Cambridge, UK (1967).

[5] Bechert, D.W., Sound absorption caused by vorticity shedding, demonstrated with a jet flow. J. Sound and Vibration 70 (1980) 389-405.

[6] Bjorno, L. & Larsen, P.N., Noise of air jets from rectangular slits, Acustica 54 (1984) 247-256.

[7] Blackstock, D.T., Fundamentals of physical acoustics, Wiley-Interscience, NY (2000).

[8] Blake, W.K., Mechanics of Flow-Induced Sound and Vibration, Vol. I and II, Academic Press, Orlando (1986).

[9] Blevins R.D., Flow-Induced Vibration, second edition, Van Nostrand Reinhold, NY (1990).

[10] Bouasse, H., Instruments à vent, vols. I & II, Librairies Delagrave, Paris (1929), reprint Blanchard, Paris (1985).

[11] Bruggeman, J.C., Hirschberg, A., van Dongen, M.E.H. & Wijnands, A.P.J., Self-sustained aero-acoustic pulsations in gas transport systems: experimental study of the influence of closed side branches, Journal of Sound and Vibration 150 (1991) 371-393.

[12] Cargill, A.M., Low frequency acoustic radiation from a jet pipe - a second order theory. J. Sound and Vibration 83 (1982) 339-354.

[13] Hirschberg A., Kergomard, J. & Weinreich, G. (edts), Mechanics of Musical Instruments, Springer Verlag, Wien (1995).

[14] Coltman, J.W., Sounding mechanism of the flute and organ pipe, J. Acoust. Soc. Am. 44 (1968) 983-992.

[15] Coltman, J.W., Jet drive mechanism in edge tones and organ pipes, J. Acoust. Soc. Am. 60 (1976) 725-733.

[16] Cousteix, J., Aérodynamique, couche limite laminaire, Cepadues, Toulouse, France (1988).

[17] Cremer L. & Heckl M., Structure-Borne Sound, second edition, Springer-Verlag, Berlin (1988).

[18] Crighton, D.G., Basic principles of aerodynamic noise generation, Prog. Aerospace Sci., 16 (1975) 31-96.

[19] Crighton, D.G., The Kutta condition in unsteady flow. Annual Review of Fluid Mechanics 17 (1985) 411-445.

[20] Crighton, D.G., Dowling, A.P., Ffwocs Williams, J.E., Heckl, M. & Leppington, F.G., Modern methods in analytical acoustics, Lecture notes, Springer-Verlag, London (1992).

[21] Crighton, D.G., The edgetone feedback cycle. Linear theory for the operating stages, J. Fluid Mech. 234 (1992) 361-391.

[22] Crocker M.J. (ed), Handbook of Acoustics, Jhon Wiley & Sons, NY (1998).

[23] Cummings, A., J. Sound and Vibration 31 (1973) 331-343.

[24] Curle, N., The influence of solid boundaries upon aerodynamic sound, Proc. Roy. Soc. A 231 (1955) 505-514.

[25] Dequand, S., Luo, X., Willems, J. & Hirschberg, A., Helmolz-like resonator self-sustained oscillations, part 1: Acoustical measurements and analytical models. AIAA Journal 41 (2003) 408-415.

[26] Disselhorst, J.H.M. & van Wijngaarden, L., Flow in the exit of open pipes during acoustic resonances, J.Fluid Mech. 99 (1980) 293-319.

[27] Doak, P.E., Fluctuating total enthalpy as a generalized field, Acoust. Phys. 44 (1995) 677-685.

[28] Dowling, A.P. & Ffowcs Williams, J.E., Sound and sources of sound, Ellis Horwood Publisher, Chichester (1983).

[29] Elder, S.A., On the mechanism of sound production in organ pipes, J. Acoust. Soc. Am. 54 (1973) 1554-1564.

[30] Elder, S.A., Forced oscillations of a separated shear layer with application to cavity flow-tone effects, J. Acoust. Soc. Am. 67 (1980) 774-781.

[31] Fabre, B., Hirschberg, A. & Wijnands, A.P.J., Vortex shedding in steady oscillations of a flue organ pipe, Acta Acustica 82 (1996) 863-877.

[32] Finch, T.L. & Nolle, A.W., Pressure wave reflections in organ note channel, J. Acoust. Soc. Am. 79 (1986) 1584-1591.

[33] Fletcher, N.H. & Rossing, T., The physics of musical instruments, Second edition, Springer-Verlag, NY (1998).

[34] Forester, J.H. & Young, D.F., Flow through a converging-diverging tube ands its implications in occlusive vascular disease, Journal of Biomechanics 3 (1970) 297-316.

[35] Ffowcs Williams, J., Hydrodynamic noise, Ann. Rev. Fluid Mechanics 1 (1969) 197-222.

[36] Glezer, A. & Amitay, M., Synthetic Jets. Ann. Rev. Fluid Mech. 34 (2002) 503-529.

[37] Goldstein, M., Aeroacoustics, McGraw-Hill, NY (1976).

[38] Gijrath, J.W.M., Verhaar, B.T. & Bruggeman, J.C., paper presented at FIV2000 conference, Lucerne, Zwitserland (2000).

[39] Heckl, M.A., Active control of noise from a Rijke tube, J. Sound and Vibration 124 (1988) 117-133.

[40] St. Hilaire, A.O., Wilson, T.A. & Beavers, G.S., Aerodynamic excitation of the harmonium reed, J. Fluid Mech., 49 (1971) 803-816.

[41] Hirschberg, A., van de Laar, R.W.A., Marrou-Maurières, J.P., Wijnands, A.P.J., Dane, J.H., Kruijswijk, S.G & Houtsma, A.J.M., A quasi-stationary model of air flow in the reed channel of single-reed woodwind instruments, Acustica 70 (1990) 146-154.

[42] Hirschberg, A., Gilbert, J., Wijnands, A.P.J. & Valkering, A.M.C., Musical aero-acoustics of the clarinet, Journal de Physique IV, Colloque C5, su. J. Physique III, vol. 4 (1994) C5-559-568.

[43] Hirschberg, A., Thielens, G. & Luijten, C., Aero-acoustic sources, Nederlandse Akoestisch Genootschap, NAG journal 129 (1995) 3-13.

[44] Hirschberg, A., Gilbert, J., Wijands, A.P.J. & Msallam, R., Shock waves in trombones, J. Acoust. Soc. Am. 99 (1996) 1754-1758.

[45] Hofmans, G.C.J., Vortex sound in confined flows, PhD thesis, Technische Universiteit Eindhoven (1998).

[46] Holger, D.K., Wilson, T.A., & Beavers, G.S., Fluid mechanics of the edgetone, J. Acoust. Soc. Am. 62 (1977) 1116-1128.

[47] Hourigan, K., Thompson, M.C., Stokes, A.N. & Welsh, M.C., Prediction of flow/acoustic interactions using vortex models: duct with baffles, in Computational Fluid Dynamics, G.de Vahl Davis and C.Fletcher (eds.), Elsevier Science Pub. B.V. (North-Holland), (1988) 427-436.

[48] Howe, M.S., Contribution to the theory of aerodynamic sound, with application to excess jet noise and the theory of the flute, J. Fluid Mech. 71 (1975) 625-673.

[49] Howe, M.S., On the theory of unsteady shearing flow over a slot, Philosophical Transactions of the Royal Society of London A 303 (1981) 151-180.

[50] Howe, M.S., On the absorption of sound by turbulence and other hydrodynamic flows, IMA J. Applied Math. 32 (1984) 187-209.

[51] Howe, M.S., Acoustics of Fluid-Structure Interactions, Cambridge University Press, Cambridge, UK (1998).

[52] Howe, M.S., Theory of Vortex Sound. Cambridge University Press, Cambridge, UK (2002).

[53] Hubbard, H.H., Aeroacoustics of flight vehicles, Acoustical Society of America (1995).

[54] Hubbard, H.H., editor. Aeroacoustics of Flight Vehicles: Theory and Practice. Volume 1, Noise Sources; Volume 2, Noise Control (Nasa Reference Publication 1258). Acoustical Society of America (1995).

[55] Ingard, U. & Ising, H., Acoustic nonlinearity of an orifice, J. Acoust. Soc. Am. 42 (1967) 6-17.

[56] Ishizaka, K. & Matsudaira, M., Fluid mechanical consideration of vocal cord vibrations, Speech Communication Research Laboratory Monograph N^{o}8, S.B., CA (1972).

[57] Junger, M.C. & Feit D., Sound, Structures and Their Interaction, second edition, MIT Press (1986).

[58] Keefe, D.H., Acoustic streaming, dimensional analysis of non-linearities, and tone hole mutual interactions in woodwinds, J. Acoust. Soc. Am. 73 (1983) 1804-1820.

[59] Keefe, D.H., Acoustical streaming, dimensional analysis of nonlinearities, and tone hole mutual interactions in woodwinds, J. Acoust. Soc. Am. 73 (1983) 1804-1820.

[60] Kinsler, L.E., Frey, A. R., Coppens, A.B. & Sanders, J.V., Fundamentals of Acoustics, third edition, John Wiley, NY (1982).

[61] Kovasnay, L.S.G., Turbulence in supersonic flow, Journal Aeronautical Sciences, 20 (1953) 657.

[62] Krasny, R., A study of singularity formation in a vortex sheet by the point vortex method, J. Fluid Mech. 167 (1986) 65-93.

[63] Kriesels, P.C., Peters, M.C.A.M., Hirschberg, A., Bruggeman, J.C. & Wijands, A.P.J., High amplitude vortex induced pulsations in a gas transport system, Journal of Sound and Vibration 184 (1995) 343-368.

[64] Kundu, P.K., Fluid mechanics, Academic Press, Harcourt (1990).

[65] Landau, L.D. & Lifshitz, E.M., Fluid Mechanics, Second edition, Pergamon Press, Oxford (1987).

[66] Levine, H. & Schwinger, J., On the radiation of sound from a unflanged circular pipe. Physical Review 73 (1948) 383-406.

[67] Lier van, L., Dequand, S. & Hirschberg, A., Aeroacoustics of diffusers: An experimental study of typical industrial diffusers at Reynolds of $O(10^5)$, J. Acoust. Soc. Am. 109 (2001) 108-115.

[68] Lighthill, M.J., On sound generated aerodynamically I & II, Proceedings of the Royal Society of London Series A 211 (1952) 564-587 & A 222 (1954) 1-32.

[69] Milne-Thomson, L.M., Theoretical Aerodynamics, Macmillan, London (1952).

[70] Möhring, W., On flows with vortex sheets and solid plates, Journal of Sound and Vibration, 38 (1975) 403-412.

[71] Möhring, W., On vortex sound at low Mach number, J. Fluid Mech. 85 (1978) 685-691.

[72] Morfey, C.L., Szewczyk, V.M. & Tester, B.J., J. Sound and Vibration, 61 (1978) 255-292.

[73] Morkovin, M.V., Fluctuations and hot-wire anemometry in compressible flows, Agardoraph 24, NATO (1956).

[74] Morse, P.M. & Ingard, K.U., Theoretical acoustics, Princeton University Press, Princeton, NJ (1968).

[75] Myers, M.K., Transport of energy by disturbances in arbitrary flows. Journal of Fluid Mechanics 226 (1991) 383-400.

[76] Myers, M.K., Transport of energy by disturbances in arbitrary flows, J. Fluid Mech. 226 (1991) 383-400.

[77] Munt, R.M., Acoustic transmission properties of a jet pipe with subsonic jet flow 1, The cold jet reflection coefficient, J. Sound and Vibration 142 (1990) 413-436.

[78] Musafir, R.E., A discussion on the structure of aeroacoustic wave equations, Proceedings of 4th French Congress on Acoustics, Marseille , Teknea, Toulouse, France (1997) 923-926.

[79] Nederveen, C.J., Acoustical aspects of woodwind instruments, second revised edition, Northern Illinois University Press, DeKlab (1998).

[80] Nelson, P.A. & Morfey, C.L., Aerodynamic sound production in low speed ducts, J. Sound and Vibration 79 (1981) 253-289.

[81] Nelson, P.A., Halliwell N.A. & Doak, P.E., Fluid dynamics of a flow excited resonance, part 2: theory, Journal of Sound and Vibration 91 (1983) 375-402.

[82] Norton M.P., Fundamental of noise and vibration analysis for engineers, Cambridge University Press, Cambridge, UK (1989).

[83] Nygrad, S., Modelling of low frequency sound in duct networks, Licentiate thesis, MWL, KTH Stockholm (2000).

[84] Obermeier, F., Aerodynamic sound generation caused by viscous processes, J. Sound and Vibration 99 (1985) 111-120.

[85] Oldham, D.J. & Ukpoho, A.U., A pressure-based technique for predicting regenerated noise levels in ventilation systems, J. Sound and Vibration, 140 (1990) 259-272.

[86] Paterson, A.R., A first course in fluid dynamics, Cambridge University Press, Cambridge (1983).

[87] Pelorson, X., Hirschberg, A., van Hassel, R.R., Wijnands, A.P.J. & Auregan, Y., Theoretical and experimental study of quasisteady-flow separation within the glottis during phonation, J. Acoust. Soc. Am. 96 (1994) 3416-3431.

[88] Peters, M.C.A.M., Aeroacoustic sources in internal flows, PhD thesis, Eindhoven University of Technology, The Netherlands (1993).

[89] Peters, M.C.A.M., Hirschberg, A., Reijnen, A.J., & Wijnands, A.P.J., Damping and reflection coefficient measurements for an open pipe at low Mach and low Helmholtz numbers, J. Fluid Mech. 256 (1993) 499-534.

[90] Pierce, A.D., Acoustics, McGraw-Hill, NY (1981), presently available from Acoustical Society of America, NY (1990).

[91] Powell, A., Vortex sound theory, J. Acoust. Soc. Am. 36 (1964) 177-195.

[92] Powell, A., Theory of vortex sound. Journal of Acoustical Society of America 36 (1964) 177-195.

[93] Powell, A., Some aspects of aeroacoustics from Rayleigh until today. Journal of Vibration and Acoustics 112 (1990)145-159.

[94] Prandtl, L., Fundamentals of hydro- and aerodynamics, Dover Pub., NY (1934).

[95] Rayleigh, J.W.S., The theory of sound (1894), Dover reprint (1954).

[96] Reethof, G. & Ward, W.C., A theoretically based valve noise prediction method for compressible fluids, J. Vibration, Acoustics, Stress and Reliability in Design, 108, Trans. ASME (1986) 329-338.

[97] Rienstra, S.W., A small number analysis of acoustic wave-jet flow-pipe interaction, J. Sound and Vibration 86 (1983) 539-556.

[98] Rienstra, S.W. & Hirschberg, A., An introduction to Acoustics, Report IWDE 99-02, Instituut Wiskundige Dienstverlening, TU Eindhoven (1999).

[99] Ronneberger, D. & Ahrens, C., Wall shear stress caused by small amplitude perturbations of turbulent boundary-layer flow: an experimental investigation, J. Fluid Mech. 83 (1977) 433-464.

[100] Roozen, N.B., Bockholts M, Eck van, P., & Hirschberg, A., Vortex sound in bass-reflex ports of loudspeakers. Part I and II, J. Acoust. Soc. Am. 104 (1998) 1914-1924.

[101] Saffman, P.G., Vortex dynamics, Cambridge University Press, Cambridge (1992).

[102] Schlichting, H., Boundary layer theory, 6th ed., McGraw-Hill, NY (1968).

[103] Schram, C. & Hirschberg, A., Application of vortex sound theory to vortex-pairing noise: sensitivity to errors in flow data. Journal of Sound and Vibrations 266 (2003) 1079-1098.

[104] Sherman, F.S., Viscous flow, McGraw-Hill, NY (1990).

[105] Spruyt, A.G., Stromings-geïnduceerde akoestische resonanties in de industrie, Nederlandse Akoestisch Genootschap, NAG Journaal 22 (1972) 1-12.

[106] St. Hilaire, A.O., Wilson, T.A. & Beavers, G.S., Aerodynamic excitation of the harmonium reed, J. Fluid Mech., 49 (1971) 803-816.

[107] Stokes, A.N. & Welsh, M.C., Flow resonant sound interaction in a duct containing a plate, 2: square leading edge, Journal of Sound and Vibration 104 (1986) 55-73.

[108] Tam, C.K.W., Noise from high speed jets. VKI Lecture Series 2001-2002, editors: J. Athoine & Scram, C., Von Karman Institute for Fluid Dynamics (2001).

[109] Temkin, S., Elements of Acoustics. Acoustical Society of America, New York, 2001. Reprint.

[110] Thompson, P.A., Compressible-fluid dynamics, McGraw-Hill, NY (1972).

[111] Verge, M.P., Fabre, B., Mahu, W.E.A., Hirschberg, A.,
van Hassel, R.R., Wijnands, A.P.J., de Vries, J.J. & Hogendoorn, C.J.,
Jet formation and jet velocity fluctuations in a flue organ pipe, J.Acoust. Soc. Am. 95 (1994) 1119-1132.

[112] Verge, M.P., Causse, R., Fabre, B., Hirschberg, A., Wijnands, A.P.J. & van Steenbergen, A., Jet oscillations and jet drive in recorder-like instruments, Acta Acustica 2 (1994) 403-419.

[113] Verge, M.P., Aeroacoustics of confined jets, PhD thesis Technische Universiteit Eindhoven (1995).

[114] Welsh, M.C. & Stokes, A.N., Flow-resonant sound interaction in a duct containing a plate, part i: Semi-circular leading edge. Journal of Sound and Vibration 95 (1984).

[115] Wilson, T.A., Beavers, G.S., De Coster, M.A., Holger, D.K. & Regenfuss, D., Experiments on the fluid mechanics of whistling, J. Acoust. Soc. Am. 50 (1971) 366-372.

[116] Wilson, T.A. & Beavers, G.S., Operating modes of the clarinet, J. Acoust. Soc. Am., 56 (1974) 653-658.

[117] Wijngaarden van, L., One-dimensional flow of liquids containing small gas bubbles. Annual Review of Fluid Mechanics 4 (1972) 369-396.